TASK-EVOKED FUNCTIONAL CONNECTIVITY AND ITS RELATIONSHIP TO BEHAVIOR IN CHILDREN

Mackenzie E. Mitchell

A thesis submitted to the faculty at the University of North Carolina at Chapel Hill in partial fulfillment of the requirements for the degree of Master of Arts in the Department of Psychology and Neuroscience in the College of Arts and Sciences.

Chapel Hill
2022

Approved by:

Jessica R. Cohen

Kelly S. Giovanello

Michael N. Hallquist

ABSTRACT

Mackenzie E. Mitchell: Task-evoked Functional Connectivity and its Relationship to Behavior in Children
(Under the direction of Jessica R. Cohen)

Studies investigating the brain basis of executive functioning and reward processing in children often use resting state functional connectivity, despite evidence in adults that functional connectivity during cognitive tasks is more predictive of behavior. This project investigated differences in functional brain network connectivity between the resting state and three tasks, probing executive function and reward processing, in the Adolescent Brain and Cognitive Development (ABCD) Study. Relationships between brain connectivity metrics and task performance were tested to determine if task-evoked brain metrics exhibited stronger relationships with task performance than resting state brain metrics. All tasks exhibited more integrated brain networks than the resting state. Additionally, preliminary evidence suggests that task-evoked brain metrics may relate more strongly to executive function task performance than resting state brain metrics. This project is a first step toward determining if resting state or task-evoked brain network organization is more predictive of behavior in children.

TABLE OF CONTENTS

LIST OF FIGURES

LIST OF TABLES

LIST OF ABBREVIATIONS

ABCD	Adolescent Brain and Cognitive Development
ARMS	ABCD Reproducible Matched Samples
BIDS	brain imaging data structure
BOLD	blood oxygen level dependent
CPM	connectome-based predictive models
dlPFC	dorsolateral prefrontal cortex
DAIC	ABCD Data Analysis and Informatics Core
dACC	dorsal anterior cingulate cortex
EN-back	emotional n-back
FC	functional connectivity
FDR	false discovery rate
FEF	frontal eye field
FIR	finite impulse response
fMRI	functional magnetic resonance imaging
HCP	Human Connectome Project
MID	monetary incentive delay
MRI	magnetic resonance imaging
NDA	NIMH Data Archive
NDI	network dissociation index
NIMH	National Institute of Mental Health
OFC	orbitofrontal cortex
SE	standard error

SES	socioeconomic status
SMA	supplementary motor area
SSD	stop signal delay
SSRT	stop signal reaction time
SST	stop signal task
STN	subthalamic nucleus
vlPFC	ventrolateral prefrontal cortex
vmPFC	ventromedial prefrontal cortex

Introduction

Cognitive abilities in childhood, such as executive functioning and reward processing, are predictive of outcomes across the lifespan. Executive functioning, which governs the abilities involved in controlling thoughts and behaviors to achieve goals (Diamond, 2013), predicts educational achievement (e.g., Follmer, 2018; Kamkar & Morton, 2017; Ribner et al., 2017) and is implicated in many clinical disorders (e.g., Demetriou et al., 2018; Nuño et al., 2021; Silverstein et al., 2020). Reward processing plays a role in risk-taking (e.g., Casey et al., 2008; Ernst, 2014; van Duijvenvoorde et al., 2016) and is implicated in substance use (e.g., Luijten et al., 2017; Yanes et al., 2018), as well as other clinical disorders (e.g., Keren et al., 2018; Nusslock & Alloy, 2017; Zald & Treadway, 2017). Maturational trajectories of executive function and reward processing are underpinned by continuing neural development into early adulthood (Casey, 2015; Grayson & Fair, 2017; Luna et al., 2010, 2015). Studies of brain function underlying executive function and reward processing have deepened our understanding of these cognitive processes (Botvinick & Braver, 2015; Casey, 2015; Luna et al., 2015) and provided foundational knowledge needed to study deviations across the lifespan and within clinical disorders.

A useful approach to understanding brain function is functional connectivity. It is widely recognized that brain regions do not act in isolation, and functional communication between brain regions is important for behavior (Biswal et al., 1995; Friston, 1994). Functional connectivity offers a statistical approximation of the similarity of variations in blood oxygen level dependent (BOLD) signaling between brain regions of interest, which can then be related to

behavior. Functional connectivity is often characterized during a resting state and offers a snapshot of the brain at 'rest' with no specific task demands, often referred to as 'intrinsic functional connectivity'(Biswal et al., 1995; Gusnard & Raichle, 2001). Resting state functional connectivity is a popular method in studies of development given in part to the ease of administration and lack of need to adjust for task difficulty across age groups. However, recent work in adults finds that functional connectivity assessed during cognitive tasks is more predictive of behavioral outcomes than resting state functional connectivity (A. S. Greene et al., 2018; Jiang et al., 2020). It is not yet known if task-evoked functional connectivity is a stronger predictor of behavior compared to the resting state in childhood.

Given that functional brain networks mature throughout childhood and adolescence (Grayson & Fair, 2017), it is possible that brain-behavior relationships shift between childhood and adulthood. One prior investigation in a cross sectional sample of youth between the ages of 8-21 years found a similar relationship to that in adults, in which task-evoked functional connectivity was more predictive of behavior than the resting state (A. S. Greene et al., 2018). However, given the wide age range used in that study, it remains unclear if brain-behavior relationships change throughout that period.

To close this knowledge gap, this project tested for differences in functional brain organization between the resting state and task-evoked states in a sample of children aged 9-10 years. Moreover, we further investigated brain network differences to test for differences in relationships with task performance between the resting state and task-evoked states. We focused on tasks probing executive functioning (response inhibition and working memory) and reward processing, given their relationship to life outcomes (e.g., Casey et al., 2008; Diamond, 2013). Understanding how resting state and task-evoked functional connectivity relate to behavior in

childhood serves three purposes: First, it improves our understanding of how brain function underlies cognitive processes. Second, it sets a foundation for studies spanning the transition to adolescence, a sensitive period with rapid neurodevelopment and changes in cognitive abilities (Casey, 2015; Di Martino et al., 2014). Third, clarifying the relationships between brain function and behavior will ultimately improve our ability to identify risk and protective factors for life outcomes, as well as develop early detection and intervention protocols (Insel et al., 2010).

I. A brief introduction to resting state and task-evoked functional brain connectivity

Functional connectivity assessed during the resting state and during task-evoked states differ in their contributions to our understanding of the brain basis of behavior. resting state functional connectivity assesses the brain in the absence of external stimuli or specific task demands and is thought to reflect a Hebbian "fire together, wire together" framework wherein brain plasticity between regions is driven by a history of coactivation, highlighting the influence of genetics and prior experience on functional brain architecture (Dosenbach et al., 2007). Brain networks, or communities of brain regions with stronger within-network than between-network connectivity, have been identified during the resting state. For example, the fronto-parietal and cingulo-opercular networks have been robustly identified during resting state and are thought to support cognitive control (Dosenbach et al., 2006, 2007, 2008; Power & Petersen, 2013). The fronto-parietal network, which includes the dorsolateral prefrontal cortex (dlPFC) and the posterior parietal cortex, is thought to support flexible adaptive control, while the cingulo-opercular network, which includes the anterior insula and dorsal anterior cingulate cortex (dACC), is thought to support stable task maintenance (Dosenbach et al., 2006, 2007, 2008; Power & Petersen, 2013). The cingulo-opercular network is closely connected to the salience

network, which includes regions of the anterior insula and the dACC as well (Seeley et al., 2007). In some atlases, the cingulo-opercular and salience networks are considered one network (e.g., Yeo et al., 2011), while in others they are considered two networks (e.g., Power et al., 2011). Across studies these two network names are largely used interchangeably. Importantly, coherent functional connectivity of networks of brain regions at rest corresponds with regional activity evoked during cognitive tasks (Power et al., 2011; Smith et al., 2009; Tavor et al., 2016; Yeo et al., 2011). It is unsurprising then that resting state functional connectivity has been found to be related to general intelligence, sensorimotor function, executive functioning, learning, memory, language, and emotional functioning (Vaidya & Gordon, 2013).

Cognitive tasks evoke a functional connectivity profile different from that of the intrinsically-driven resting state in a context-driven way. Functional connectivity patterns during the resting state and cognitive tasks are largely similar (Cole et al., 2014; Gratton et al., 2018; Krienen et al., 2014). However, cognitive tasks evoke small but meaningful changes in functional brain connectivity compared to intrinsic resting states, suggesting that brain network configuration is driven by an intrinsic architecture and then shaped by context (J. R. Cohen & D'Esposito, 2016; Cole et al., 2014; Gratton et al., 2018; Krienen et al., 2014; Schultz & Cole, 2016; Shine et al., 2016). For example, cognitively-demanding tasks, such as those probing working memory, language, and decision making, show increased integration, or increases in connectivity between brain networks (e.g., Braun et al., 2015; Cohen & D'Esposito, 2016; Shine et al., 2016), while more simple tasks, such as those probing sustained attention (Sadaghiani et al., 2015) and motor learning , display decreased between-network integration and increased within-network coherence (Chen & Deem, 2015). Overall, resting state and task-evoked functional connectivity both contribute to our understanding of behavior and delimiting the

similarities and differences is critical to understanding the neurobiological mechanisms underlying behavior.

II. Tasks strengthen brain-behavior relationships compared to the resting state

Several recent studies have directly tested how relationships with behavior differ between the resting state and task-evoked functional connectivity in adults. Greene and colleagues implemented connectome-based predictive models (CPM) utilizing adult data from the Human Connectome Project (HCP), as well as youth data from the Philadelphia Neurodevelopmental Cohort (PNC; aged 8-21 years) to predict IQ (A. S. Greene et al., 2018). In CPM, an iterative, leave-one-subject-out cross-validation is performed on the functional connectivity matrices to predict IQ from the left-out subject. They found that CPM during all task states was more predictive of IQ than CPM during the resting state in both children and adults (A. S. Greene et al., 2018). Jiang and colleagues replicated the work of Greene and colleagues using the HCP dataset and partial least squares regression. They similarly found that prediction of IQ, reading comprehension, cognitive flexibility ability, and working memory ability was better during tasks than during the resting state (Jiang et al., 2020). Together, this literature indicates that although task-evoked functional connectivity changes compared to the resting state are small (e.g., Cole et al., 2014; Gratton et al., 2018), they are functionally relevant manipulations that tap into task-relevant brain circuitry (A. S. Greene et al., 2018).

Greene and colleagues proposed a theoretical framework explaining the manipulation of functional connectivity by cognitive tasks. They suggested that cognitive tasks may tax the brain in a manner akin to how a cardiac stress test can tax the heart to make visible clinically-relevant features of functioning that are not observed at rest (A. S. Greene et al., 2018). For example, a

task tapping inhibitory control might tax the brain in such a way to highlight functional brain features related to impulsivity and self-control, features which may not be easily observable during the resting state and that are relevant to clinical and educational outcomes. This project will employ this theoretical framework to probe relationships between functional connectivity and behaviors relevant to life outcomes in children.

III. Developmental changes in functional connectivity

Resting state functional connectivity data collected across childhood and adolescence has been used to characterize trajectories of functional brain development. Functional connectivity shifts from local to distributed across development, such that with increased age there is a strengthening of long-range connections and a weakening of short-range connections (Grayson & Fair, 2017; Rubia, 2013; Wang et al., 2012). Additionally, while functional brain network organization is largely established prior to adolescence (Grayson & Fair, 2017; Gu et al., 2015; Marek et al., 2015), connectivity patterns continue to be refined into adulthood (Betzel et al., 2014; Grayson et al., 2014; Grayson & Fair, 2017; Gu et al., 2015; Lopez et al., 2020; Marek et al., 2015; Rubia, 2013). From childhood into adulthood, there is a general trend of decreases in within-network communication and increases in between-network communication (Betzel et al., 2014; Marek et al., 2015; Rubia, 2013; Wang et al., 2012).

The maturational trajectories of within- and between-network connectivity differ across networks (Gu et al., 2015; Lopez et al., 2020; Marek et al., 2015). For example, one study using wavelet coherence to estimate functional connectivity found decreases in both within- and between-network connectivity of brain networks involved in higher order cognitive processes (e.g., fronto-parietal, cingulo-opercular, dorsal attention; Gu et al., 2015). Other studies using

correlations to estimate functional connectivity found an increase in between-network connectivity of the cingulo-opercular network, but a decrease in between-network connectivity of the fronto-parietal network into adulthood (Marek et al., 2015; Lopez et al., 2019). These discrepant findings may be explained by the method used to estimate functional connectivity in each study. However, each study highlights how the trajectory of between-network connectivity from childhood to adulthood differs by network (Gu et al., 2015; Marek et al., 2015; Lopez et al., 2019).

Given that brain network organization changes between childhood and adulthood, it is possible that relationships between functional brain network organization and behaviors, such as executive functioning and reward processing, change as well. The above cross-sectional studies of resting state data lend an initial understanding of network maturation and relationships to behavior (Gu et al., 2015; Marek et al., 2015; Lopez et al., 2019), but fail to address how task-evoked connectivity, which directly underlies and better predicts behavior (Greene et al., 2018; Jiang et al., 2020), may change across childhood and adolescence. The following sections will briefly review relationships between functional connectivity and inhibitory control, working memory, and reward processing.

IV. Inhibitory control and functional connectivity in youth

Inhibitory control is a core component of executive function that governs the ability to withhold or suppress prepotent behaviors or thoughts (Diamond, 2013; Miyake et al., 2000; Miyake & Friedman, 2012). Basic inhibitory control is evident in early childhood and maturation of inhibitory control ability continues through adolescence, showing marked improvements in consistency (Luna et al., 2013). Inhibitory control plays a critical role in self-control, impulsivity,

and risk-taking behaviors (Casey et al., 2008; Diamond, 2013; Luna et al., 2013) and has been implicated in psychological resilience and several clinical disorders (Afek et al., 2021; Arnsten & Rubia, 2012; Diamond, 2013; Enticott et al., 2008; Gohier et al., 2009).

During tasks of inhibitory control, children engage regions of the fronto-parietal network (e.g., ventrolateral prefrontal cortex (vlPFC), dlPFC, posterior parietal cortex) and cingulo-opercular network (e.g., dACC, pre-supplementary motor area (pre-SMA)), as well as the bilateral frontal eye fields (FEF), subthalamic nucleus (STN), and striatum (Engelhardt et al., 2019; Luna et al., 2010; McKenna et al., 2017). Engagement of and communication between these regions changes with development into adulthood and is associated with improvements in inhibitory control ability (Luna et al., 2010).

During the resting state, inhibitory control ability relates to resting state functional connectivity measures of the default mode, cingulo-opercular, and visual networks. In a sample of children aged 8-13 years, stronger resting state functional connectivity between regions in the cingulo-opercular and default mode networks was related to better performance on the stop signal task (Mennes et al., 2012). Better response inhibition performance was also related to reduced functional connectivity between the pre-SMA of the cingulo-opercular network and the right dlPFC of the fronto-parietal network, as well as reduced anticorrelations (i.e., less negative functional connectivity) between the right caudate and the left intracalcarine cortex of the visual network (Mennes et al., 2012). In a sample of youth aged 10-26 years, it was found that increased cingulo-opercular/salience network integration with other large-scale brain networks was related to better response inhibition during an antisaccade task (Marek et al., 2015). Finally, anticorrelations between 'task-positive' cognitive control networks and the default mode network have been shown to contribute to response inhibition ability. Barber and colleagues (2013) found

that stronger anticorrelations between regions of the cognitive control networks (cingulo-opercular and fronto-parietal) and regions of the default mode network were related to better response inhibition performance on a go/no-go task in adults, but not in children. They thus suggested that the development of strong anticorrelations supports adult-like response inhibition (Barber et al., 2013).

Functional connectivity estimated during the execution of inhibitory control, as opposed to during the resting state, also implicates networks involved in cognitive control (fronto-parietal, cingulo-opercular), sensory and motor networks, and the striatum (Hwang et al., 2010; Mehnert et al., 2013; Rubia et al., 2007; Stevens, 2016; Stevens et al., 2007; Vink et al., 2014). Children display stronger local functional connectivity in the frontal and parietal cortices during tasks probing inhibitory control compared to adults (Hwang et al., 2010; Mehnert et al., 2013). Connections between frontal, parietal, subcortical, and cerebellar regions increase from childhood into adulthood and enable successful inhibitory control performance (Rubia et al., 2007; Stevens et al., 2007; Hwang et al., 2010; Vink et al., 2014). During an incentivized inhibitory control task, connectivity between the dorsal attention and cingulo-opercular/salience networks increases with age (Hallquist et al., 2018). Further, connectivity within the cingulo-opercular/salience network and between sensorimotor regions and the visual, control, motor, and attention networks decreases with age (Hallquist et al., 2018).

To my knowledge, only two studies have directly tested for differences in functional connectivity between the resting state and a task probing inhibitory control in children. Mitchell and colleagues found that functional connectivity during a simple go/no-go task evoked a less integrated whole brain organization compared to the resting state in a sample of children aged 8-12 years (Mitchell et al., In Prep). This whole brain segregation was driven by network-level

decreases in integration in the fronto-parietal, default mode, and sensorimotor networks. No relations were found between functional brain organization and task performance (Mitchell et al., In Prep). This is perhaps explained by the knowledge that during easy tasks, the brain doesn't need to be as efficiently configured to achieve high performance, and thus variability in brain configuration across individuals can obscure group-wide brain-behavior relationships (Kitzbichler et al., 2011). Dwyer and colleagues found that a task probing cognitive inhibition (i.e., an interference task combining the Simon and Erikson Flanker tasks) also evokes reconfiguration of cognitive control and default mode brain networks compared to the resting state in adolescents aged 12-19 years. They also found that both weaker functional connectivity within the default mode and greater functional connectivity between regions in the cognitive control and default mode networks related to better task performance (Dwyer et al., 2014). The brain metric-task performance relationships identified in these two studies differ, which may be due to differences in the tasks used as well as differences in the functional brain networks investigated.

Overall, functional connectivity of the fronto-parietal, cingulo-opercular, default mode, sensorimotor networks are implicated in inhibitory control (Marek et al., 2015; Hwang et al., 2010; Mehnert et al., 2013; Rubia et al., 2007; Stevens, 2016; Stevens et al., 2007; Vink et al., 2014; Hallquist et al., 2018). Increased integration of functional brain networks during rest is related to better inhibitory control (Marek et al., 2015), while the relationship between functional brain organization during tasks of inhibitory control and behavioral task performance is still unclear. Clarifications of the relationship between inhibitory control performance and measures of functional connectivity during rest and task would further our understanding of the neurobiological mechanisms of self-control and impulsivity.

V. Working memory and functional connectivity in youth

Working memory is a core executive function encompassing the ability to hold information in mind for a short period of time and manipulate it. The ability to hold information in mind is present in infancy, but capacity and the ability to flexibly manipulate information improve slowly into adulthood (Best & Miller, 2010; Diamond, 2013; Luna et al., 2004). Working memory is related to fluid intelligence (Salthouse & Pink, 2008), and working memory impairments are noted in many clinical disorders (e.g., Gohier et al., 2009; Kofler et al., 2008; Lee & Park, 2005).

Tasks of working memory engage a core executive function-related architecture consisting of distributed frontal and parietal regions in children (Engelhardt et al., 2019; McKenna et al., 2017), including vlPFC, dlPFC, bilateral anterior insula, dACC, SMA, bilateral superior parietal cortex, bilateral inferior parietal cortex, striatum, and cerebellum (Engelhardt et al., 2019; Luna et al., 2010; McKenna et al., 2017). Engagement of and communication between these regions, especially prefrontal regions, changes with development into adulthood and is associated with improvements in working memory ability (Luna et al., 2010).

Resting state functional connectivity between the fronto-parietal, cingulo-opercular, and default mode networks relates to working memory ability (Vaidya & Gordon, 2013). In adults, greater working memory ability is related to stronger intrinsic connectivity of regions within the default mode network (Hampson et al., 2006, 2010; Sala-Llonch et al., 2012), as well as between the cingulo-opercular network and the caudate (Gordon et al., 2015; Vaidya & Gordon, 2013). Weaker functional connectivity between some regions is important to working memory as well. Specifically, better working memory ability is related to reduced functional connectivity between the default mode and fronto-parietal networks in adults (Hampson et al., 2010; Markett et al.,

2018). However, there is little work investigating the relationship between working memory performance and resting state functional connectivity in children (Camacho et al., 2020). In children, working memory ability is related to increased functional connectivity within the fronto-parietal network (Barnes et al., 2016) and between the thalamus and the right dlPFC of the fronto-parietal network (Mills et al., 2012). Decreased functional connectivity between the thalamus and striatum is related to working memory performance as well (Mills et al., 2012).

Similar to the resting state, during working memory tasks functional connectivity of the fronto-parietal and default mode networks is related to working memory ability (Bosch et al., 2014; White et al., 2011). In youth aged 9-19 years, Bosch et al. (2014) identified a network involving regions of the left PFC, left parietal cortex, and right cerebellum that increased functional connectivity with increased working memory load. Additionally, functional connectivity of this network decreased with age (Bosch et al., 2014). In youth aged 8-19 years, White et al. (2011) found that functional connectivity between the medial frontal lobe, ACC, occipital lobe, and cerebellum increased with increasing working memory load. While few studies have investigated functional connectivity during working memory tasks, preliminary evidence suggests that working memory relates to network-level modulations of distributed brain regions involved in the fronto-parietal, cingulo-opercular, default mode, and visual networks.

A handful of studies have directly tested for differences in functional brain networks between the resting state and tasks of working memory in adults (e.g., Cohen & D'Esposito, 2016; Shine et al., 2016) and children (Le et al., 2020). In both adults and children, working memory tasks evoke a more integrated whole brain network organization compared to the resting state (Cohen & D'Esposito, 2016; Le et al., 2020; Shine et al., 2016). In adults, integration of the fronto-parietal, dorsal attention, cingulo-opercular and visual networks drive the increases in

whole brain integration observed during tasks probing working memory relative to the resting state (Shine et al., 2016). During working memory tasks, better task performance is related to greater integration and less segregation of the whole brain (Cohen & D'Esposito, 2016), as well as integration of fronto-parietal, striatal, and thalamic regions (Shine et al., 2016). Together, these two studies converge on the idea that a globally integrated brain state is critical for working memory performance (Cohen & D'Esposito, 2016; Shine et al., 2016), a notion supported by a number of additional studies (for a review, see (Shine & Poldrack, 2018). Similar results have been found in children. During a working memory task, children's whole brain networks reconfigured to a more integrated state (Le et al., 2020). However, diverging from the adult literature, Le et al. (2020) found that greater integration during the working memory task related to worse working memory performance.

Overall, working memory ability is related to functional connectivity of the fronto-parietal, cingulo-opercular, default mode, dorsal attention, and visual networks both at rest (Hampson et al., 2006, 2010; Sala-Llonch et al., 2012; Gordon et al., 2015; Vaidya & Gordon, 2013; Markett et al., 2018; Barnes et al., 2016; Mills et al., 2012) and during tasks probing working memory (Bosch et al., 2014; White et al., 2011; Cohen & D'Esposito, 2016; Shine et al., 2016; Le et al., 2020). The literature reviewed above also emphasizes the importance of an integrated whole brain architecture for working memory ability (Cohen & D'Esposito, 2016; Le et al., 2020; Shine et al., 2016). Critically, to my knowledge only three published studies have investigated functional connectivity during tasks probing working memory in children (Barnes et al., 2016; Le et al., 2020; Mills et al., 2012), and none of these studies have probed organization of specific networks, despite evidence for the involvement of brain networks in working memory in adults (e.g., Braun et al., 2015; Cohen & D'Esposito, 2016; Shine et al., 2016). Thus, the

relationship between functional brain organization during tasks of working memory and behavioral task performance is still unclear. Clarifications of the relationship between working memory performance and measures of functional connectivity during rest and task would further our understanding of the neurobiological mechanisms of higher level cognitive functions as well as contribute to our understanding of cognitive impairments across clinical disorders (Diamond, 2013). Further, this information provides foundational knowledge critical to further studies tracking the brain basis of working memory longitudinally across development.

VI. Reward processing and functional connectivity in youth

Rewards are important motivators of behavior. External rewards modulate the neural architecture underlying cognitive control and improve cognitive control ability (for a review, see (Botvinick & Braver, 2015). Rewards are especially salient during development (e.g., Geier & Luna, 2009; Jazbec et al., 2006; Luna et al., 2015, 2015); they improve cognitive control performance to a greater extent in children and adolescents compared to adults (Casey, 2015). Neurobiological models of development suggest that reward saliency arises as a function of early maturation of limbic reward processing regions, which peak in sensitivity in adolescence, and protracted linear maturation of prefrontal cortex regions involved in top-down cognitive control (Casey, 2015; Casey et al., 2008; Ernst, 2014; Galvan, 2010; Galvan et al., 2006; Geier & Luna, 2009; Luna et al., 2015; Somerville & Casey, 2010). These models suggest that the combination of heightened neural sensitivity to rewards and immature cognitive control circuitry results in risk-taking behaviors. These models have been extended to explain trajectories of atypical neurodevelopment, specifically disruptive behavioral disorders, as manifesting from reward-control circuitry imbalances more exaggerated than those seen in typically developing

populations (Bjork & Pardini, 2015). Indeed, altered reward processing and reward circuitry in the brain are linked to substance use disorders (Crane et al., 2017; Heitzeg et al., 2015; Jollans et al., 2016; Weissman et al., 2015; Zhu et al., 2017), as well as many clinical disorders (Black et al., 2014; Chau et al., 2004; Clark et al., 2019; García-García et al., 2013; Ma, van Duijvenvoorde, et al., 2016; Pan et al., 2017; Quevedo et al., 2017; Sutcubasi et al., 2020). Altogether, rewards are critical motivators of behavior across the lifespan, but especially in late childhood and adolescence.

The neural circuitry supporting reward processing has been robustly characterized. Brain regions implicated in reward processing include the ventral striatum, amygdala, orbitofrontal cortex (OFC), ventromedial prefrontal cortex (vmPFC), ACC, and insula (Camara et al., 2009; Geier & Luna, 2009). The neural architecture supporting reward processing is mostly established in childhood (Geier et al., 2010; Padmanabhan et al., 2011), but engagement of reward processing regions, as well as regions in the frontal and parietal cortices, changes from childhood into adulthood (Geier et al., 2010; Padmanabhan et al., 2011; Teslovich et al., 2014). For example, Padmanabhan et al. (2011) tested children, adolescents, and adults on an incentivized antisaccade task. They found that during rewarded trials adolescents showed increased striatal activation, while adults showed increased OFC activation, and children relied on prefrontal regions more than the adolescents and adult groups.

During the resting state, reward processing is related to intrinsic functional connectivity between reward-related limbic regions and regions of the cingulo-opercular/salience and default mode networks in adults and children. Functional connectivity between limbic regions and the cingulo-opercular/salience and default mode networks is stronger in childhood (Tooley et al., 2022). The ventral striatum, a key region implicated in reward processing, exhibits decreasing

functional connectivity with regions of the cingulo-opercular/salience networks (Porter et al., 2015) and with the amygdala, inferior temporal gyrus, and regions of the cerebellum from childhood into adulthood (Padmanabhan et al., 2013). In childhood, the network of reward-related regions includes the OFC and subcortical limbic regions observed in adults, as well as additional regions of the medial and lateral PFC (Tooley et al., 2022). Additionally, regions considered part of the default mode network in adulthood are more integrated with the limbic reward-related regions in childhood (Tooley et al., 2022). Functional connectivity of reward-related brain regions is related to behavior: In adulthood the propensity to seek out rewarding events is related to greater resting state functional connectivity between brain regions involved in reward processing: the caudate, putamen, and bilateral OFC (Angelides et al., 2017).

In adults, the receipt of external rewards has been shown to evoke integration across the whole brain (Shine et al., 2016), as well as between striatal and frontal regions (Bahlmann et al., 2015; Boehler et al., 2014; Cubillo et al., 2019; Dixon & Christoff, 2012; Teslovich et al., 2014). In children and adolescents, striatal-frontal connectivity increases during reward processing (Cao et al., 2019; Cho et al., 2013) and probabilistic learning (van den Bos et al., 2012). Connectivity between the vmPFC, of the reward and default mode networks, and the dlPFC, a key region of the fronto-parietal network, strengthens with age during childhood and is related to improved delay discounting (Steinbeis et al., 2016). Additionally, in adolescence, functional integration of motor regions with reward and salience regions increases during reward processing (Cao et al., 2019) and is related to better task performance (Ma, van Holstein, et al., 2016).

In children, tasks tapping reward processing evoke differences in functional network organization compared to the resting state (Le et al., 2020; Mitchell et al., In Prep), but there are discrepancies in the direction of reconfiguration. Le and colleagues (2020) found that integration

increased during a two choice rewarded decision-making task, wherein acquiring money was the primary goal, compared to the resting state. Conversely, Mitchell and colleagues (In Prep) found that the addition of rewards to a go/no-go task evoked decreased integration of the whole brain, driven by decreased integration in the fronto-parietal, cingulo-opercular, salience, default mode, reward, somatomotor, and visual networks compared to the resting state. The discrepancy may highlight the importance of specific task demands for network reconfiguration. For example, perhaps when response inhibition is a primary task goal (rewarded go/no-go task; Mitchell et al., In Prep), rewards may invoke a stronger task-relevant decrease in functional integration, but when acquiring money is the primary task goal (two-choice rewarded decision task; Le et al., 2020), rewards may invoke an increase in functional integration. However, there are other differences in these tasks and it is still unclear how rewards influence brain network organization in children.

In summary, reward processing in children is related to functional connectivity of reward-related circuitry and regions in the fronto-parietal, cingulo-opercular, and default mode networks (Cao et al., 2019; Cho et al., 2013; Ma, van Holstein, et al., 2016; Mitchell et al., In Prep). Reward processing is implicated in the development of risk taking behaviors and clinical disorders (Casey et al., 2008; Chau et al., 2004; Bjork & Pardini, 2015), so it is critical to understand how individual differences in functional brain networks relate to reward processing. Additionally, given that reward circuitry undergoes dramatic changes during adolescence (Casey et al., 2008), studying brain-behavior relationships during late childhood prior to these within- and between-individual shifts can provide a strong foundation from which longitudinal work can progress.

VII. Current project

In adults, there is mounting evidence that task-evoked functional brain connectivity better predicts behavior than functional connectivity during the resting state (A. S. Greene et al., 2018, 2020; Jiang et al., 2020). However, in children, much of the literature linking functional connectivity to cognitive abilities, specifically inhibition, working memory, and reward processing, uses resting state data. Without also interrogating task-evoked functional connectivity, we are missing information about how these cognitive processes emerge from brain network function (Stevens, 2016). Further, given that individual differences in inhibition, working memory, and reward processing relate to differences in life outcomes (e.g., Casey et al., 2008; Demetriou et al., 2018; Ernst, 2014; Follmer, 2018; Kamkar & Morton, 2017; Keren et al., 2018; Luijten et al., 2017; Nuño et al., 2021; Nusslock & Alloy, 2017; Ribner et al., 2017; Silverstein et al., 2020; van Duijvenvoorde et al., 2016; Yanes et al., 2018; Zald & Treadway, 2017), characterizing brain-behavior relationships provides foundational insight to understand educational and clinical outcomes. Ultimately, this line of work will inform efforts toward early detection and intervention of learning and clinical disorders (Insel et al., 2010). To fill this gap, this study leveraged the Adolescent Brain and Cognitive Development (ABCD) study dataset and investigated differences in brain-behavior relationships between the resting state and tasks probing response inhibition, working memory, and reward processing in children aged 9-10 years.

Aim 1: Characterize group-level differences in functional brain networks between the resting state and tasks probing response inhibition, working memory, and reward processing. Brain graphs were constructed for each subject and each state (rest, stop signal task (SST), emotional n-back task (EN-back), monetary incentive delay task (MID)). From each brain

graph, we calculated graph metrics to characterize segregation and integration of the whole brain, as well as for key networks implicated in cognitive control (i.e., fronto-parietal, cingulo-opercular), attention (i.e., dorsal and ventral attention), adaptive functioning (i.e., salience), and task execution (i.e., dorsal somatomotor, visual), as well as the default mode network. Mixed effects models were then estimated to test for differences in segregation and integration between states. *Hypotheses*: We expected that whole brain integration would be greater in the EN-back and MID tasks compared to rest, while integration during the SST would be lower than during rest. Further, during the SST, we hypothesized that network integration would decrease in the fronto-parietal, default mode, and dorsal somatomotor networks compared to rest. During the EN-back task, we hypothesized that network integration would increase in the fronto-parietal, cingulo-opercular, dorsal attention, default mode, and visual networks. During the MID task, we hypothesized that network integration would increase in the cingulo-opercular, salience and default mode networks.

Aim 2: Characterize and compare resting state and task-evoked brain network relationships with task performance. The second aim of this project consisted of two parts. The first was to assess whether resting state and task-evoked functional connectivity exhibited relationships to task performance in children. Thus, we estimated relationships between brain metrics and task performance separately for the resting state and each task-evoked state. For each state, mixed effects models were estimated wherein functional connectivity was predicted by task performance. Second, we tested if there were significantly different relationships between task performance and task-evoked brain metrics compared to the resting state brain metrics. For each task, mixed effects models were estimated wherein functional connectivity was predicted by an interaction between brain state (rest vs. task) and task performance to test for brain state-

driven modulations of relationships between functional connectivity and behavior. *Hypotheses*: First, we expected that we would find that both resting state and task-evoked brain metrics would exhibit significant relationships to behavior. Second, we expected that task-evoked brain metrics would exhibit stronger relationships to task performance compared to resting state brain metrics. Further, the task-evoked brain metrics exhibiting stronger relationships with task performance compared to the resting state would be brain metrics identified in Aim 1 as significantly different between the resting state and the task-evoked states. For example, if modularity was decreased during the SST compared to the resting state, I predicted that modularity during the SST would exhibit a significantly stronger relationship to task performance than modularity during the resting state.

Together, this project characterizes changes in brain network organization between the resting state and task-evoked states and then directly tests the importance of brain state in investigations of brain-behavior relationships. Given that functional brain networks mature throughout childhood and adolescence and it is not yet fully known how functional brain networks support cognition (e.g., response inhibition, working memory, reward processing) in childhood, this project will contribute information critical to effectively understand brain network mechanisms supporting cognitive functions in children. Further, this project tests the utility of task-evoked functional connectivity to highlight neurobiological features relevant to behavior in childhood.

Methods

Participants

Data from the Adolescent Brain and Cognitive Development (ABCD) study was used for this project. The ABCD study baseline collection includes neuroimaging, demographic, and

behavioral data from a demographically diverse sample of 11,875 children aged 9-10 years old. This data collection was conducted across 21 sites in the United States and is made available through the National Data Archive (NDA) at the National Institutes of Health (NIH). The ABCD Reproducible Matched Samples (ARMS), a program which divides the full behavioral sample into discovery and replication datasets matched on demographic variables (i.e., site location, age, sex, ethnicity, grade, parent education, handedness, family income, exposure to anesthesia), was used to select matching discovery and replication datasets for this analysis (https://osf.io/7xn4f/; Feczko et al., 2020). For this project, only subjects with usable MRI and behavioral data across all tasks were included. Thus, the discovery sample consisted of 498 children and the replication sample consisted of 513 children.

Study measures

The ABCD neuroimaging protocol includes a resting state scan and three cognitive tasks. The full ABCD study neuroimaging protocol, including descriptions of the fMRI tasks, is described in Casey et al. (2018). Relevant information for the current analyses is included here. All neuroimaging data, as well as task performance and demographic measures were downloaded from the NDA 3.0 Release.

Resting state: Up to four runs of resting state scans (5 minutes each) were collected from each subject. During the resting state scans, subjects passively viewed a cross hair. Between 12 and 20 minutes of resting state data was collected for each subject.

Stop signal task (SST): The SST paradigm employed in the ABCD study (**Figure 1**) was modeled after (Logan, 1994). In the SST, subjects were tasked to withhold, or stop, the execution of a motor response with the presentation of a rare, unpredictable signal to stop. The SST is well

characterized in developmental populations and robustly engages neural circuitry underlying response inhibition, including the dorsal striatum, ACC, and vlPFC (Casey et al., 2018). 'Go' signals were horizontal arrows pointing left or right, while 'stop' signals were vertical arrows pointing up (16.67% of all trials). The greater frequency of go in comparison to stop signals creates a prepotent motor response. Stop signals appeared at a variable duration of time after the onset of the go signal, causing subjects to engage inhibitory control brain mechanisms to stop the ongoing motor response. The task included a staircase procedure that adjusts the stop signal onset time so that over the course of the task run there are approximately 50% successful and 50% unsuccessful inhibition (stop) trials. Each trial lasted 1000ms. Go trials began with a go signal (left or right arrow), which was terminated by subject response (button press) and followed by a fixation cross presented until the end of the trial. Stop trials began with a go signal presented for a variable duration determined by the staircase mechanism, denoted the Stop Signal Delay (SSD), and followed by the stop signal (vertical arrow) presented for 300ms and a fixation cross presented until the end of the trial. The initial SSD was 50ms and subsequent SSDs were determined by the staircase procedure, such that the SSD was increased by 50ms following successful inhibitions and decreased by 50ms following failed inhibitions. Inter-trial intervals are jittered between 700-2000ms. Participants completed two runs of the SST, with each run containing 180 trials and lasting a duration of 5 minutes and 49 seconds. Each run contained 150 go trials and 30 stop trials. The stair stepping mechanism was expected to have 15 failed inhibitions and 15 successful inhibitions. For the SST, we indexed performance with the mean stop signal reaction time (SSRT) across both runs. The SSRT was equal to the mean reaction time on correct go trials minus the mean SSD (Rosenberg et al., 2020).

Recently, Bissett and colleagues raised concerns about the utility of the stop signal task in measuring response inhibition (Bissett et al., 2021). They claimed that the SST used in the ABCD Study violates the assumption of contextual independence in the independent race model and identified several coding errors. These claims were addressed by Garavan and colleagues (Preprint), who affirmed that some of the issues presented were not issues but rather intentional design features and others were due to incorrect data analysis and incorrect exclusion criteria used by Bissett and colleagues (Garavan et al., Preprint). Garavan and colleagues assert that the independent race model is robust to violations of the independence assumption, but they implemented code corrections and released a set of exclusion criteria in the ABCD Release 3.0. The exclusionary criteria identify subjects (a) who experienced coding errors during the task and (b) who exhibited longer failed stop response times compared to go response times. They also state that the neuroimaging data which passes the exclusionary criteria is unaffected and can be used (Garavan et al., Preprint). For this project, we excluded all subjects and runs that did not pass the exclusionary criteria set forth by Garavan and colleagues.

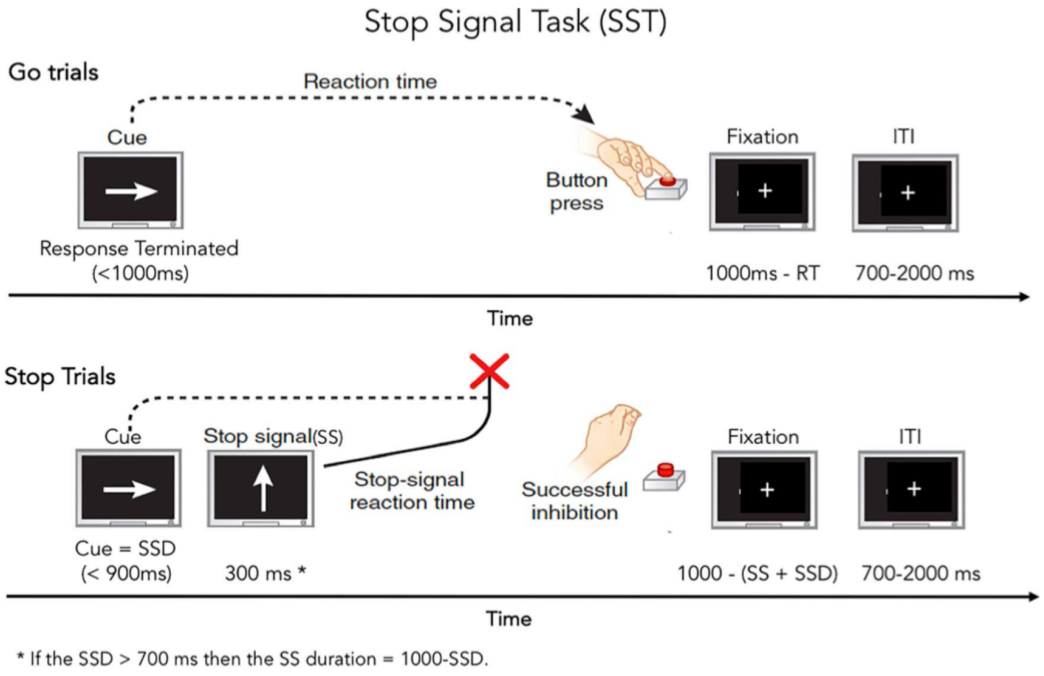

Figure 1. Stop Signal Task (SST). Figure from Casey et al. (2018).

Monetary Incentive Delay (MID) task: The MID task employed in the ABCD study (**Figure 2**) was modeled after Knutson et al. (2000) and Yau et al. (2012) and robustly engages the neural circuitry of reward processing, including the ventral striatum, OFC, mPFC, and vmPFC (Casey et al., 2018). Each MID trial included cue, anticipation, target, and feedback phases. The cue phase indicated which trial type will follow (Win $0.20, Win $5, Lose $0.20, Lose $5, $0) and lasted a duration of 2000ms. The cue was followed by a variable length anticipation phase, where the participant viewed a fixation cross for 1500-4000ms. In the target phase, a target appeared for 150-500ms and the participant pressed a button to either win or avoid losing money. The feedback phase informed the participant if they had won money, lost money, or neither and lasted for 1500-1850ms such that the total duration of the target and feedback phases was 2000ms. Target duration was adjusted such that each participant achieved a

60% success rate across the course of the task. After every third win or loss trial, task difficulty was either increased by lengthening the target duration or decreased by shortening the target duration. Participants were paid based on their performance, such that participants earned an average of $21. Participants completed one run of the MID task containing 50 trials (10 trials of each type presented pseudorandomly). The run lasted 5 minutes and 42 seconds in duration. For the MID task, we indexed performance as the mean of the monetary value won across both runs.

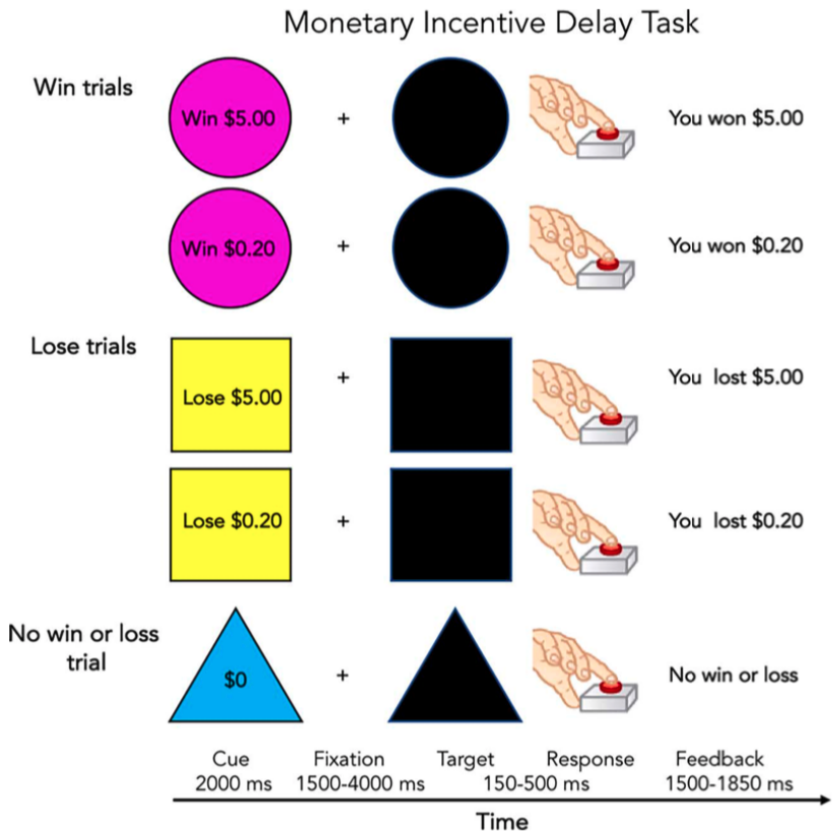

Figure 2. Monetary Incentive Delay task (MID). Figure from Casey, et al. (2018).

Emotional N-back (EN-back) task: The EN-back task employed in the ABCD study (**Figure 3**) was modeled after the HCP n-back task (Barch et al., 2013) and adapted to engage

emotion regulation processes (Cohen et al., 2016). The EN-back task robustly engages neural circuitry involved in working memory (including the dlPFC, parietal, premotor cortex, and hippocampus) and emotion regulation (dlPFC, vlPFC, vmPFC, amygdala, ventral striatum) (Casey et al., 2018). Emotional stimuli included pictures of faces with happy, fearful, and neutral expressions (Conley et al., 2018; Tottenham et al., 2009). Non-emotional stimuli included pictures of places (Kanwisher, 2001; O'Craven & Kanwisher, 2000; Park & Chun, 2009). One stimulus was presented at a time and subjects were asked to press a button to indicate whether the picture is a match or not. The task was presented in blocks, with one stimulus type per block. A cue at the beginning of each block indicated whether the task was 0-back or a 2-back. During 0-back blocks, subjects pressed to indicate if the stimulus matched the target stimulus presented at the beginning of the block. During 2-back blocks, subjects pressed to indicate if the stimulus matched the stimulus presented two trials prior. Participants completed two runs of the EN-back task, each containing four 2-back blocks (one for each stimulus type: places, neutral faces, fearful faces, and happy faces) and four 0-back blocks (one for each stimulus type). Each block began with a 2500ms cue specifying if the task was 2-back or 0-back for that block. Each block included 10 trials (2500ms each) with a stimulus (2000ms) followed by a fixation (500ms). Each block was followed by 500ms of colored fixation to denote the end of the block and the switch to a new block. There were a total of 160 trials across both runs of the EN-back task, with 40 trials of each of the four stimulus types. For this analysis, only 2-back blocks of all stimulus types were used to capture brain networks during working memory. In this project, the EN-back task was used in analyses to assess working memory. The inclusion of emotional stimuli in this analysis should not hinder the elucidation of brain-behavior relationships of working memory given that the EN-back task robustly engages core brain networks implicated in working memory

for all conditions (Casey et al., 2018). For the EN-back task, we indexed performance with average percent accuracy on the 2-back blocks across both runs.

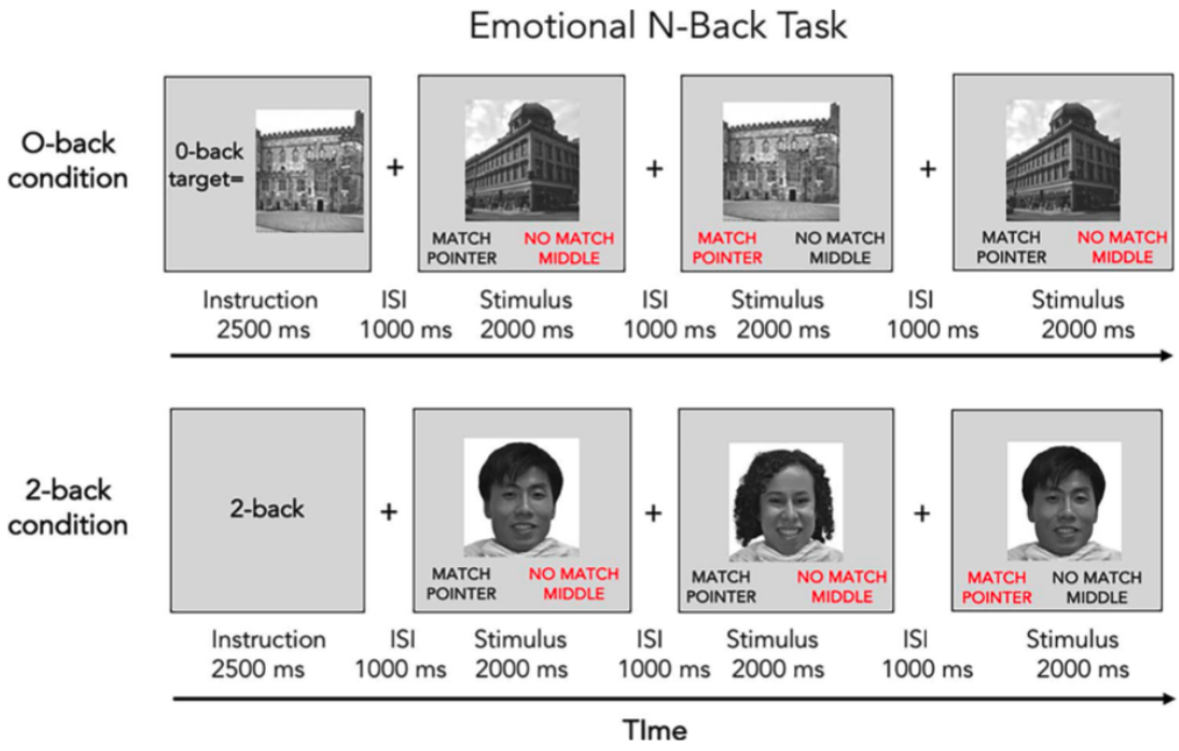

Figure 3. Emotional N-back task (EN-back). Figure from Casey, et al. (2018).

Demographic Information: Demographic measures captured included: age, sex, race, ethnicity, parental education, family income, and parental marital status. Family income was collected in categorical bins of varying sizes (e.g., "$5,000 through $11,999", "$75,000 through $99,999"), so we converted the bins into numeric quantities by taking the highest value of the lowest bin (i.e., "Less than $5,000": $5,000), the lowest value from the highest bin (i.e., "$200,000 and greater": $200,000), and the average value from every other bin (e.g., "$75,000 through $99,999": $87,499.50). Parental education was captured categorically (e.g., "GED or equivalent"), so we converted each category into a numeric value representing years of education

(e.g., “GED or equivalent”: 12 years). A socioeconomic status composite score was calculated from family income and parental education in years via a principal components analysis with the *FactoMineR* package in R (Lê et al., 2008). Missing data was imputed with the *missMDA* package in R (Josse & Husson, 2016).

Image acquisition

Neuroimaging data available in the ABCD-BIDS Collection 3165 from the NIMH Data Archive (NDA) was utilized for this project (https://collection3165.readthedocs.io/en/stable/). Neuroimaging data were collected on three 3T scanner platforms (Siemens Prisma, n=7101; General Electric 750, n=2974; and Philips, n=1516) with multi-channel head coils at 21 sites in the United States. Participants completed 3D T1-weighted images, 3D T2-weighted images, diffusion weighted images, up to four runs of resting state fMRI, and then the three fMRI tasks. The fMRI task order was counterbalanced across participants. A high-resolution anatomical T1-weighted scan (1mm isotropic) was collected. Whole brain functional data were collected with a T2-weighted multiband EPI sequence with a slice acceleration factor of 6 (60 slices, 90x90 matrix, TR = 800 ms, TE = 30 ms, field of view 216 x 216mm, voxel dimensions: 2.4 mm x 2.4 mm x 2.4 mm). Acquisition parameters were harmonized across the three scanner platforms (full details are described in Casey et al., 2018), see **Table 1** for details.

Image processing

Image processing steps were implemented within the ABCD-BIDS pipeline (https://github.com/ABCD-STUDY/abcd-hcp-pipeline; Fair et al., 2020; Glasser et al., 2013). Source data was first converted into the standardized Brain Imaging Data Structure (BIDS)

format and then processed. Structural MRI (T1w and T2w) preprocessing steps include corrections for gradient non-linearity distortions specific to each scanner, rigid body alignment, co-registration of the T2w scan to the T1w scan, correction for spatial intensity variation, bias field correction, and a rigid registration and resampling into alignment with the in-house reference brain in standard space. Cortical and subcortical segmentation, as well as surface reconstruction, were implemented with FreeSurfer.

Functional MRI preprocessing steps included registration to the first frame to correct for head motion, distortion correction with spin echo field maps, gradient nonlinearity correction, and rigid body alignment of all scans for each subject. Sixteen initial frames were discarded from each scan run; details on specifics for each scanner manufacturer are in (Hagler et al., 2019). Data were mapped into CIFTI grayordinates space ("surface space") and then underwent additional processing through DCANBOLDProcessing. Additional preprocessing steps included time series normalization, nuisance regression, temporal filtering, and motion scrubbing. Nuisance regression includes six motion parameters, mean time series and first derivatives for white matter, cerebrospinal fluid, and global signal, as well as derivatives and squares for each, and regression of the mean greyordinate time series. Temporal notch filtering between 0.31-0.43Hz was employed to attenuate respiration artifacts (Fair et al., 2020). Additionally, band-pass filtering was applied between 0.009 and 0.08 Hz using a 2nd order Butterworth filter (Hallquist et al., 2013). Motion scrubbing was included to remove timepoints with framewise displacement (FD) greater than 0.2mm from the time series (Power et al., 2012). Each functional run was demeaned and detrended and then concatenated across runs within each state (i.e., rest, SST, EN-back, MID). For the EN-back task, only the 2-back condition blocks were retained in

the time series. For the resting state, SST, and MID task all time points were included in the time series.

Functional connectivity brain graph construction

The concatenated time series data was then parcellated with regard to the Gordon cortical parcellation (**Figure 4**; Gordon et al., 2016). This parcellation includes 14 functional networks, all of which will be included in the whole brain analyses. Parcellated time series for each subject and each state were downloaded from the ABCD-BIDS Collection 3165 available on the NIMH Data Archive (NDA) in Amazon Web Services (AWS) Simple Storage Service (S3) via a GitHub tool (https://github.com/ABCD-STUDY/nda-abcd-s3-downloader).

Functional connectivity (FC) between each pair of ROIs was estimated using Pearson's correlation coefficient (**Figure 4**). This resulted in a 333 x 333 correlation matrix for each participant and for each state (i.e., rest, SST, EN-back, MID). Correlation matrices were Fisher z-transformed prior to the construction of brain graphs. The Fisher z-transformed correlation matrices were thresholded to reduce noise due to spurious low magnitude correlations. Edge weights were retained after thresholding. Given that there is no universal benchmark for threshold specification, we tested across a range of FC thresholds, from z-transformed r-values of 0.2-0.45 in increments of 0.05. These FC thresholds approximate common brain graph densities reported consistently in the literature (2-25%) and corresponding to small world architecture (Bullmore & Bassett, 2011; Seitzman et al., 2020). We then calculated the proportion of disconnected nodes in each brain graph averaged across each task at each threshold. An elbow point was estimated from the distribution of these disconnected nodes using the *akmedoids* package in R (Adepeju et al., 2020). This determined the maximum curvature of

the distribution as the point in which the costs of including the additional thresholds (i.e., disconnected nodes) outweigh the benefits (i.e., power) to be between the 0.35 and 0.40 z-transformed r-value thresholds. FC thresholds included in the analyses included all thresholds below the elbow point (i.e., 0.20, 0.25, 0.30, 0.35).

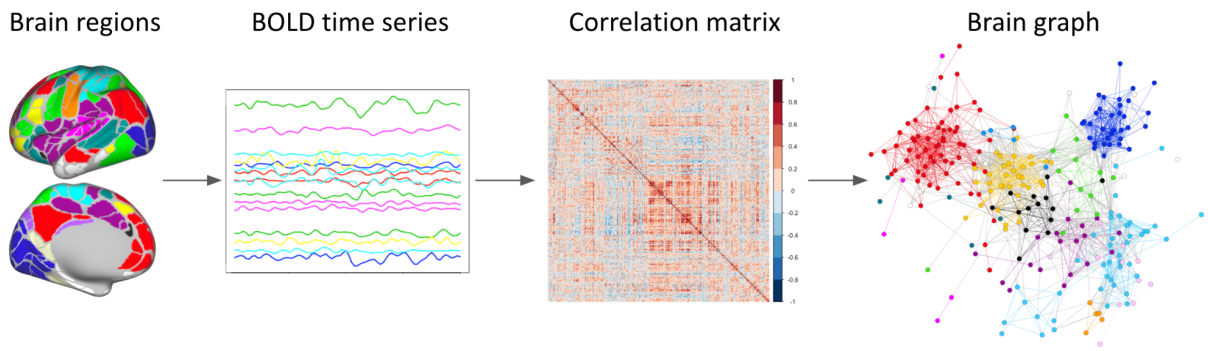

Figure 4. From brain regions to brain graphs. 333 brain regions form distinct networks, depicted with colors. A BOLD time series is extracted from each region and then correlated with the BOLD time series of all other regions. From this correlation matrix a brain graph is constructed, consisting of nodes representing brain regions and edges representing the strength of correlation between BOLD time series of those regions.

Weighted, undirected brain graphs were calculated from the Fisher transformed, thresholded connectivity matrices using the *igraph* package in R (Csardi & Nepusz, 2006). Network assignments were pre-assigned from the Gordon parcellation (Gordon et al., 2016). Graph metrics were calculated at each threshold and averaged across thresholds prior to analysis.

Graph metrics

Weighted metrics quantifying network segregation and integration were calculated from the brain graph for each subject and each state (**Figure 5**). Whole brain metrics of modularity

and global efficiency were calculated to quantify network segregation and network integration, respectively. Modularity is a measure of the degree to which the brain segregates into distinct subnetworks, or communities, with many connections within these subnetworks and fewer connections between subnetworks (Bullmore & Bassett, 2011). A weighted variant of modularity was calculated using the pre-assigned network memberships from the Gordon parcellation (Gordon et al., 2016) with the *igraph* package in R (Csardi & Nepusz, 2006). Greater values of modularity indicate that the whole brain system more readily decomposes into subnetworks. Global efficiency is a measure of information transfer across the whole brain system without regard for network membership. A weighted variant of global efficiency was calculated as the average of the shortest weighted path length defined on the inverse brain graph (Latora & Marchiori, 2001) and implemented with the *brainGraph* package in R (Watson, 2020).

Node dissociation index, which indexes between-network connectivity, was calculated for each node as the sum of weighted connections to nodes in every other network divided by the total weighted connections (Cary et al., 2016). Node dissociation index was then averaged across nodes in each of eight networks of interest (fronto-parietal, cingulo-opercular, default mode, salience, dorsal attention, ventral attention, dorsal somatomotor, and visual networks), which resulted in one value per network. When averaged across nodes in each network, node dissociation index quantifies the strength of connectivity of a network to other networks, and will therefore be referred to as 'network dissociation index' henceforth. Finally, mean functional connectivity (FC) of the whole brain was calculated as the average of all edge values in the matrix remaining after thresholding.

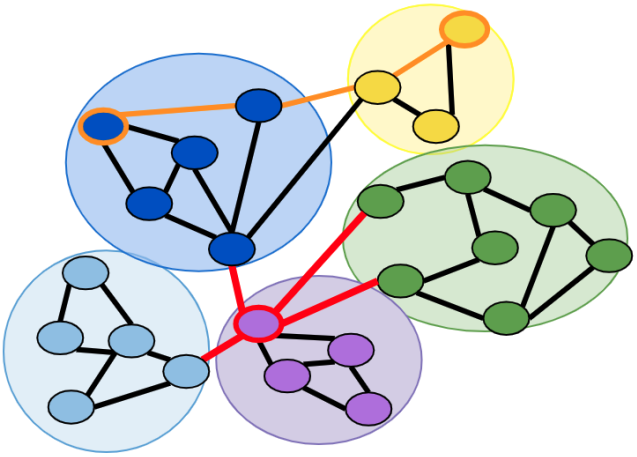

Figure 5. Graph metrics on a toy brain graph. Modularity is the degree to which the graph segregates into discrete networks. Network membership is shown by the color of each node (brain region). Global efficiency is the inverse of the average shortest path length between all nodes. For example, the shortest path length between the nodes highlighted in orange is the sum of each edge weight in the shortest path between them (shown in orange). Node dissociation index for the purple node highlighted in red is the sum of between-network edges (shown in red) divided by the total edges connected to that node.

Analyses

Aim 1. Test for differences in functional brain network organization between the resting state and task-evoked states

First, we characterized differences in functional brain networks between the resting state and tasks tapping response inhibition, working memory, and reward processing. Ten mixed effects models were estimated to test for differences in segregation (modularity) and integration (global efficiency, network dissociation index) between the resting state and each task-evoked state. Age, sex, race, ethnicity, parental marital status, SES composite score, and scanner manufacturer were included in each model as fixed effects, and a random intercept of subject

was used to control for inter-subject variation, per recommendation by the ABCD Data Analysis and Informatics Core (DAIC). Mean FC was also included as a fixed effect covariate, given the impact of differences in mean FC on network inferences (Hallquist & Hillary, 2019). Mixed effects models were implemented with the *lme4* package in R (Bates et al., 2015). Initially the models were tested with nested random intercepts of site and subject, but the site level random effect was removed due to convergence issues.

In total, 10 mixed effects models (one for each brain metric: modularity, global efficiency, and network dissociation index for eight networks) were estimated. Omnibus effects (F-statistics) were investigated first, to identify models with significant differences in brain metrics between brain states (rest, SST, EN-back, MID). Omnibus test *p*-values were corrected for multiple comparisons with the Benjamini-Hochberg false discovery rate (FDR) $p < .05$ correction (Benjamini & Hochberg, 1995) for each of the ten models.

Models with significant omnibus tests were further investigated to identify which states (rest vs. SST, rest vs. EN-back, rest vs. MID, SST vs. MID, SST vs. EN-back, MID vs. EN-back) were significantly different. Resulting *p*-values were corrected for multiple comparisons with the Benjamini-Hochberg false discovery rate (FDR) $p < .05$ correction (Benjamini & Hochberg, 1995) for each brain metric (modularity, global efficiency, network dissociation index). This resulted in 10 corrections with six *p*-values each. Given that the brain metrics likely exhibit some dependence, correlations between brain metrics for each state were calculated and *p*-values were also corrected with the Benjamini-Yekutieli procedure (Benjamini & Yekutieli, 2001); see **Appendices**. All analyses were run separately and identically for both the discovery and replication samples.

Aim 2a. Test for relationships between brain network organization and task performance

Next, we assessed how brain metrics related to task performance. For each task-evoked state, we tested if brain metrics during that state were related to task performance during that state (e.g., how brain metrics during the SST related to SSRT). For the resting state, we tested if brain metrics were related to task performance in each of the task-evoked states (e.g., how brain metrics during the resting state were related to SSRT, 2-back percent accuracy, monetary value won). Sixty linear regressions were estimated wherein task performance was predicted by brain metrics for each brain state separately. Mean FC, age, sex, race, ethnicity, parental marital status, scanner manufacturer, and the SES composite score were included in each model as fixed effects.

Resulting *p*-values were corrected for multiple comparisons with the Benjamini-Hochberg false discovery rate (FDR) $p < .05$ correction (Benjamini & Hochberg, 1995) within each task performance measure (i.e., SSRT, 2-back percent accuracy, monetary value won) separately for the resting state and each task. This resulted in six corrections with 10 *p*-values each. The *p*-values were also corrected with the Benjamini-Yekutieli procedure (Benjamini & Yekutieli, 2001); see **Appendices**. All analyses were run separately and identically for both the discovery and replication samples.

Aim 2b. Test for modulation of brain-behavior relationships by brain state

Lastly, we characterized brain state-driven modulations of functional connectivity brain-behavior relationships. Thirty mixed effects models wherein brain network organization (modularity, global efficiency, network dissociation index for each of the 8 networks of interest) was predicted by an interaction between brain state and task performance were estimated to test

for brain state-driven modulations of relationships between network organization and task performance. For each task performance metric, only rest and the task from which performance was captured were included (e.g., for SSRT models only the resting state and SST were included) such that the interaction term would denote a significant difference in the brain-behavior relationship between the resting state and the task state of interest. Mean FC, age, sex, race, ethnicity, parental marital status, SES composite score, and scanner manufacturer were included in each model as fixed effects, and a random intercept of subject was used to control for inter-subject variation. Similar to Aim 1, the models were initially tested with nested random intercepts of site and subject, but the site level random effect was removed due to convergence issues.

Each model was investigated to identify significant interaction effects between the resting state and the task state. *P*-values were corrected for multiple comparisons with the Benjamini-Hochberg false discovery rate (FDR) $p < .05$ correction (Benjamini & Hochberg, 1995) for each task performance measure (i.e., SSRT, 2-back percent accuracy, monetary value won) and each brain metric (i.e., modularity, global efficiency, network dissociation index of each of the eight networks of interest). As such, three *p*-value corrections were calculated (i.e., one for each task performance measure), with 10 *p*-values each (i.e., whole brain and network-level metrics). The *p*-values were also corrected with the Benjamini-Yekutieli procedure (Benjamini & Yekutieli, 2001); see **Appendices** All analyses were run separately and identically for both the discovery and replication samples.

Results

Aim 1 Results: Differences in brain network organization between the resting state and task-evoked states

To quantify differences in whole brain organization between the resting state and task-evoked states, modularity and global efficiency were estimated. All omnibus tests were found to be significant, indicating differences in whole brain organization between the states (modularity: F(3, 1608.46) = 818.49, raw p = 4.45e-323, adjusted-p = 4.45e-322; global efficiency: F(3, 1577.38) = 584.70, raw p = 1.87E-255, adjusted-p = 9.37E-255). Compared to the resting state, we observed significantly decreased modularity during all tasks (SST: β = -0.73, adjusted-p = 5.73e-189; MID: β = -0.63 , adjusted-p = 5.05e-160; EN-back: β = -1.65, adjusted-p = 2.33e-318) and significantly decreased global efficiency during the SST (β = -0.29, adjusted-pI = 2.06e-35) and MID tasks (β = -0.56, adjusted-p = 2.58e-124), but significantly increased global efficiency during the EN-back task (β = 0.67, adjusted-p = 1.20e-66); see **Figure 6** and **Table 2**.

Comparing brain organization between the task states, we found that modularity in the MID task was significantly greater than modularity in the SST (β = 0.10, adjusted-p = 2.96e-06). Modularity in the EN-back was significantly less than in the SST (β = -0.92, adjusted-p = 2.64e-165) and the MID task (β = -1.02, adjusted-p = 2.30e-166). Global efficiency in the EN-back task was significantly greater than the SST (β = 0.96, adjusted-p = 1.36e-158) and the MID task (β = 1.23, adjusted-p = 4.55e-202). Global efficiency in the MID task was significantly less than in the SST (β = -0.28, adjusted-p = 3.72e-35); see **Table 2**.

To quantify differences in network-level organization between the resting state and task-evoked states, between-network integration (network dissociation index) was estimated for each network of interest. All omnibus tests were found to be significant, indicating differences in

network-level organization between the states (fronto-parietal: F(3,1553.35) = 49.39, raw p = 1.73E-30, adjusted-p = 1.92E-30; cingulo-opercular: F(3,1582.49) = 364.82, raw p = 4.66E-180, adjusted-p = 9.33E-180; default mode: F(3,1593.13) = 421.34, raw p = 1.79E-201, adjusted-p = 4.46E-201; salience: F(3,1614.44) = 44.65, raw p = 1.03E-27, adjusted-p = 1.03E-27; dorsal attention: F(3,1587.72) = 202.88, raw p = 2.23E-111, adjusted-p = 3.71E-111; ventral attention: F(3,1580.12) = 155.56, raw p = 2.45E-88, adjusted-p = 3.06E-88; somatomotor hand: F(3,1586.24) = 200.81, raw p = 2.18E-110, adjusted-p = 3.11E-110; visual: F(3,1620.89) = 529.99, raw p = 5.75E-240, adjusted-p = 1.92E-239). Compared to the resting state, during the SST we observed significantly increased network dissociation index in all networks (cingulo-opercular: β = 0.39, adjusted-p = 5.56e-39; default mode: β = 0.33, adjusted-p = 1.10e-25; salience: β = 0.24, adjusted-p = 2.22e-06; dorsal attention: β = 0.40, adjusted-p = 8.37e-25; ventral attention: β = 0.60, adjusted-p = 7.04e-59; dorsal somatomotor: β = 0.07, adjusted-p = 0.036; visual: β = 0.71, adjusted-p = 8.22e-123), except for the fronto-parietal network in which we observed a trend toward significantly increased network dissociation index (β = 0.08, adjusted-p = 0.059). In the MID task, we observed significantly decreased network dissociation index in the fronto-parietal network (β = -.29, adjusted-p = 8.08e-13), but significantly increased network dissociation index in all other networks (cingulo-opercular: β = 0.44, adjusted-p = 1.00e-53; default mode: β = 0.50, adjusted-p = 2.58e-57; salience: β = 0.34, adjusted-p = 3.84e-12; dorsal attention: β = 0.74, adjusted-p = 1.60e-80; ventral attention: β = 0.20, adjusted-p = 2.79e-09; visual: β = 0.50, adjusted-p = 1.51e-72), except for the dorsal somatomotor network in which we observed a trend toward significantly increased network dissociation index (β = 0.06, adjusted-p = 0.053). In the EN-back task, we observed significantly increased network dissociation index in all networks (fronto-parietal: β = 0.40, adjusted-p = 6.27e-09; cingulo-

opercular: β = 1.54, adjusted-p = 4.30e-179; default mode: β = 1.74, adjusted-p = 1.32e-192; salience: β = 0.87, adjusted-p = 8.28e-26; dorsal attention: β = 1.23, adjusted-p = 1.99e-76; ventral attention: β = 1.15, adjusted-p = 8.70e-76; dorsal somatomotor: β = 1.13, adjusted-p = 3.81e-94; visual: β = 1.74, adjusted-p = 6.90e-246); see **Figure 6** and **Table 2.**

Across all networks tested, network dissociation index in the EN-back was greater than in the MID task (fronto-parietal: β = 0.69, adjusted-p = 1.17e-24; cingulo-opercular: β = 1.10, adjusted-p = 2.86e-111; default mode: β = 1.24, adjusted-p = 3.86e-120; salience: β = 0.53, adjusted-p = 6.20e-12; dorsal attention: β = 0.49, adjusted-p = 8.26e-16; ventral attention: β = 0.95, adjusted-p = 7.04e-59; dorsal somatomotor: β = 1.07, adjusted-p = 1.01e-93; visual: β = 1.24, adjusted-p = 1.45e-155) and in the SST (fronto-parietal: β = 0.34, adjusted-p = 2.93e-08; cingulo-opercular: β = 1.15, adjusted-p = 2.94e-143; default mode: β = 1.40, adjusted-p = 4.92e-174; salience: β = 0.63, adjusted-p = 4.14e-19; dorsal attention: β = 0.83, adjusted-p = 1.62e-49; ventral attention: β = 0.55, adjusted-p = 2.42e-26; dorsal somatomotor: β = 1.06, adjusted-p = 3.94e-109; visual: β = 1.03, adjusted-p = 9.44e-135). The MID task exhibited significantly greater network dissociation index than the SST in the cingulo-opercular (β = 0.06, adjusted-p = 0.04), default mode (β = 0.17, adjusted-p = 4.91e-08), salience (β = 0.10, adjusted-p = 0.04), and dorsal attention (β = 0.34, adjusted-p = 9.12e-20) networks. Conversely, the MID task exhibited significantly decreased network dissociation index than the SST in the fronto-parietal (β = -0.36, adjusted-p = 5.61e-19), ventral attention (β = -0.40, adjusted-p = 2.55e-29), and visual networks (β = -0.21, adjusted-p = 1.87e-14). Network dissociation index of the dorsal somatomotor network did not differ between the MID task and the SST (β = -0.01, adjusted-p = 0.74). See **Table 2**.

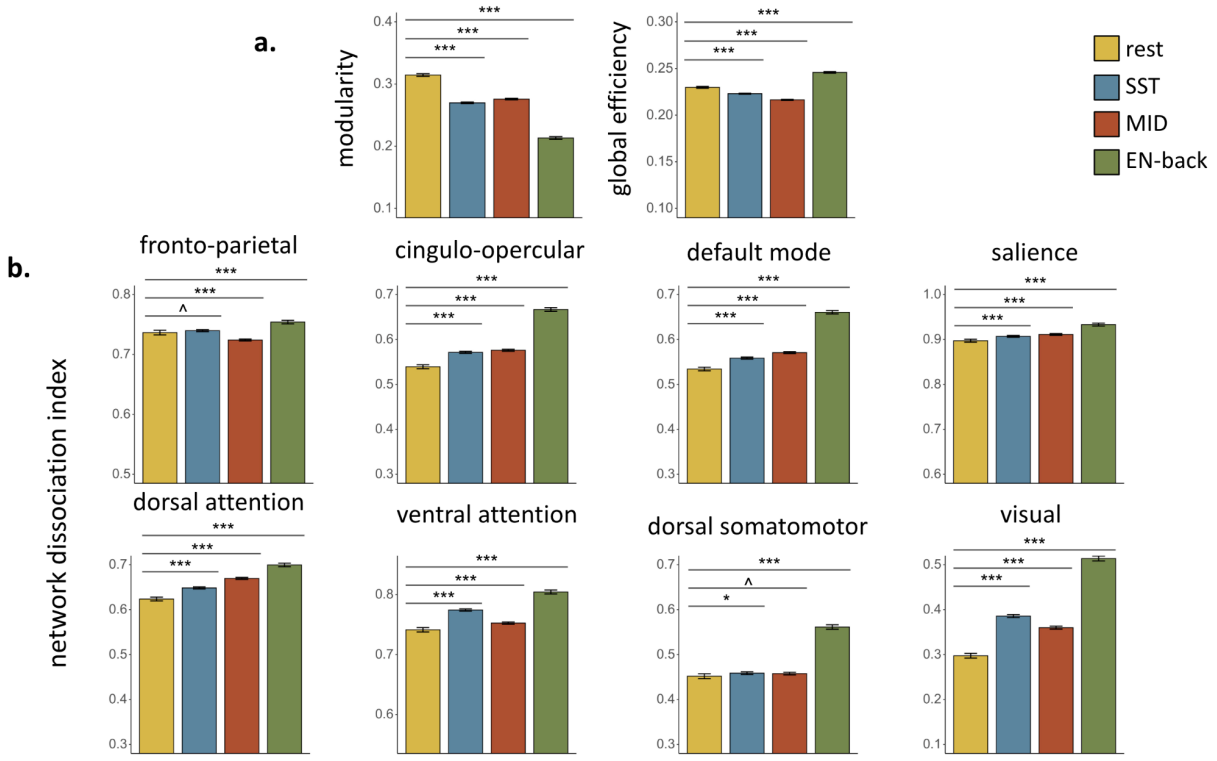

Figure 6. Differences in brain organization between the resting state and task-evoked states. a. Whole brain organization (modularity, global efficiency) during the states. **b.** Network dissociation index across the eight networks of interest during the resting state and the cognitive tasks. Output from the mixed effects models are plotted for visualization. The means and standard errors for the resting state (yellow) shown in this figure are the beta and standard error, respectively, for the intercept in each model. The means shown for each task (blue, red, green) were calculated by adding the beta for each comparison to the beta for the intercept in each model. The standard errors shown for the tasks are from the comparison in each model. Significant differences between the resting state (yellow) and the task states are indicated with regard to the adjusted *p*-values: ^$p < .10$, *$p < .05$, **$p < .01$, ***$p < .001$

Aim 2a Results: Relationships between brain network organization and task performance

First, we assessed if brain organization during the resting state was related to SST task performance (i.e., SSRT scores). We found no significant relationships after multiple comparison correction. All adjusted-*p*s > .32; see **Figure 7c** and **Table 3**. Then, we assessed if brain organization during the SST was related to SSRT. After correction there were no significant relationships, but we found trends such that increased SSRT (worse task performance) was related to increased modularity (β = 0.12, adjusted-*p* = .09), increased global efficiency (β = 0.14, adjusted-*p* = .09), and decreased network dissociation index of the default mode network (β = -0.10, adjusted-*p* = .09); see **Figure 7d** and **Table 3**.

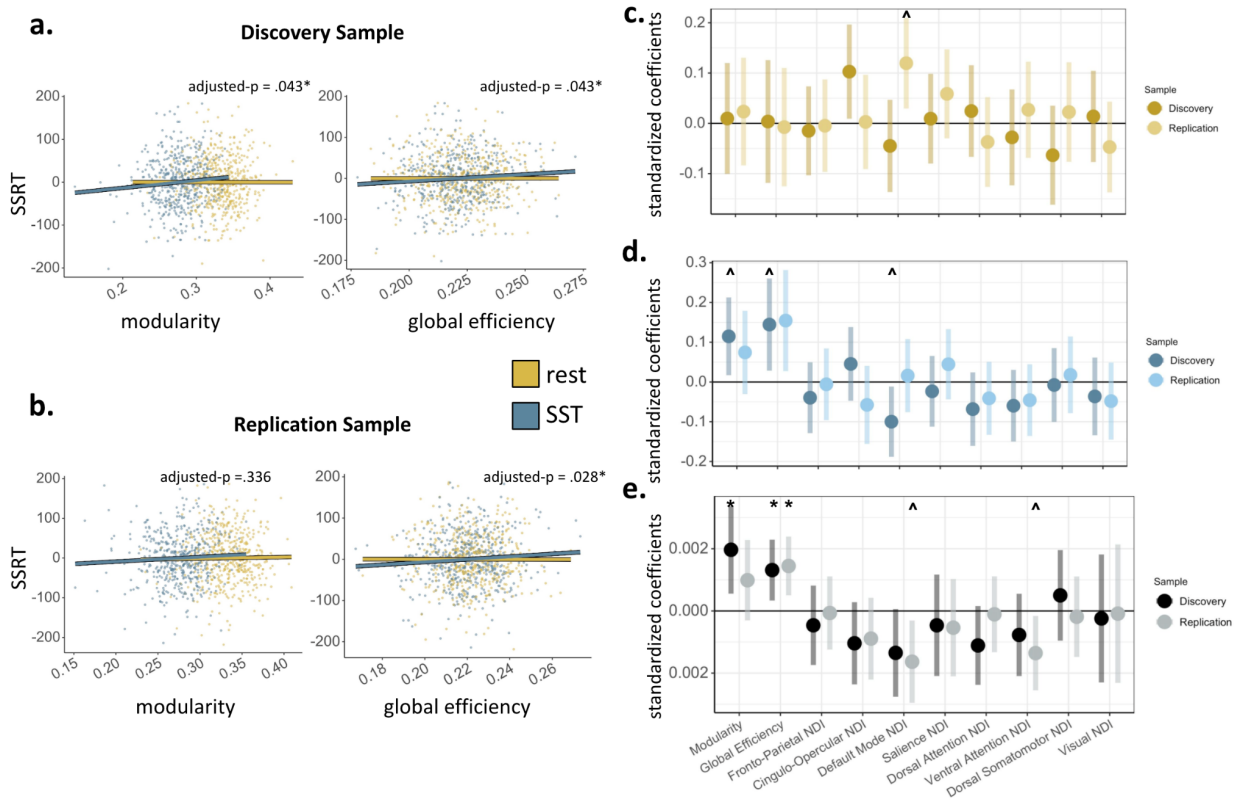

Figure 7. Relationships between SSRT and brain metrics in the resting state and the SST. Relationships of SSRT with modularity and global efficiency shown during the resting state (yellow) and the SST (blue) in the discovery sample **(a)** and the replication sample **(b)**. *P*-values

shown are for the difference in slopes between the resting state and the SST. Residualized brain metrics are plotted for visualization. Standardized coefficients and confidence intervals for **(c)** the relationship between resting state brain metrics and SSRT, **(d)** the relationship between SST brain metrics and SSRT, and **(e)** the difference between SSRT with SST brain metrics and resting state brain metrics. Significance is indicated with regard to the adjusted *p*-values: ^$p <$ .10, *$p <$ .05, **$p <$ .01, ***$p <$ .001

Next, we assessed if brain organization during the resting state was related to MID task performance (i.e., monetary value won). We found no significant relationships after multiple comparison correction. All adjusted-*p*s > .23; see **Figure 8c** and **Table 4**. Then, we assessed if brain organization during the MID task was related to monetary value won. After correction, we found that higher monetary value won was significantly related to lower global efficiency during the MID task (β = -0.21, adjusted-p = .02); see **Figure 8d** and **Table 4**.

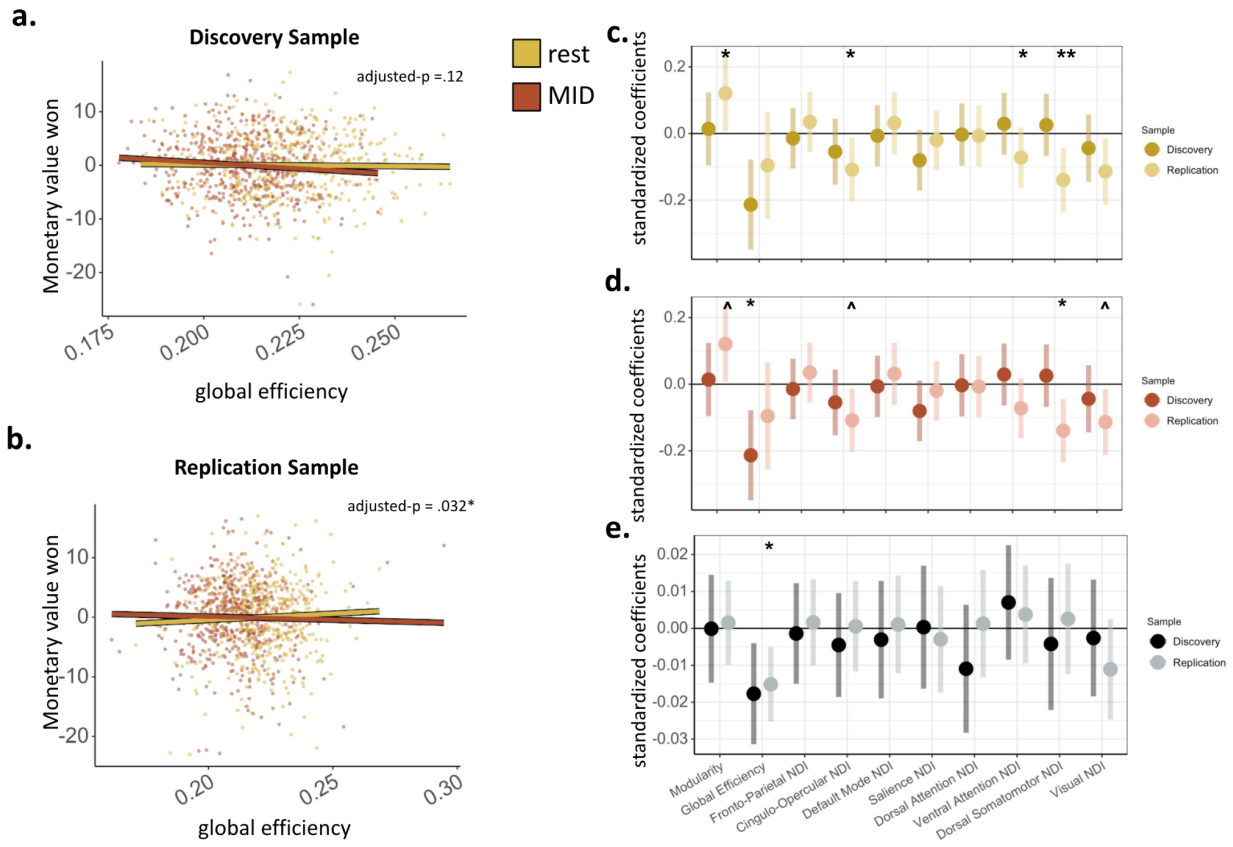

Figure 8. Relationships between monetary value won and brain metrics in the resting state and the MID task. Relationships of monetary value won with global efficiency shown during the resting state (yellow) and the MID task (red) in the discovery sample **(a)** and the replication sample **(b)**. *P*-values shown are for the difference in slopes between the resting state and the MID task. Residualized brain metrics are plotted for visualization. Standardized coefficients and confidence intervals for **(c)** the relationship between resting state brain metrics and monetary value won, **(d)** the relationship between MID brain metrics and monetary value won, and **(e)** the difference between monetary value won with MID brain metrics and resting state brain metrics. Significance is indicated with regard to the adjusted *p*-values: ^$p < .10$, *$p < .05$, **$p < .01$, ***$p < .001$

Last, we assessed if brain organization during the resting state was related to EN-back task performance (i.e., 2-back task accuracy). We found no significant results after multiple comparison correction. All adjusted-*p*s > .59; see **Figure 9c** and **Table 5**. Then, we assessed if brain organization during the EN-back task was related to 2-back percent accuracy. After correction there were no significant relationships, but we found a trend such that increased 2-back percent accuracy was related to decreased network dissociation index of the dorsal attention network (β = *-0.12,* adjusted-*p* = .08); see **Figure 9d** and **Table 5**.

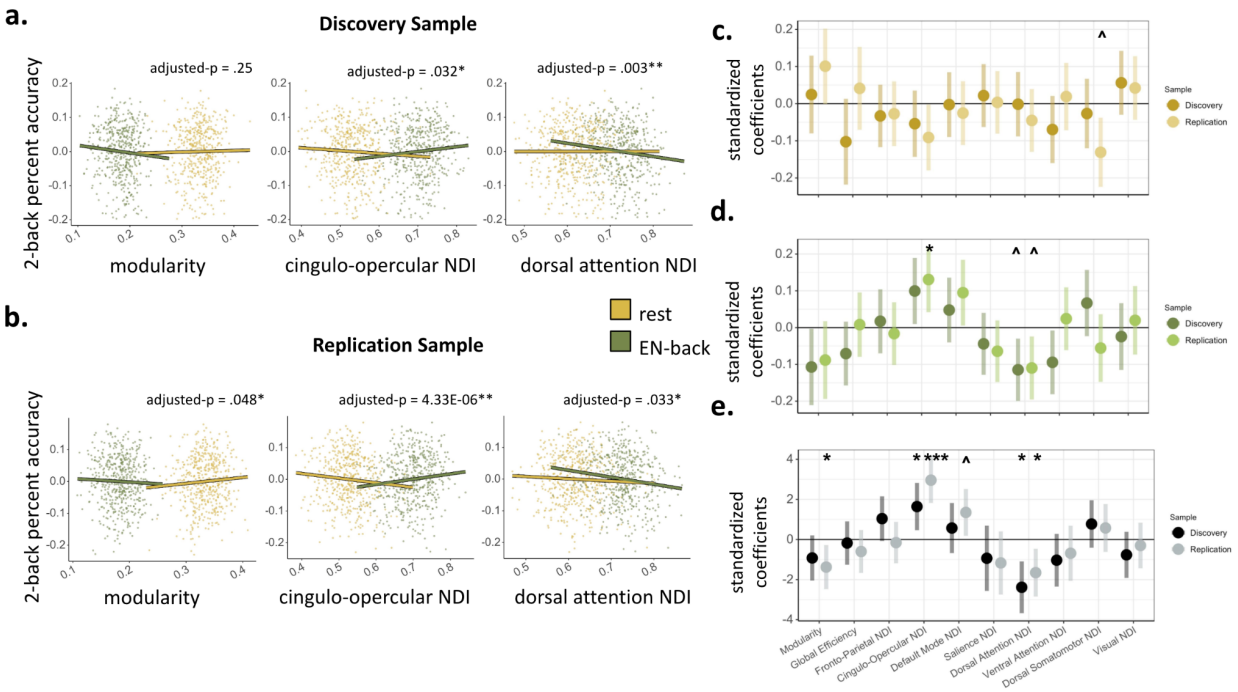

Figure 9. Relationships between 2-back percent accuracy and brain metrics in the resting state and the EN-back task. Relationships of 2-back percent accuracy with modularity, cingulo-opercular network dissociation index (NDI), and dorsal attention NDI shown during the resting state (yellow) and the EN-back task (green) in the discovery sample **(a)** and the replication sample **(b)**. P-values shown are for the difference in slopes between the resting state and the EN-back. Residualized brain metrics are plotted for visualization. Standardized coefficients and

confidence intervals for **(c)** the relationship between resting state brain metrics and 2-back accuracy, **(d)** the relationship between EN-back brain metrics and 2-back accuracy, and **(e)** the difference between 2-back accuracy with EN-back brain metrics and resting state brain metrics. Significance is indicated with regard to the adjusted p-values: ^$p < .10$, *$p < .05$, **$p < .01$, ***$p < .001$

Aim 2b Results: Modulation of brain-behavior relationships by brain state

We investigated if relationships between functional brain network organization and task performance differed between the resting state and the task-evoked states. First, we assessed whether the relationship between SST brain organization and SSRT was stronger than the relationship between the resting state brain organization and the SSRT; see **Figure 7a,b,e** and **Table 6**. We found that modularity and global efficiency during the SST had significantly stronger positive relationships with SSRT compared to modularity ($\beta = 0.08$, adjusted-$p = .04$) and global efficiency ($\beta = 0.08$, adjusted-$p = .04$) in the resting state, respectively; see **Figure 7a,b,e** and **Table 6**. All other adjusted-p values > .20; see **Table 6**.

Next, we assessed whether the relationship between MID brain organization and the monetary value won was stronger than the relationship between the resting state brain organization and the monetary value won. We did not find any significant differences between how brain organization in the MID related to average monetary value won compared to the resting state. All adjusted-p values > .11; see **Figure 8a,b,e** and **Table 7**.

Lastly, we assessed whether the relationship between EN-back brain organization and 2-back percent accuracy was stronger than the relationship between the resting state brain organization and 2-back percent accuracy; see **Table 8**. We found that the EN-back network

dissociation index of the cingulo-opercular network was significantly more positively related to 2-back percent accuracy than the network dissociation index of the cingulo-opercular network during the resting state ($\beta = 0.07$, adjusted-p = .03); see **Figure 9a,b,e** and **Table 8**. Additionally, the network dissociation index of the dorsal attention network was significantly more negatively related to 2-back percent accuracy than the network dissociation index of the dorsal attention network during the resting state ($\beta = -0.13$, adjusted-p = .003); see **Figure 9a,b,e** and **Table 8**. All other adjusted-p values > .22; see **Table 8**.

Results: Replication analyses

We used a separate, demographically matched sample (n=513) to test if the effects reported above replicate. We focused on replicating the results identified in the discovery sample, though results that emerged in the replication but were not seen in the discovery sample are included in the respective tables. With regard to differences in brain organization between the resting state and the task, we successfully replicated all significant results reported above; see **Figure 10** and **Table 9**. With regard to differences in brain organization between the tasks, we successfully replicated all significant results reported above, except in the replication sample network dissociation index of the cingulo-opercular network did not differ between the SST and the MID task (β = 0.003, raw p = .13, adjusted-p = .13); see **Table 9**.

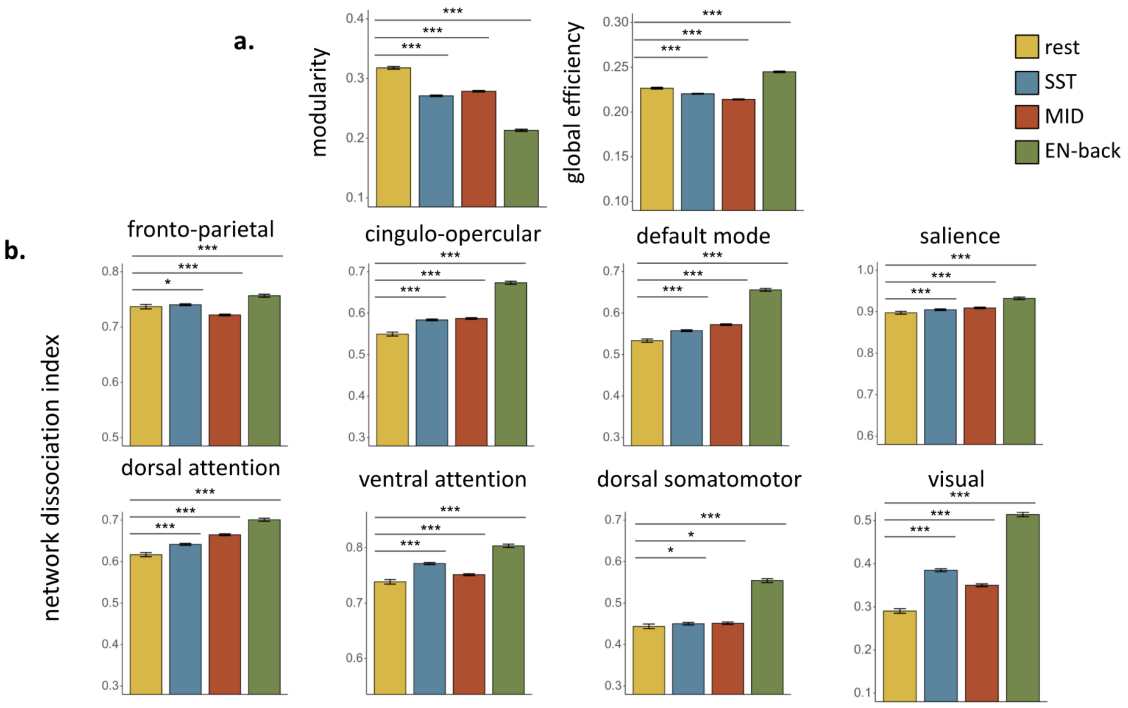

Figure 10. Replication of differences in brain organization between the resting state and task-evoked states. **a.** Whole brain organization (modularity, global efficiency) during the states. **b.** Network dissociation index across the eight networks of interest during the resting state and the cognitive tasks. Output from the mixed effects models are plotted for visualization. The means and standard errors for the resting state (yellow) shown in this figure are the beta and standard error, respectively, for the intercept in each model. The means shown for each task (blue, red, green) were calculated by adding the beta for each comparison to the beta for the intercept in each model. The standard errors shown for the tasks are from the comparison in each model. Significant differences between the resting state (yellow) and the task states are indicated with regard to the adjusted *p*-values: ^$p < .10$, *$p < .05$, **$p < .01$, ***$p < .001$

With regard to the relationships between brain organization and task performance, we replicated only a few of the effects reported above and found additional relationships. For SST

performance, no relationships were significant after multiple comparisons correction. As such, we failed to replicate the results reported above; see **Figure 7c,d** and **Table 10**.

For MID task performance, no relationships identified in the discovery sample were significant after multiple comparisons correction in the replication sample; see **Figure 8c,d** and **Table 11**.

For EN-back task performance, while no relationships identified in the discovery sample were significant after multiple comparisons correction in the replication sample, we did find a trend that greater 2-back percent accuracy was significantly related to lower network dissociation index of the dorsal attention network during the EN-back task (β = *-0.11,* adjusted-p = .06); see **Figure 9c,d** and **Table 12**. This trending relationship aligns with the significant relationship we found between network dissociation index of the dorsal attention network and 2-back percent accuracy in the discovery sample.

With regard to the modulation of brain-behavior relationships by brain state, we replicated some but not all of the effects reported above. In the replication sample, we found that global efficiency during the SST was significantly more positively related to the SSRT compared to global efficiency during the resting state (β = 0.09*,* adjusted-p = .03); see **Figure 7a,b,e** and **Table 13**. Thus, we replicated the finding that global efficiency is modulated by the SST to relate more strongly to SSRT compared to the resting state, but we did not replicate the above finding with modularity (β = 0.04*,* adjusted-p = .34).

Next, while no differences were found in the relationship between monetary value won with MID and resting state organization in the discovery sample, we ran the replication analysis anyway; see **Figure 8a,b,e** and **Table 14** for results from the replication sample.

Lastly, in the replication sample, we found that the EN-back task network dissociation index of the cingulo-opercular network was significantly more positively related to 2-back percent accuracy than the network dissociation index of the cingulo-opercular network during the resting state (β = 0.12, adjusted-p = 4.33E-06). Additionally, the network dissociation index of the dorsal attention network was significantly more negatively related to 2-back percent accuracy than the network dissociation index of the dorsal attention network during the resting state (β = -0.09, adjusted-p = .03); see **Figure 9a,b,e** and **Table 15**. Overall, we replicated the findings that network dissociation indices of the cingulo-opercular and dorsal attention networks are modulated by the EN-back task to relate more strongly to 2-back percent accuracy compared to the resting state.

Discussion

In this study, we investigated differences in functional brain network organization between the resting state, a stop signal task (SST) state, a monetary incentive delay (MID) task state, and an emotional N-back (EN-back) task state in children ages 9-10 years from the ABCD Study sample. We also assessed relationships between brain organization and task performance and, critically, whether task-evoked states elicited stronger relationships between functional brain organization and task performance compared to the resting state. We used demographic-matched discovery and replication samples to test the reproducibility of our results in all analyses.

We found that compared to the resting state, each task state evoked a more integrated brain network organization. Differences in brain organization between the resting state and task-evoked states were successfully replicated. Metrics of brain organization in each task-evoked

state were weakly related to task performance, such that complex relationships to behavior emerged across networks and few relationships replicated across samples. However, most of the task-evoked brain metrics found to be significantly related to task performance in the discovery sample exhibited a similar pattern of effects in the replication sample despite not meeting our significance criteria. Notably, these same task-evoked brain metrics also exhibited significantly stronger relationships to task performance compared to the resting state brain metrics in the discovery sample with trends in the replication sample. Together, these results contribute preliminary evidence to the idea that, in children, cognitive tasks may evoke changes in functional brain network organization that result in a stronger relationship to behavioral performance on the tasks.

Differences in functional brain organization between the resting state and cognitive tasks

We found that overall, brain network integration increased in each of the cognitive tasks compared to the resting state. In each cognitive task, we observed decreased whole-brain modularity and increased network dissociation index in most networks compared to the resting state. Increased integration during tasks compared to the resting state aligns with the idea that coordination across distributed regions of the brain is important for cognitive processes (Dehaene et al., 1998). Despite immaturities in functional brain network organization in childhood (Grayson & Fair, 2017), this work validates prior findings that similar to adults, children exhibit global reconfiguration from the resting state into a more integrated configuration during task states probing complex cognitive abilities, including inhibition (Mitchell et al., In Prep), working memory (Braun et al., 2015; Cohen & D'Esposito, 2016; Le et al., 2020; Shine et al., 2016), and reward processing (Le et al., 2020; Mitchell et al., In Prep; Shine et al., 2016).

These results provide evidence for the involvement of functional network reconfiguration in cognitive tasks in children. The functional architecture of response inhibition involves distributed brain regions (e.g., Aron et al., 2014; Aron & Poldrack, 2006), including the cingulo-opercular, default mode, somatomotor, and visual networks (Engelhardt et al., 2019; McKenna et al., 2017; Hwang et al., 2010; Mehnert et al., 2013; Rubia et al., 2007; Stevens, 2016; Stevens et al., 2007; Vink et al., 2014; Mitchell et al., In Prep). To our knowledge, only one prior study has investigated functional brain network reconfiguration between the resting state and a task probing response inhibition. Mitchell and colleagues observed increased segregation and decreased integration during a go/no-go task compared to the resting state in a sample of children aged 8-12 years (Mitchell et al., In Prep). The discrepancy between this work and the prior study could be due to differences in cognitive processes probed by the tasks: Mitchell and colleagues used a go/no-go task (Mitchell et al., In Prep), while ABCD used a stop signal task (Casey et al., 2018). While both go/no-go tasks and stop signal tasks are considered to probe response inhibition, the two tasks evoke unique cognitive processes (Littman & Takács, 2017; Raud et al., 2020; Schachar et al., 2007). A study directly comparing a go/no-go task and a stop signal task found that two tasks evoked different neural and physiological responses. The go/no-go task signatures aligned more closely with response selection (an index of attention), whereas the stop signal task signatures aligned more closely with response inhibition (Raud et al., 2020). This could explain why the segregated functional brain network signatures derived from the go/no-go task used by Mitchell and colleagues aligns with findings of network reconfiguration during sustained attention in adults (e.g., Mitchell et al., In Prep; Sadaghiani et al., 2015). While on the other hand, the largely integrated functional brain network signatures obtained from the SST here

align with cognitive control-demanding tasks in adults (e.g., Braun et al., 2015; Cohen & D'Esposito, 2016; Shine et al., 2016) and children (Le et al., 2020).

The network integration we observed during the MID task includes networks involved in the theorized MID-evoked "motivational salience" circuit consisting of salience, default mode, cognitive control, and attention network regions (Wilson et al., 2018). However, we observed a decrease in integration in the fronto-parietal network during the MID task compared to the resting state. It is unclear why the fronto-parietal network would deviate from the pattern of reconfiguration seen in all other networks tested and future investigation into the role of the fronto-parietal network during reward processing in childhood is warranted. In contrast to the pattern of reconfiguration observed between the resting state and the MID here, we previously found that the addition of rewards during a go/no-go task increased segregation of functional brain networks (e.g, cingulo-opercular, salience, and visual networks; Mitchell et al., In Prep). However, the MID task specifically probes reward anticipation and receipt (Casey et al., 2018), while in the rewarded go/no-go task used by Mitchell and colleagues rewards incentivized good go/no-go task performance. Notably, the pattern of reconfiguration we observed here does align with one prior study in children that found increases in whole brain integration during a two-choice rewarded decision making task (Le et al., 2020). The combination of these three studies suggests that the impact of rewards on brain network reconfiguration may differ based on the task demands, such that rewards will increase a task-specific brain organization, promoting segregation in tasks where performance benefits from segregation (e.g., a go/no-go task) and vice versa in tasks where performance benefits from increased integration (e.g., a MID task; a two-choice rewarded decision making task).

During working memory, increased functional integration is observed in the fronto-parietal, cingulo-opercular, dorsal attention, and visual networks in adults when compared to the resting state (Shine et al., 2016), as well as to less demanding cognitive task states (Cohen et al., 2014; Braun et al., 2015). Additionally, this work aligns with two prior studies in children that find increased connectivity between distributed regions in the prefrontal cortex, parietal cortex, visual cortex, and cerebellum (Bosch et al., 2014; White et al., 2011). In this study, we extend the prior literature by characterizing significant integration across all networks tested, including the fronto-parietal, cingulo-opercular, salience, dorsal attention, and visual networks.

During both the SST and the MID task, we found an interesting pattern of decreased global efficiency and increased network dissociation index in most networks compared to the resting state. While global efficiency and network dissociation index are both conceptualized as metrics of integration, each measures integration differently. Global efficiency is a calculation of the shortest path lengths between all nodes regardless of network membership (Latora & Marchiori, 2001) and network dissociation index quantifies the sum of between network connections relative to all connections for each network (Cary et al., 2016). Given that network dissociation indices largely increased during the SST and MID task, the decrease in global efficiency could be explained by a decrease in within-network connectivity during the SST and MID task compared to the resting state. Increased between-network connectivity relative to decreased within-network connectivity might suggest that functional network membership shifts, such that new communities are formed during these tasks relative to the resting state, but further analyses would be needed to probe this possibility. Additionally, interpretation of this pattern as an artifact of immature brain networks would require further work with an adult sample for comparison.

Overall, our results align with patterns of increased integration during working memory observed in adults, but as there is less literature characterizing brain network organization during response inhibition and reward processing our comparisons are less clear. Additionally, across all cognitive processes tested, we are unable to make direct claims about developmental change in brain network reconfiguration. Studies of activation and functional connectivity between individual regions note that the functional brain correlates of inhibition, working memory, and reward processing continue to change into adulthood (Luna et al., 2010; Rubia et al., 2007; Stevens et al., 2007; Hwang et al., 2010; Vink et al., 2014; Geier et al., 2010; Padmanabhan et al., 2011; Teslovich et al., 2014; Porter et al., 2015), even after behavioral abilities reach adult levels (Best & Miller, 2010). Future work should include an adult comparison group and would ideally track brain network organization changes longitudinally across childhood and adolescence. Future waves of the ABCD Study will make longitudinal investigations possible.

Relationships between brain network organization and task performance

In the discovery sample, resting state brain metrics did not significantly relate to any of the task performance measures. However, in the replication sample resting state brain metrics related to task performance measures from each of the tasks. For each of the tasks, relationships between task-evoked brain metrics and task performance were identified, but none were successfully replicated after multiple comparison correction. Alignment of brain-behavior relationships across both the discovery and replication samples, even if not significant after correction, did occur in a few cases and those are described here.

During the SST, better task performance (i.e., decreased SSRT) was related to decreased global efficiency in the discovery sample. In the replication sample, there was a similar

relationship between SST global efficiency and SSRT that did not survive multiple comparison correction. Overall, global efficiency was decreased in the SST compared to the resting state and decreased SST global efficiency was related to better task performance.

When investigating relationships between brain organization and monetary value won during the MID task, none of the findings replicated across both samples. There are several possible explanations. First, given the impact of pubertal maturation on brain-behavior relationships (Gracia-Tabuenca et al., 2021), variability in functional brain connectivity between individuals in different stages of pubertal maturation (Piekarski et al., 2017) may obscure the elucidation of brain-behavior relationships in a cross-sectional sample of this age. Indeed, functional brain organization underlying reward processing changes rapidly during this developmental period (Fareri et al., 2015) and may thus be variable in our sample. Second, in tasks that evoke more cognitive effort, the brain reconfigures to better facilitate behavior (Dehaene et al., 1998; Hearne et al., 2017; Kitzbichler et al., 2011). Relatedly, in tasks with low cognitive demands, comparable levels of task performance can be achieved with variable patterns of brain organization across individuals (Kitzbichler et al., 2011). Given that the cognitive demands of the MID task used here are low, it is conceivable that individuals in our sample exhibited varying patterns of brain organization, which occluded the elucidation of brain-behavior relationships. This explanation would fit with work that finds that varying attentional demands during the MID task elicit variation in brain activation in adults (Stoppel et al., 2011). Third, the functional brain features that relate to behavior during the MID task may not have been included in these analyses. The ventral striatum, a primary brain region targeted by the MID task (Oldham et al., 2018; Wilson et al., 2018), was not included in these analyses as it was not included in the functional networks identified in the cortical brain parcellation used (Gordon

et al., 2016). Future work should consider functional connectivity between large-scale functional brain networks and subcortical regions.

During the EN-back task, in both the discovery and replication samples, we observed a trend toward significance such that better task performance (i.e., 2-back percent accuracy) related to decreased network dissociation index of the dorsal attention network. The dorsal attention network is thought to facilitate flexible, goal-directed attention (Corbetta & Shulman, 2002). In a previous study, we found that increased flexibility, or rapid changes on the order of seconds, in network organization resulted in decreased estimates of network integration captured across minutes of a scan (Duffy et al., 2021). As such, perhaps a less integrated, or more flexible on the order of seconds, dorsal attention network may facilitate better working memory ability in children. While on average the network dissociation index of the dorsal attention network increased during the EN-back task compared to the resting state, less dorsal attention network dissociation index during the EN-back task was better for task performance. Relatedly, another study using the ABCD Study found that less resting state integration between the dorsal attention network and the default mode network is related to higher general cognitive ability (Marek et al., 2019). It is possible that our result could also be due to the inclusion of emotional stimuli in the task. During working memory, the introduction of salient, distracting stimuli decreases the connectivity between the dorsal and ventral attention networks (Greene & Soto, 2014). It is possible that the emotional face stimuli blocks included in the EN-back task data used in this analysis impacted connectivity between the dorsal attention network and other networks, such as the ventral attention network, during the EN-back task. Future work is needed to parse differences in functional connectivity underlying the emotional and non-emotional blocks of the EN-back task.

Given that we had a relatively small sample size and were somewhat underpowered (Marek et al., 2022), in exploratory analyses we examined patterns of results without correction for multiple comparisons. Specifically, we looked to see if any of the significant results surviving correction in the replication sample showed the same effect, even if not surviving correction, in the discovery sample. Only one effect met this criteria: increased EN-back cingulo-opercular network integration was related to better task performance (i.e., higher 2-back accuracy) prior to correction in the discovery sample (raw p = .03; adjusted-p = 0.11) and survived correction in the replication sample (raw p = .004; adjusted-p = .04). This result should be taken with caution, but it is noteworthy that it aligns with prior literature finding that the cingulo-opercular network is highly integrated with other large scale brain networks during working memory in adults (J. R. Cohen et al., 2014; Shine et al., 2016) and the purported role of the cingulo-opercular network in task set maintenance (Dosenbach et al., 2006, 2007, 2008; Power & Petersen, 2013).

Altogether, while a handful of trends were observed across the samples, we failed to replicate any brain-behavior relationships. The lack of replication of significant relationships between functional brain metrics and task performance aligns with the idea that recovery of stable brain-behavior relationships requires sample sizes close to n=2,000 (Marek et al., 2022). In this analysis, we only included subjects with usable fMRI and task performance data in all tasks, which drastically reduced our sample size (discovery n = 498; replication n = 513).

Differences in relationships between task-evoked and resting state brain network organization and task performance

In both the discovery and replication samples, SST and EN-back brain metrics exhibited stronger relationships with task performance compared to brain organization during the resting state. With regard to the SST, we found that better task performance (i.e., lower SSRT) was

significantly more strongly related to SST global efficiency than resting state global efficiency in both the discovery and replication samples. With regard to the EN-back task, we found that 2-back accuracy was significantly more negatively related to EN-back dorsal attention network dissociation index and significantly more positively related to EN-back cingulo-opercular network dissociation index compared to the respective metrics in the resting state in both the discovery and replication samples.

Thus, across all tasks tested, we identified a pattern of effects such that many of the task-evoked brain metrics that exhibited relationships with task performance also showed stronger relationships to task performance compared to those metrics in the resting state. However, these findings should be interpreted with caution as none of our brain-behavior relationships survived multiple comparison correction in both the discovery and replication samples. This work aligns with prior literature which finds that task-evoked functional connectivity is more predictive of task performance (Rosenberg et al., 2016), as well as behaviors like IQ and reading comprehension (Gao et al., 2019; Greene et al., 2018; Jiang et al., 2020), compared to resting state functional connectivity. Future work with larger samples of children is needed to replicate these results.

It is worth noting that there are a few differences between these prior studies and this work. First, these prior studies have utilized the full connectivity matrix in predictive models (i.e., CPM, partial least squares regression), while this work calculated graph metrics summarizing network topology from the connectivity matrix. While graph metrics have shown clear relationships to cognition (e.g., Cohen & D'Esposito, 2016), they are a dimension reduction technique that inherently removes some of the information present in the full connectivity matrix. It is possible that the calculation of graph metrics here eliminated or obscured features of

the connectivity matrix that relate to task performance. Second, this study focused on a sample of children aged 9-10 years, while prior work has largely utilized adult samples (Rosenberg et al., 2015; Greene et al., 2018; Jiang et al., 2020) or a broad age range in youth (i.e., 8-21 years; Greene et al., 2018).

Given that refinement of functional brain networks continues into early adulthood (Grayson & Fair, 2017), it is possible that there are qualitative and/or quantitative shifts in brain-behavioral relationships across the course of childhood and adolescence. Qualitative shifts could include different brain networks relating to behavior in childhood (e.g., cingulo-opercular) and adulthood (e.g., fronto-parietal). Quantitative shifts could include alterations in the magnitude of relationships between brain metrics and behavior (e.g., strengthening relationships with age). In order to determine if either type of shift occurs, future work will need to include an adult comparison group and track these relationships longitudinally.

Limitations

It is important to note task and rest data have different influences. Resting state brain function is considered entirely endogenously driven, while brain function during tasks is a combination of an endogenous background state and activity related to stimuli and response encodings (Turk-Browne, 2013). These event locked changes in the BOLD signal related to task stimuli and responses can increase estimates of functional connectivity between regions that are not interacting (Cole et al., 2019). In this project, all data was processed identically. Thus, the analyses presented above likely include inflated functional connectivity estimates, which may bias task-evoked graph metrics and result in spurious relationships with behavior. To control for this inflation in functional connectivity estimates, task events can be regressed from the

functional brain time series using finite impulse response (FIR) functions (Cole et al., 2019) to create a 'background connectivity' profile capturing only the endogenous activity during a given cognitive state (Norman-Haignere et al., 2012). Future work should implement task event regression to eliminate the biasing of functional connectivity estimates during cognitive tasks.

There are also several analysis considerations to note. First, we did not replicate brain-behavior metrics in this project. Recent work has shown that brain-behavior relationships do not stabilize until sample sizes reach approximately 2,000 (Marek et al., 2022), which offers an explanation for the differences in brain-behavior relationships identified across discovery (n = 498) and replication samples (n = 513). In this project, the sample was limited to subjects with good MRI and behavioral data in all three tasks, which dramatically reduced the sample size. Future work can address this by using all available data, rather than limiting analyses to subjects with complete data as this project did. This approach would allow for larger sample sizes and thus more power in some task-evoked states. Additionally, when implementing a more restricted multiple comparison correction that accounts for dependence between the brain organization metrics (see **Appendices**), most of the brain-behavior relationships did not survive correction; thus our results should be interpreted with caution.

Second, the parcellation employed in this study (Gordon et al., 2016) includes subcortical structures critical for the SST and MID tasks (e.g., putamen, ventral striatum), but they are not assigned membership into large scale brain networks and were thus omitted from these analyses. The discrepancies in our findings compared to prior literature may be due to the omission of these brain regions from consideration, especially given that fronto-striatal connections are widely implicated in both response inhibition (Luna et al., 2010) and reward processing (Cao et

al., 2019; Cho et al., 2013). Future work should utilize a brain parcellation that includes subcortical structures in functional brain networks (e.g., Ji et al., 2019).

Conclusions

In this study, we found that functional brain networks reconfigured between the resting state and tasks probing working memory, response inhibition, and reward processing in children aged 9-10 years. Overall, functional brain organization during all three tasks was more integrated than during the resting state. We did not find any consistent relationships between brain metrics and task performance, but we did find that a few task-specific brain metrics in the SST and EN-back task were more strongly related to task performance than resting state brain metrics. Overall, this work cautiously contributes preliminary evidence that in childhood, task-evoked functional connectivity may be able to highlight neurobiological features relevant to task performance to a greater extent than the resting state. Additional work probing these relationships in larger samples is critical to determine the stability of these relationships. Additionally, future work in children should test if these relationships can be extended to behaviors relevant to educational and clinical outcomes, such as general cognitive ability and reward responsiveness.

Table 1. ABCD imaging scanning parameters harmonized for Siemens Prisma, Phillips, and GE 750 3T scanners. Figure from Casey et al. (2018).

Siemens (Prisma VE11B-C)	***Matrix***	***Slices***	***FOV***	***% FOV Phase***	***Resolution (mm)***	***TR (ms)***	***TE (ms)***	***TI (ms)***	***Flip Angle (deg)***	***Parallel Imaging***	***MultiBand Acceleration***
T1	256 × 256	176	256 × 256	100%	1.0×1.0×1.0	2500	2.88	1060	8	2×	Off
T2	256 × 256	176	256 × 256	100%	1.0×1.0×1.0	3200	565	N/A	Variable	2×	Off
fMRI	90×90	60	216×216	100%	2.4×2.4×2.4	800	30	N/A	52	Off	6
Philips (Achieva dStream, Ingenia)	***Matrix***	***Slices***	***FOV***	***% FOV Phase***	***Resolution (mm)***	***TR (ms)***	***TE (ms)***	***TI (ms)***	***Flip Angle (deg)***	***Parallel Imaging***	***MultiBand Acceleration***
T1	256 × 256	225	256 × 240	93.75%	1.0×1.0×1.0	6.31	2.9	1060	8	1.5×2.2	Off
T2	256 × 256	256	256 × 256	100%	1.0×1.0×1.0	2500	251.6	N/A	90	1.5×2.0	Off
fMRI	90×90	60	216×216	100%	2.4×2.4×2.4	800	30		N/A	52	Off
GE (MR750, DV25-26)	***Matrix***	***Slices***	***FOV***	***% FOV Phase***	***Resolution (mm)***	***TR (ms)***	***TE (ms)***	***TI (ms)***	***Flip Angle (deg)***	***Parallel Imaging***	***MultiBand Acceleration***
T1	256 × 256	208	256 × 256	100%	1.0×1.0×1.0	2500	2	1060	8	2×	Off
T2	256 × 256	208	256 × 256	100%	1.0×1.0×1.0	3200	60	N/A	Variable	2×	Off
fMRI	90×90	60	216×216	100%	2.4×2.4×2.4	800	30	N/A	52	Off	6

Table 2. Differences in brain network organization between the resting state and task states.

Task 1 (Reference)	*Task 2*	*b*	*β*	*SE*	*t*	*df*	*raw p*	*adjusted-p*
Modularity								
Intercept (Resting state)		0.314	0.715	0.00214	146.632	734.9		
Resting state	Stop Signal task	-0.045	-0.727	0.00131	-34.028	1530.07	1.91E-189***	5.73e-189***
Resting state	Monetary Incentive Delay task	-0.039	-0.63	0.00126	-30.637	1482.41	4.21E-160***	5.05e-160***
Resting state	Emotional N-back task	-0.101	-1.646	0.00215	-47.136	1847.88	3.88e-319***	2.33e-318***
Stop Signal task	Monetary Incentive Delay task	0.006	0.098	0.001	4.69	1500.15	2.96E-06***	2.96e-06***
Stop Signal task	Emotional N-back task	-0.056	-0.919	0.002	-30.56	1793.11	1.76E-165***	2.64e-165***
Monetary Incentive Delay task	Emotional N-back task	-0.063	-1.017	0.002	-30.62	1832.12	1.15E-166***	2.30e-166***
Global efficiency								
Intercept (Resting state)		0.23	0.02	0.00101	227.631	662.37		
Resting state	Stop Signal task	-0.007	-0.285	0.00053	-12.759	1516.57	1.72E-35***	2.06e-35***
Resting state	Monetary Incentive Delay task	-0.013	-0.561	0.00051	-26.202	1478.92	1.29E-124***	2.58e-124***
Resting state	Emotional N-back task	0.016	0.671	0.00089	18.025	1771.75	8.03E-67***	1.20e-66***
Stop Signal task	Monetary Incentive Delay task	-0.007	-0.276	0.001	-12.70	1492.97	3.72E-35***	3.72e-35***
Stop Signal task	Emotional N-back task	0.023	0.956	0.001	29.95	1724.78	4.52E-159***	1.36e-158***
Monetary Incentive Delay task	Emotional N-back task	0.029	1.232	0.001	34.86	1757.86	7.59E-203***	4.55e-202***

NDI of the Fronto-parietal network								
Intercept (Resting state)		0.736	0.132	0.0039	188.775	611.64		
Resting state	Stop Signal task	0.003	0.076	0.00176	1.889	1507.53	0.059^	0.059^
Resting state	Monetary Incentive Delay task	-0.012	-0.282	0.00169	-7.321	1478.84	4.04E-13***	8.08e-13***
Resting state	Emotional N-back task	0.018	0.403	0.00298	5.908	1702	4.18E-09***	6.27e-09***
Stop Signal task	Monetary Incentive Delay task	-0.016	-0.359	0.002	-9.15	1489.57	1.87E-19***	5.61e-19***
Stop Signal task	Emotional N-back task	0.014	0.327	0.003	5.60	1665.33	2.44E-08***	2.93e-08***
Monetary Incentive Delay task	Emotional N-back task	0.030	0.685	0.003	10.59	1691.05	1.95E-25***	1.17e-24***
NDI of the Cingulo-opercular network								
Intercept (Resting state)		0.539	-0.634	0.00441	122.354	672.89		
Resting state	Stop Signal task	0.032	0.386	0.00238	13.453	1519.42	4.63E-39***	5.56e-39***
Resting state	Monetary Incentive Delay task	0.037	0.444	0.00228	16.106	1480.45	6.67E-54***	1.00e-53***
Resting state	Emotional N-back task	0.127	1.539	0.00395	32.218	1783.15	7.16E-180***	4.30e-179***
Stop Signal task	Monetary Incentive Delay task	0.005	0.057	0.002	2.05	1494.99	0.04*	0.04*
Stop Signal task	Emotional N-back task	0.095	1.152	0.003	28.13	1734.92	9.81E-144***	2.94e-143***
Monetary Incentive Delay task	Emotional N-back task	0.091	1.095	0.004	24.15	1768.93	1.43E-111***	2.86e-111***

NDI of the Default mode network								
Intercept (Resting state)		0.534	-0.741	0.00399	133.896	697.06		
Resting state	Stop Signal task	0.024	0.333	0.00227	10.689	1524.01	9.18E-26***	1.10e-25***
Resting state	Monetary Incentive Delay task	0.036	0.5	0.00218	16.699	1481.55	1.72E-57***	2.58e-57***
Resting state	Emotional N-back task	0.126	1.735	0.00375	33.669	1810.11	2.20E-193***	1.32e-192***
Stop Signal task	Monetary Incentive Delay task	0.012	0.167	0.002	5.48	1497.38	4.91E-08***	4.91e-08***
Stop Signal task	Emotional N-back task	0.102	1.402	0.003	31.66	1758.79	1.64E-174***	4.92e-174***
Monetary Incentive Delay task	Emotional N-back task	0.090	1.235	0.004	25.23	1795.09	1.93E-120***	3.86e-120***
NDI of the Salience network								
Intercept (Resting state)		0.897	-0.228	0.00322	278.906	751.38		
Resting state	Stop Signal task	0.01	0.236	0.00203	4.788	1531.76	1.85E-06***	2.22e-06***
Resting state	Monetary Incentive Delay task	0.014	0.337	0.00196	7.1	1481.78	1.92E-12***	3.84e-12***
Resting state	Emotional N-back task	0.036	0.868	0.00331	10.838	1863.15	1.38E-26***	8.28e-26***
Stop Signal task	Monetary Incentive Delay task	0.004	0.101	0.002	2.09	1500.37	0.04*	0.04*
Stop Signal task	Emotional N-back task	0.026	0.632	0.003	9.16	1807.33	1.38E-19***	4.14e-19***
Monetary Incentive Delay task	Emotional N-back task	0.022	0.532	0.003	6.98	1847.25	4.13E-12***	6.20e-12***
NDI of the								

Dorsal attention network								
Intercept (Resting state)		0.624	-0.584	0.00425	146.906	684.45		
Resting state	Stop Signal task	0.025	0.399	0.00235	10.507	1521.82	5.58E-25***	8.37e-25***
Resting state	Monetary Incentive Delay task	0.046	0.742	0.00225	20.339	1481.21	2.66E-81***	1.60e-80***
Resting state	Emotional N-back task	0.076	1.228	0.00389	19.491	1796.13	6.63E-77***	1.99e-76***
Stop Signal task	Monetary Incentive Delay task	0.021	0.342	0.002	9.25	1496.35	7.60E-20***	9.12e-20***
Stop Signal task	Emotional N-back task	0.051	0.829	0.003	15.32	1746.39	8.11E-50***	1.62e-49***
Monetary Incentive Delay task	Emotional N-back task	0.030	0.486	0.004	8.13	1781.51	8.26E-16***	8.26e-16***
NDI of the Ventral attention network								
Intercept (Resting state)		0.741	-0.46	0.00366	202.492	667.37		
Resting state	Stop Signal task	0.033	0.603	0.00195	16.954	1518.67	3.52E-59***	7.04e-59***
Resting state	Monetary Incentive Delay task	0.011	0.204	0.00187	5.98	1480.64	2.79E-09***	2.79e-09***
Resting state	Emotional N-back task	0.063	1.153	0.00324	19.453	1776.16	1.45E-76***	8.70e-76***
Stop Signal task	Monetary Incentive Delay task	-0.022	-0.399	0.002	-11.52	1494.83	1.70E-29***	2.55e-29***
Stop Signal task	Emotional N-back task	0.030	0.549	0.003	10.81	1728.88	2.02E-26***	2.42e-26***
Monetary Incentive Delay task	Emotional N-back task	0.052	0.949	0.003	16.86	1762.19	2.92E-59***	7.04e-59***

NDI of the Dorsal somatomotor network								
Intercept (Resting state)		0.452	-0.324	0.00545	82.959	682.05		
Resting state	Stop Signal task	0.007	0.07	0.00301	2.26	1520.33	0.02*	0.036*
Resting state	Monetary Incentive Delay task	0.006	0.06	0.00289	2.018	1479.71	0.04*	0.053^
Resting state	Emotional N-back task	0.109	1.131	0.00499	21.927	1794.89	1.27E-94***	3.81e-94***
Stop Signal task	Monetary Incentive Delay task	-0.001	-0.010	0.003	-0.33	1494.86	0.74	0.74
Stop Signal task	Emotional N-back task	0.103	1.061	0.004	23.96	1745.06	6.56E-110***	3.94e-109***
Monetary Incentive Delay task	Emotional N-back task	0.104	1.071	0.005	21.86	1780.24	5.06E-94***	1.01e-93***
NDI of the Visual network								
Intercept (Resting state)		0.297	-0.6	0.00525	56.647	768.17		
Resting state	Stop Signal task	0.088	0.709	0.00341	25.897	1534.82	5.48E-123***	8.22e-123***
Resting state	Monetary Incentive Delay task	0.062	0.502	0.00328	19.061	1483.03	1.26E-72***	1.51e-72***
Resting state	Emotional N-back task	0.216	1.739	0.00551	39.268	1875.79	1.15E-246***	6.90e-246***
Stop Signal task	Monetary Incentive Delay task	-0.026	-0.207	0.003	-7.74	1502.28	1.87E-14***	1.87e-14***
Stop Signal task	Emotional N-back task	0.128	1.030	0.005	26.97	1819.68	4.72E-135***	9.44e-135***
Monetary Incentive Delay task	Emotional N-back task	0.154	1.237	0.005	29.36	1859.97	4.82E-156***	1.45e-155***

The tests are reported for the difference between Task 2 from the Intercept (Task 1) in each model. Significance is indicated with: ^$p < .10$, *$p < .05$, **$p < .01$, ***$p < .001$

Table 3. Relationships between brain organization and task performance on the SST.

Fixed Effects	*b*	*β*	*SE*	*t*	*raw p*	*adjusted-p*
Modularity						
resting state	20.293	0.010	118.320	0.172	0.86	0.95
Stop Signal Task (SST)	234.167	0.115	101.526	2.306	0.02*	0.09^
Global efficiency						
resting state	14.523	0.004	250.204	0.058	0.95	0.95
Stop Signal Task (SST)	629.076	0.144	256.943	2.448	0.01*	0.09^
NDI of the Fronto-parietal network						
resting state	-22.236	-0.015	67.015	-0.332	0.74	0.95
Stop Signal Task (SST)	-60.973	-0.040	69.897	-0.872	0.38	0.55
NDI of the Cingulo-opercular network						
resting state	123.858	0.103	57.436	2.156	0.03*	0.32
Stop Signal Task (SST)	56.389	0.045	58.534	0.963	0.34	0.55
NDI of the Default mode network						
resting state	-62.374	-0.045	64.826	-0.962	0.34	0.95
Stop Signal Task (SST)	-134.155	-0.100	60.365	-2.222	0.03*	0.09^
NDI of the Salience network						
resting state	14.618	0.009	71.710	0.204	0.84	0.95
Stop Signal Task (SST)	-36.915	-0.023	71.070	-0.519	0.60	0.67
NDI of the Dorsal attention						

network						
resting state	28.350	0.024	53.910	0.526	0.60	0.95
Stop Signal Task (SST)	-94.489	-0.068	65.073	-1.452	0.15	0.37
NDI of the Ventral attention network						
resting state	-38.766	-0.028	67.408	-0.575	0.57	0.95
Stop Signal Task (SST)	-86.704	-0.060	66.566	-1.303	0.19	0.39
NDI of the Dorsal somatomotor network						
resting state	-57.426	-0.063	45.408	-1.265	0.21	0.95
Stop Signal Task (SST)	-7.148	-0.008	44.760	-0.160	0.87	0.87
NDI of the Visual network						
resting state	16.188	0.014	54.272	0.298	0.77	0.95
Stop Signal Task (SST)	-30.910	-0.036	42.363	-0.730	0.47	0.58

Tests are reported from separate models for the resting state and the SST. Significance is indicated with: ^$p < .10$, *$p < .05$, **$p < .01$, ***$p < .001$

Table 4. Relationships between brain organization and task performance on the MID.

Fixed Effects	***b***	***β***	***SE***	***t***	***raw p***	***adjusted-p***
Modularity						
resting state	5.703	0.028	11.762	0.485	0.63	0.78
Monetary Incentive Delay (MID) Task	2.781	0.014	11.081	0.251	0.80	0.95
Global efficiency						
resting state	-11.928	-0.031	24.872	-0.480	0.63	0.78
Monetary Incentive Delay (MID) Task	-101.498	-0.213	32.730	-3.101	0.002**	0.02*
NDI of the Fronto-						

parietal network						
resting state	-2.258	-0.016	6.663	-0.339	0.73	0.78
Monetary Incentive Delay (MID) Task	-2.090	-0.014	6.726	-0.311	0.76	0.95
NDI of the Cingulo-opercular network						
resting state	-5.387	-0.046	5.733	-0.940	0.35	0.78
Monetary Incentive Delay (MID) Task	-5.957	-0.055	5.488	-1.086	0.28	0.93
NDI of the Default mode network						
resting state	1.778	0.013	6.452	0.276	0.78	0.78
Monetary Incentive Delay (MID) Task	-0.898	-0.007	6.388	-0.141	0.89	0.95
NDI of the Salience network						
resting state	-16.176	-0.106	7.092	-2.281	0.02*	0.23
Monetary Incentive Delay (MID) Task	-10.995	-0.080	6.338	-1.735	0.08	0.42
NDI of the Dorsal attention network						
resting state	4.705	0.042	5.358	0.878	0.38	0.78
Monetary Incentive Delay (MID) Task	-0.422	-0.003	6.218	-0.068	0.95	0.95
NDI of the Ventral attention network						
resting state	-4.296	-0.032	6.702	-0.641	0.52	0.78
Monetary	3.974	0.029	6.469	0.614	0.54	0.95

Incentive Delay (MID) Task						
NDI of the Dorsal somatomotor network						
resting state	3.216	0.037	4.520	0.711	0.48	0.78
Monetary Incentive Delay (MID) Task	2.621	0.026	4.863	0.539	0.59	0.95
NDI of the Visual network						
resting state	-7.146	-0.063	5.387	-1.327	0.19	0.78
Monetary Incentive Delay (MID) Task	-3.651	-0.044	4.254	-0.858	0.39	0.95

Tests are reported from separate models for the resting state and the MID task. Significance is indicated with: ^$p <$ .10, *$p <$ .05, **$p <$ .01, ***$p <$ .001

Table 5. Relationships between brain organization and task performance on the EN-back.

Fixed Effects	***b***	***β***	***SE***	***t***	***raw p***	***adjusted-p***
Modularity						
resting state	0.072	0.025	0.156	0.462	0.64	0.81
Emotional N-back (EN-back) Task	-0.337	-0.107	0.166	-2.027	0.04*	0.11
Global efficiency						
resting state	-0.574	-0.102	0.330	-1.742	0.08^	0.59
Emotional N-back (EN-back) Task	-0.455	-0.071	0.284	-1.602	0.11	0.22
NDI of the Fronto-parietal network						
resting state	-0.068	-0.033	0.089	-0.773	0.44	0.81
Emotional N-back (EN-back) Task	0.036	0.017	0.093	0.388	0.70	0.70

NDI of the Cingulo-opercular network						
resting state	-0.090	-0.054	0.076	-1.188	0.24	0.59
Emotional N-back (EN-back) Task	0.168	0.099	0.077	2.175	0.03*	0.11
NDI of the Default mode network						
resting state	-0.005	-0.003	0.086	-0.060	0.95	0.97
Emotional N-back (EN-back) Task	0.085	0.048	0.080	1.068	0.29	0.38
NDI of the Salience network						
resting state	0.048	0.022	0.095	0.504	0.61	0.81
Emotional N-back (EN-back) Task	-0.140	-0.044	0.136	-1.030	0.30	0.38
NDI of the Dorsal attention network						
resting state	-0.002	-0.001	0.071	-0.033	0.97	0.97
Emotional N-back (EN-back) Task	-0.198	-0.115	0.074	-2.664	0.008**	0.08^
NDI of the Ventral attention network						
resting state	-0.135	-0.070	0.089	-1.514	0.13	0.59
Emotional N-back (EN-back) Task	-0.234	-0.094	0.109	-2.142	0.03*	0.11
NDI of the Dorsal somatomotor network						
resting state	-0.034	-0.027	0.060	-0.559	0.58	0.81
Emotional N-back (EN-back) Task	0.091	0.067	0.062	1.456	0.15	0.24
NDI of the						

Visual network						
resting state	0.092	0.056	0.072	1.282	0.20	0.59
Emotional N-back (EN-back) Task	-0.031	-0.024	0.058	-0.529	0.60	0.66

Tests are reported from separate models for the resting state and the EN-back task. Significance is indicated with: ^p < .10, *p< .05, **p< .01, ***p< .001

Table 6. Differences in brain-task performance relationships between the resting state and the SST state.

Fixed Effects	**Task Performance Metric**	***b***	***β***	***SE***	***t***	***df***	***raw p***	***adjusted-p***
Modularity	**SSRT**							
Intercept (Resting state)		0.315	0.502	0.00261	120.64	609.45		
Stop Signal Task (SST)		0.00006	0.083	0.00002	2.74	492.47	0.0064**	0.04*
Global efficiency	**SSRT**							
Intercept (Resting state)		0.230	0.152	0.00115	199.25	586.52		
Stop Signal Task (SST)		0.00002	0.081	0.00001	2.64	491.84	0.0086**	0.04*
NDI of the Fronto-parietal network	**SSRT**							
Intercept (Resting state)		0.734	0.080	0.00434	169.31	575.78		
Stop Signal Task (SST)		-0.00002	-0.028	0.00003	-0.71	488.08	0.48	0.62
NDI of the Cingulo-opercular network	**SSRT**							
Intercept (Resting state)		0.533	-0.463	0.00501	106.37	590.90		
Stop Signal Task (SST)		-0.00005	-0.058	0.00003	-1.55	491.79	0.12	0.25

NDI of the Default mode network	**SSRT**							
Intercept (Resting state)		0.531	-0.462	0.00465	114.06	590.96		
Stop Signal Task (SST)		-0.00006	-0.075	0.00003	-1.88	492.41	0.06^	0.20
NDI of the Salience network	**SSRT**							
Intercept (Resting state)		0.900	0.049	0.00397	226.75	611.25		
Stop Signal Task (SST)		-0.00002	-0.027	0.00003	-0.56	492.54	0.58	0.64
NDI of the Dorsal attention network	**SSRT**							
Intercept (Resting state)		0.623	-0.244	0.00496	125.50	591.55		
Stop Signal Task (SST)		-0.00006	-0.068	0.00003	-1.72	492.00	0.08^	0.22
NDI of the Ventral attention network	**SSRT**							
Intercept (Resting state)		0.739	-0.368	0.00437	169.23	590.01		
Stop Signal Task (SST)		-0.00003	-0.042	0.00003	-1.15	491.23	0.25	0.42
NDI of the Dorsal somatomotor network	**SSRT**							
Intercept (Resting state)		0.460	0.032	0.00634	72.65	605.55		
Stop Signal Task (SST)		0.00003	0.030	0.00005	0.68	489.61	0.50	0.62
NDI of the Visual network	**SSRT**							
Intercept (Resting state)		0.295	-0.355	0.00589	50.07	625.22		

Stop Signal Task (SST)		-0.00001	-0.009	0.00005	-0.23	490.52	0.82	0.82

The test is reported for the interaction term in each model. Significance is indicated with: ^p < .10, *p< .05, **p< .01, ***p< .001

Table 7. Differences in brain-task performance relationships between the resting state and the MID task state.

Fixed Effects	**Task Performance Metric**	***b***	***β***	***SE***	***t***	***df***	***raw p***	***adjusted-p***
Modularity	**Monetary value won**							
Intercept (Resting state)		0.313	0.438	0.00248	126.17	624.14		
Monetary Incentive Delay (MID) Task		0.0000	-0.001	0.00022	-0.02	490.71	0.99	0.99
Global efficiency	**Monetary value won**							
Intercept (Resting state)		0.230	0.388	0.00101	226.93	616.39		
Monetary Incentive Delay (MID) Task		-0.0002	-0.084	0.00008	-2.55	488.46	0.01*	0.11
NDI of the Fronto-parietal network	**Monetary value won**							
Intercept (Resting state)		0.731	0.257	0.00443	164.84	580.10		
Monetary Incentive Delay (MID) Task		-0.0001	-0.008	0.00027	-0.20	489.73	0.84	0.99
NDI of the Cingulo-opercular network	**Monetary value won**							
Intercept (Resting state)		0.539	-0.397	0.00514	104.88	601.89		
Monetary Incentive		-0.0002	-0.025	0.00038	-0.63	490.13	0.53	0.99

Delay (MID) Task								
NDI of the Default mode network	**Monetary value won**							
Intercept (Resting state)		0.534	-0.533	0.00447	119.43	607.40		
Monetary Incentive Delay (MID) Task		-0.0001	-0.016	0.00034	-0.38	490.65	0.70	0.99
NDI of the Salience network	**Monetary value won**							
Intercept (Resting state)		0.895	-0.074	0.00415	215.89	622.08		
Monetary Incentive Delay (MID) Task		0.00001	0.002	0.00036	0.04	490.10	0.97	0.99
NDI of the Dorsal attention network	**Monetary value won**							
Intercept (Resting state)		0.624	-0.406	0.00496	125.74	610.50		
Monetary Incentive Delay (MID) Task		-0.0005	-0.052	0.00039	-1.24	490.61	0.21	0.99
NDI of the Ventral attention network	**Monetary value won**							
Intercept (Resting state)		0.742	-0.102	0.00437	169.65	606.95		
Monetary Incentive Delay (MID) Task		0.0003	0.040	0.00033	0.89	490.64	0.37	0.99
NDI of the Dorsal somatomotor network	**Monetary value won**							
Intercept (Resting		0.446	-0.102	0.00609	73.16	619.35		

state)								
Monetary Incentive Delay (MID) Task		-0.0002	-0.022	0.00051	-0.47	489.90	0.64	0.99
NDI of the Visual network	**Monetary value won**							
Intercept (Resting state)		0.295	-0.189	0.00580	50.88	636.46		
Monetary Incentive Delay (MID) Task		-0.0002	-0.015	0.00056	-0.33	489.38	0.74	0.99

The test is reported for the interaction term in each model. Significance is indicated with: ^$p < .10$, *$p < .05$, **$p <$ .01, ***$p < .001$

Table 8. Differences in brain-task performance relationships between the resting state and the EN-back task state.

Fixed Effects	**Task Performance Metric**	***b***	***β***	***SE***	***t***	***df***	***raw p***	***adjusted-p***
Modularity	**2-back percent accuracy**							
Intercept (Resting state)		0.309	0.517	0.00229	135.21	676.83		
Emotional N-back (EN-back) Task		-0.024	-0.025	0.01507	-1.61	490.57	0.11	0.25
Global efficiency	**2-back percent accuracy**							
Intercept (Resting state)		0.230	-0.356	0.00126	182.15	651.33		
Emotional N-back (EN-back) Task		-0.002	-0.008	0.00707	-0.32	490.88	0.75	0.75
NDI of the Fronto-parietal network	**2-back percent accuracy**							
Intercept (Resting		0.739	0.079	0.00427	173.03	639.03		

state)								
Emotional N-back (EN-back) Task		0.041	0.077	0.02240	1.84	490.05	0.067^	0.22
NDI of the Cingulo-opercular network	**2-back percent accuracy**							
Intercept (Resting state)		0.541	-0.628	0.00489	110.69	663.29		
Emotional N-back (EN-back) Task		0.081	0.067	0.02953	2.73	490.88	0.0065**	0.03*
NDI of the Default mode network	**2-back percent accuracy**							
Intercept (Resting state)		0.539	-0.721	0.00448	120.16	676.54		
Emotional N-back (EN-back) Task		0.026	0.025	0.02951	0.90	490.40	0.37	0.41
NDI of the Salience network	**2-back percent accuracy**							
Intercept (Resting state)		0.898	-0.250	0.00336	267.10	671.78		
Emotional N-back (EN-back) Task		-0.025	-0.049	0.02175	-1.13	488.10	0.26	0.33
NDI of the Dorsal attention network	**2-back percent accuracy**							
Intercept (Resting state)		0.625	-0.493	0.00511	122.22	666.59		
Emotional N-back (EN-back) Task		-0.114	-0.127	0.03152	-3.62	490.77	0.0003***	0.003**
NDI of the Ventral attention network	**2-back percent accuracy**							
Intercept (Resting state)		0.747	-0.347	0.00387	193.14	655.84		

Emotional N-back (EN-back) Task		-0.034	-0.046	0.02232	-1.54	490.92	0.12	0.25
NDI of the Dorsal somatomotor network	**2-back percent accuracy**							
Intercept (Resting state)		0.460	-0.393	0.00615	74.76	662.00		
Emotional N-back (EN-back) Task		0.047	0.035	0.03684	1.28	490.90	0.20	0.29
NDI of the Visual network	**2-back percent accuracy**							
Intercept (Resting state)		0.295	-0.607	0.00580	50.86	678.24		
Emotional N-back (EN-back) Task		-0.050	-0.027	0.03853	-1.31	490.76	0.19	0.29

The test is reported for the interaction term in each model. Significance is indicated with: ^p < .10, *p< .05, **p< .01, ***p< .001

Table 9. Replication of differences in brain network organization between the resting state and task states.

Task 1 (reference)	***Task 2***	***b***	***β***	***SE***	***t***	***df***	***raw p***	***adjusted-p***
Modularity								
Intercept (Resting state)		0.318	0.748	0.00225	141.41	693.87		
Resting state	Stop Signal task	-0.047	-0.750	0.00122	-38.33	1566.07	2.73E-227***	8.19E-227***
Resting state	Monetary Incentive Delay task	-0.039	-0.628	0.00118	-33.05	1529.01	3.21E-181***	3.85E-181***
Resting state	Emotional N-back task	-0.105	-1.678	0.00191	-54.84	1880.73	0***	0.00E+00***
Stop Signal task	Monetary Incentive Delay task	0.008	0.123	0.001	6.36	1548.59	2.63E-10***	2.63E-10***
Stop Signal task	Emotional N-back	-0.058	-0.927	0.002	-34.48	1825.50	4.37E-201***	6.56E-201***

	task							
Monetary Incentive Delay task	Emotional N-back task	-0.066	-1.050	0.002	-35.49	1868.42	2.72E-211***	5.44E-211***
Global efficiency								
Intercept (Resting state)		0.227	-0.089	0.00102	222.51	653.02		
Resting state	Stop Signal task	-0.006	-0.254	0.00051	-12.22	1553.31	7.86E-33***	7.86E-33***
Resting state	Monetary Incentive Delay task	-0.012	-0.507	0.00049	-25.19	1520.10	2.50E-117***	5.00E-117***
Resting state	Emotional N-back task	0.018	0.745	0.00081	22.69	1837.46	1.06E-100***	1.59E-100***
Stop Signal task	Monetary Incentive Delay task	-0.006	-0.253	0.001	-12.38	1537.66	1.24E-33***	1.49E-33***
Stop Signal task	Emotional N-back task	0.025	0.998	0.001	34.68	1786.08	5.89E-202***	1.77E-201***
Monetary Incentive Delay task	Emotional N-back task	0.031	1.252	0.001	39.46	1825.86	8.57E-247***	5.14E-246***
NDI of the Fronto-parietal network								
Intercept (Resting state)		0.737	0.130	0.00404	182.18	605.70		
Resting state	Stop Signal task	0.004	0.082	0.00165	2.20	1551.36	0.02*	0.03*
Resting state	Monetary Incentive Delay task	-0.015	-0.335	0.00160	-9.32	1527.84	3.82E-20***	7.64E-20***
Resting state	Emotional N-back task	0.020	0.446	0.00266	7.47	1751.44	1.25E-13***	1.88E-13***
Stop Signal task	Monetary Incentive Delay task	-0.019	-0.416	0.002	-11.40	1540.30	5.80E-29***	1.74E-28***
Stop Signal task	Emotional N-back	0.016	0.365	0.002	6.98	1714.29	4.16E-12***	4.99E-12***

	task							
Monetary Incentive Delay task	Emotional N-back task	0.035	0.781	0.003	13.53	1742.94	9.65E-40***	5.79E-39***
NDI of the Cingulo-opercular network								
Intercept (Resting state)		0.550	-0.479	0.00467	117.77	657.07		
Resting state	Stop Signal task	0.034	0.415	0.00230	14.89	1560.64	5.76E-47***	6.91E-47***
Resting state	Monetary Incentive Delay task	0.038	0.457	0.00222	16.92	1528.78	5.70E-59***	8.55E-59***
Resting state	Emotional N-back task	0.124	1.502	0.00363	34.05	1832.45	2.51E-197***	1.51E-196***
Stop Signal task	Monetary Incentive Delay task	0.003	0.042	0.002	1.52	1545.63	0.13	0.13
Stop Signal task	Emotional N-back task	0.090	1.087	0.003	28.10	1783.21	3.75E-144***	1.13E-143***
Monetary Incentive Delay task	Emotional N-back task	0.086	1.045	0.004	24.51	1821.31	6.78E-115***	1.36E-114***
NDI of the Default mode network								
Intercept (Resting state)		0.533	-0.741	0.00402	132.78	678.54		
Resting state	Stop Signal task	0.024	0.333	0.00210	11.45	1563.83	3.29E-29***	3.95E-29***
Resting state	Monetary Incentive Delay task	0.039	0.535	0.00204	18.97	1528.82	2.99E-72***	4.49E-72***
Resting state	Emotional N-back task	0.122	1.695	0.00330	37.11	1861.78	3.85E-226***	2.31E-225***
Stop Signal task	Monetary Incentive Delay task	0.015	0.202	0.002	7.05	1547.33	2.75E-12***	2.75E-12***

Stop Signal task	Emotional N-back task	0.098	1.362	0.003	33.96	1808.72	5.99E-196***	1.80E-195***
Monetary Incentive Delay task	Emotional N-back task	0.084	1.160	0.003	26.27	1849.87	1.65E-129***	3.30E-129***
NDI of the Salience network								
Intercept (Resting state)		0.897	-0.220	0.00344	260.87	712.55		
Resting state	Stop Signal task	0.007	0.179	0.00195	3.79	1568.66	0.00016***	1.91E-04***
Resting state	Monetary Incentive Delay task	0.012	0.285	0.00189	6.21	1529.26	6.99E-10***	1.05E-09***
Resting state	Emotional N-back task	0.035	0.842	0.00303	11.47	1901.78	1.76E-29***	1.06E-28***
Stop Signal task	Monetary Incentive Delay task	0.004	0.106	0.002	2.27	1550.06	0.02*	0.02*
Stop Signal task	Emotional N-back task	0.027	0.663	0.003	10.26	1844.51	4.80E-24***	1.44E-23***
Monetary Incentive Delay task	Emotional N-back task	0.023	0.557	0.003	7.84	1889.15	7.34E-15***	1.47E-14***
NDI of the Dorsal attention network								
Intercept (Resting state)		0.617	-0.686	0.00477	129.21	652.12		
Resting state	Stop Signal task	0.025	0.385	0.00231	10.79	1559.79	3.08E-26***	4.62E-26***
Resting state	Monetary Incentive Delay task	0.048	0.742	0.00224	21.46	1528.65	1.72E-89***	5.16E-89***
Resting state	Emotional N-back task	0.084	1.300	0.00367	22.97	1825.41	8.22E-103***	4.93E-102***
Stop Signal task	Monetary Incentive Delay task	0.023	0.357	0.002	10.14	1545.12	1.89E-23***	1.89E-23***

Stop Signal task	Emotional N-back task	0.059	0.915	0.003	18.44	1777.13	1.29E-69***	2.58E-69***
Monetary Incentive Delay task	Emotional N-back task	0.036	0.558	0.004	10.20	1814.47	8.28E-24***	9.94E-24***
NDI of the Ventral attention network								
Intercept (Resting state)		0.738	-0.441	0.00413	178.71	637.82		
Resting state	Stop Signal task	0.033	0.578	0.00191	17.27	1557.11	2.80E-61***	5.60E-61***
Resting state	Monetary Incentive Delay task	0.013	0.227	0.00185	7.01	1528.12	3.52E-12***	3.52E-12***
Resting state	Emotional N-back task	0.065	1.137	0.00305	21.35	1804.42	2.20E-90***	1.32E-89***
Stop Signal task	Monetary Incentive Delay task	-0.020	-0.351	0.002	-10.65	1543.46	1.36E-25***	1.63E-25***
Stop Signal task	Emotional N-back task	0.032	0.560	0.003	12.00	1759.10	6.21E-32***	9.32E-32***
Monetary Incentive Delay task	Emotional N-back task	0.052	0.910	0.003	17.68	1794.12	1.23E-64***	3.69E-64***
NDI of the Dorsal somatomotor network								
Intercept (Resting state)		0.444	-0.388	0.00561	79.15	683.47		
Resting state	Stop Signal task	0.006	0.065	0.00297	2.16	1564.26	0.03*	0.04*
Resting state	Monetary Incentive Delay task	0.008	0.078	0.00288	2.70	1528.50	0.007**	0.01*
Resting state	Emotional N-back task	0.110	1.112	0.00466	23.66	1868.49	1.90E-108***	5.70E-108***
Stop Signal task	Monetary Incentive	0.001	0.014	0.003	0.46	1547.40	0.64	0.64

	Delay task							
Stop Signal task	Emotional N-back task	0.104	1.048	0.004	25.36	1814.57	1.05E-121***	6.30E-121***
Monetary Incentive Delay task	Emotional N-back task	0.103	1.034	0.005	22.74	1856.42	3.78E-101***	7.56E-101***
NDI of the Visual network								
Intercept (Resting state)		0.290	-0.660	0.00531	54.71	774.53		
Resting state	Stop Signal task	0.095	0.749	0.00340	27.86	1575.94	3.05E-139***	4.58E-139***
Resting state	Monetary Incentive Delay task	0.060	0.472	0.00330	18.05	1529.97	3.79E-66***	4.55E-66***
Resting state	Emotional N-back task	0.224	1.772	0.00517	43.33	1956.72	3.86E-288***	2.32E-287***
Stop Signal task	Monetary Incentive Delay task	-0.035	-0.277	0.003	-10.45	1554.20	9.75E-25***	9.75E-25***
Stop Signal task	Emotional N-back task	0.129	1.023	0.005	28.30	1896.99	3.03E-147***	6.06E-147***
Monetary Incentive Delay task	Emotional N-back task	0.164	1.300	0.005	32.82	1944.16	2.15E-188***	6.45E-188***

The tests are reported for the difference between Task 2 from the Intercept (Task 1) in each model. Significance is indicated with: ^$p < .10$, *$p < .05$, **$p < .01$, ***$p < .001$

Table 10. Replication of relationships between brain organization and task performance on the SST.

Fixed Effects	***b***	***β***	***SE***	***t***	***raw p***	***adjusted-p***
Modularity						
Resting state	52.642	0.023	122.851	0.428	0.67	0.95
Stop Signal Task (SST)	152.656	0.074	109.557	1.393	0.16	0.54
Global efficiency						

Resting state	-34.005	-0.008	270.006	-0.126	0.90	0.95
Stop Signal Task (SST)	674.552	0.154	282.755	2.386	0.017*	0.17
NDI of the Fronto-parietal network						
Resting state	-7.566	-0.005	73.268	-0.103	0.92	0.95
Stop Signal Task (SST)	-9.454	-0.006	74.131	-0.128	0.90	0.90
NDI of the Cingulo-opercular network						
Resting state	3.448	0.003	60.289	0.057	0.95	0.95
Stop Signal Task (SST)	-71.373	-0.058	62.007	-1.151	0.25	0.54
NDI of the Default mode network						
Resting state	186.216	0.120	71.338	2.610	0.009**	0.09^
Stop Signal Task (SST)	22.995	0.016	66.941	0.344	0.73	0.81
NDI of the Salience network						
Resting state	99.805	0.059	76.746	1.300	0.19	0.95
Stop Signal Task (SST)	71.202	0.045	71.804	0.992	0.32	0.54
NDI of the Dorsal attention network						
Resting state	-44.543	-0.037	54.423	-0.818	0.41	0.95
Stop Signal Task (SST)	-53.430	-0.041	60.787	-0.879	0.38	0.54
NDI of the Ventral attention network						
Resting state	35.955	0.027	64.847	0.554	0.58	0.95
Stop Signal Task (SST)	-63.968	-0.046	64.199	-0.996	0.32	0.54
NDI of the Dorsal somatomotor network						
Resting state	20.934	0.022	46.916	0.446	0.66	0.95
Stop Signal Task (SST)	17.389	0.018	47.455	0.366	0.71	0.81
NDI of the Visual network						
Resting state	-62.983	-0.047	61.337	-1.027	0.31	0.95
Stop Signal Task (SST)	-40.976	-0.048	41.940	-0.977	0.33	0.54

Tests are reported from separate models for the resting state and the SST. Significance is indicated with: ^$p < .10$,

*$p < .05$, **$p < .01$, ***$p < .001$

Table 11. Replication of relationships between brain organization and task performance on the MID task.

Fixed Effects	*b*	*β*	*SE*	*t*	*raw p*	*adjusted-p*
Modularity						
Resting state	32.195	0.145	11.977	2.688	0.007**	0.037*
Monetary Incentive Delay (MID) Task	23.414	0.121	11.163	2.097	0.036*	0.091^
Global efficiency						
Resting state	34.352	0.077	26.465	1.298	0.20	0.325
Monetary Incentive Delay (MID) Task	-42.202	-0.096	36.141	-1.168	0.24	0.406
NDI of the Fronto-parietal network						
Resting state	2.820	0.018	7.193	0.392	0.70	0.815
Monetary Incentive Delay (MID) Task	5.144	0.035	6.722	0.765	0.45	0.635
NDI of the Cingulo-opercular network						
Resting state	-13.995	-0.112	5.886	-2.378	0.018*	0.044*
Monetary Incentive Delay (MID) Task	-12.332	-0.108	5.496	-2.244	0.025*	0.084^
NDI of the Default mode network						
Resting state	-0.334	-0.002	7.052	-0.047	0.96	0.962
Monetary Incentive Delay (MID) Task	4.365	0.031	6.611	0.660	0.51	0.637
NDI of the Salience network						

Resting state	-2.567	-0.015	7.547	-0.340	0.734	0.815
Monetary Incentive Delay (MID) Task	-2.735	-0.020	6.348	-0.431	0.667	0.741
NDI of the Dorsal attention network						
Resting state	-2.669	-0.023	5.346	-0.499	0.62	0.815
Monetary Incentive Delay (MID) Task	-0.886	-0.007	5.943	-0.149	0.88	0.882
NDI of the Ventral attention network						
Resting state	-15.111	-0.115	6.332	-2.386	0.017*	0.044*
Monetary Incentive Delay (MID) Task	-9.818	-0.072	6.222	-1.578	0.12	0.230
NDI of the Dorsal somatomotor network						
Resting state	-15.652	-0.170	4.553	-3.438	0.001**	0.006**
Monetary Incentive Delay (MID) Task	-13.949	-0.139	4.821	-2.894	0.004**	0.040*
NDI of the Visual network						
Resting state	-10.745	-0.082	6.009	-1.788	0.074	0.149
Monetary Incentive Delay (MID) Task	-9.897	-0.114	4.410	-2.244	0.025*	0.084^

Tests are reported from separate models for the resting state and the MID task. Significance is indicated with: ^$p <$ .10, *$p <$ .05, **$p <$ .01, ***$p <$ .001

Table 12. Replication of relationships between brain organization and task performance on the EN-back task.

Fixed Effects	*b*	*β*	*SE*	*t*	*raw p*	*adjusted-p*
Modularity						
resting state	0.298	0.101	0.152	1.956	0.051^	0.17
Emotional N-back (EN-back) Task	-0.278	-0.088	0.169	-1.642	0.10	0.25
Global efficiency						
resting state	0.244	0.041	0.336	0.725	0.47	0.70
Emotional N-back (EN-back) Task	0.049	0.008	0.274	0.181	0.86	0.86
NDI of the Fronto-parietal network						
resting state	-0.056	-0.027	0.091	-0.613	0.54	0.70
Emotional N-back (EN-back) Task	-0.034	-0.016	0.090	-0.377	0.71	0.79
NDI of the Cingulo-opercular network						
resting state	-0.151	-0.091	0.075	-2.021	0.044*	0.17
Emotional N-back (EN-back) Task	0.213	0.131	0.073	2.896	0.004**	0.04*
NDI of the Default mode network						
resting state	-0.052	-0.025	0.089	-0.582	0.56	0.70
Emotional N-back (EN-back) Task	0.168	0.095	0.080	2.087	0.037*	0.13
NDI of the Salience network						
resting state	0.008	0.003	0.096	0.081	0.94	0.94
Emotional N-back (EN-back) Task	-0.198	-0.064	0.131	-1.506	0.13	0.27
NDI of the Dorsal attention						

network						
resting state	-0.071	-0.045	0.068	-1.050	0.29	0.67
Emotional N-back (EN-back) Task	-0.180	-0.110	0.072	-2.518	0.012*	0.06^
NDI of the Ventral attention network						
resting state	0.033	0.019	0.081	0.413	0.68	0.76
Emotional N-back (EN-back) Task	0.060	0.024	0.109	0.557	0.58	0.79
NDI of the Dorsal somatomotor network						
resting state	-0.160	-0.131	0.058	-2.762	0.006**	0.06^
Emotional N-back (EN-back) Task	-0.074	-0.056	0.062	-1.187	0.24	0.39
NDI of the Visual network						
resting state	0.074	0.042	0.076	0.968	0.33	0.67
Emotional N-back (EN-back) Task	0.024	0.020	0.057	0.416	0.68	0.79

Tests are reported from separate models for the resting state and the EN-back task. Significance is indicated with: ^p < .10, *p< .05, **p< .01, ***p< .001

Table 13. Replication of differences in brain-task performance relationships between the resting state and the SST state.

Fixed Effects	**Task Performance Metric**	***b***	***β***	***SE***	***t***	***df***	***raw p***	***adjusted-p***
Modularity	**SSRT**							
Intercept (Resting state)		0.318	0.557	0.0027	117.94	620.61		
Stop Signal Task (SST)		0.00003	0.042	0.0000	1.50	507.00	0.13	0.34
Global efficiency	**SSRT**							

Intercept (Resting state)		0.227	0.086	0.0012	196.30	596.50		
Stop Signal Task (SST)		0.00002	0.089	0.0000	3.01	501.20	0.0028**	0.03*
NDI of the Fronto-parietal network	**SSRT**							
Intercept (Resting state)		0.738	0.168	0.0044	168.41	596.04		
Stop Signal Task (SST)		-0.000003	-0.004	0.0000	-0.11	507.39	0.91	0.94
NDI of the Cingulo-opercular network	**SSRT**							
Intercept (Resting state)		0.549	-0.148	0.0052	106.40	615.12		
Stop Signal Task (SST)		-0.00004	-0.050	0.0000	-1.33	507.66	0.18	0.37
NDI of the Default mode network	**SSRT**							
Intercept (Resting state)		0.525	-0.558	0.0046	114.17	603.35		
Stop Signal Task (SST)		-0.00007	-0.091	0.0000	-2.43	505.92	0.016*	0.08^
NDI of the Salience network	**SSRT**							
Intercept (Resting state)		0.899	0.052	0.0042	215.06	625.23		
Stop Signal Task (SST)		-0.00002	-0.032	0.0000	-0.68	507.92	0.50	0.83
NDI of the Dorsal attention network	**SSRT**							
Intercept (Resting state)		0.621	-0.272	0.0056	111.41	603.36		
Stop Signal Task (SST)		-0.00001	-0.007	0.0000	-0.17	507.44	0.86	0.94

NDI of the Ventral attention network	**SSRT**							
Intercept (Resting state)		0.735	-0.353	0.0050	147.50	599.01		
Stop Signal Task (SST)		-0.00006	-0.079	0.0000	-2.23	504.60	0.02*	0.09^
NDI of the Dorsal somatomotor network	**SSRT**							
Intercept (Resting state)		0.455	-0.023	0.0067	68.18	618.63		
Stop Signal Task (SST)		-0.00001	-0.012	0.0000	-0.28	507.56	0.78	0.94
NDI of the Visual network	**SSRT**							
Intercept (Resting state)		0.289	-0.443	0.0060	48.45	652.54		
Stop Signal Task (SST)		-0.000004	-0.003	0.0001	-0.08	506.83	0.94	0.94

The test is reported for the interaction term in each model. Significance is indicated with: ^$p < .10$, *$p < .05$, **$p < .01$, ***$p < .001$

Table 14. Replication of differences in brain-task performance relationships between the resting state and the MID task state.

Fixed Effects	Task Performance Metric	*b*	*β*	*SE*	*t*	*df*	*raw p*	*adj-p*
Modularity	**Monetary value won**							
Intercept (Resting state)		0.317	0.481	0.0026	121.70	604.62		
Monetary Incentive Delay (MID) Task		0.00005	0.008	0.0002	0.26	508.29	0.80	0.930
Global efficiency	**Monetary value won**							
Intercept (Resting state)		0.228	0.324	0.0010	228.41	602.18		
Monetary Incentive Delay (MID) Task		-0.00021	-0.087	0.0001	-2.97	504.48	0.0032**	0.032*
NDI of the Fronto-parietal network	**Monetary value won**							
Intercept (Resting state)		0.738	0.378	0.0045	163.21	578.95		
Monetary Incentive Delay (MID) Task		0.00007	0.010	0.0002	0.27	507.67	0.79	0.930
NDI of the Cingulo-opercular network	**Monetary value won**							
Intercept (Resting state)		0.544	-0.255	0.0054	101.38	592.03		
Monetary Incentive Delay (MID) Task		0.00003	0.003	0.0003	0.09	508.34	0.93	0.930
NDI of the Default mode network	**Monetary value won**							
Intercept		0.534	-0.539	0.0045	119.09	597.37		

(Resting state)								
Monetary Incentive Delay (MID) Task		0.00005	0.006	0.0003	0.15	507.89	0.89	0.930
NDI of the Salience network	**Monetary value won**							
Intercept (Resting state)		0.897	-0.057	0.0044	205.98	609.34		
Monetary Incentive Delay (MID) Task		-0.00013	-0.020	0.0003	-0.41	507.56	0.69	0.930
NDI of the Dorsal attention network	**Monetary value won**							
Intercept (Resting state)		0.616	-0.532	0.0055	112.80	596.31		
Monetary Incentive Delay (MID) Task		0.00006	0.007	0.0004	0.17	508.38	0.87	0.930
NDI of the Ventral attention network	**Monetary value won**							
Intercept (Resting state)		0.737	-0.133	0.0049	150.14	590.90		
Monetary Incentive Delay (MID) Task		0.00017	0.022	0.0003	0.56	507.76	0.58	0.930
NDI of the Dorsal somatomotor network	**Monetary value won**							
Intercept (Resting state)		0.445	-0.125	0.0063	70.26	609.10		
Monetary Incentive Delay (MID) Task		0.00016	0.015	0.0005	0.34	507.48	0.74	0.930
NDI of the Visual	**Monetary value won**							

network								
Intercept (Resting state)		0.289	-0.237	0.0057	50.69	627.95		
Monetary Incentive Delay (MID) Task		-0.00078	-0.071	0.0005	-1.60	508.50	0.11	0.547

The test is reported for the interaction term in each model. Significance is indicated with: ^$p < .10$, *$p < .05$, **$p <$ .01, ***$p < .001$

Table 15. Replication of differences in brain-task performance relationships between the resting state and the EN-back task state.

Fixed Effects	**Task Performance Metric**	***b***	***β***	***SE***	***t***	***df***	***raw p***	***adjusted-p***
Modularity	**2-back percent accuracy**							
Intercept (Resting state)		0.316	0.599	0.0023	136.14	669.03		
Emotional N-back (EN-back) Task		-0.036	-0.036	0.0145	-2.46	507.89	0.014*	0.048*
Global efficiency	**2-back percent accuracy**							
Intercept (Resting state)		0.225	-0.517	0.0013	176.22	654.41		
Emotional N-back (EN-back) Task		-0.008	-0.026	0.0072	-1.10	507.73	0.27	0.431
NDI of the Fronto-parietal network	**2-back percent accuracy**							
Intercept (Resting state)		0.739	0.049	0.0044	169.18	628.55		
Emotional N-back (EN-back) Task		-0.006	-0.011	0.0209	-0.30	507.66	0.77	0.77
NDI of the Cingulo-opercular network	**2-back percent accuracy**							

Intercept (Resting state)		0.548	-0.531	0.0051	107.40	654.93		
Emotional N-back (EN-back) Task		0.149	0.122	0.0291	5.12	507.36	4.33E-07***	4.33E-06***
NDI of the Default mode network	**2-back percent accuracy**							
Intercept (Resting state)		0.536	-0.733	0.0045	120.39	666.98		
Emotional N-back (EN-back) Task		0.063	0.058	0.0275	2.27	507.60	0.02*	0.06^
NDI of the Salience network	**2-back percent accuracy**							
Intercept (Resting state)		0.899	-0.248	0.0034	265.04	669.55		
Emotional N-back (EN-back) Task		-0.031	-0.064	0.0213	-1.46	507.87	0.15	0.29
NDI of the Dorsal attention network	**2-back percent accuracy**							
Intercept (Resting state)		0.614	-0.654	0.0055	111.45	649.07		
Emotional N-back (EN-back) Task		-0.082	-0.088	0.0303	-2.72	506.99	0.0067**	0.03*
NDI of the Ventral attention network	**2-back percent accuracy**							
Intercept (Resting state)		0.744	-0.332	0.0042	175.80	647.80		
Emotional N-back (EN-back) Task		-0.022	-0.029	0.0230	-0.98	507.75	0.33	0.43
NDI of the Dorsal somatomotor network	**2-back percent accuracy**							
Intercept		0.449	-0.478	0.0063	71.33	661.92		

(Resting state)								
Emotional N-back (EN-back) Task		0.035	0.026	0.0375	0.95	507.85	0.34	0.43
NDI of the Visual network	**2-back percent accuracy**							
Intercept (Resting state)		0.284	-0.686	0.0057	49.50	682.97		
Emotional N-back (EN-back) Task		-0.020	-0.011	0.0394	-0.52	507.66	0.60	0.67

The test is reported for the interaction term in each model. Significance is indicated with: ^$p < .10$, *$p < .05$, **$p < .01$, ***$p < .001$

APPENDIX 1: CORRELATIONS BETWEEN BRAIN NETWORK ORGANIZATION METRICS DURING THE RESTING STATE (DISCOVERY SAMPLE).

	density	mean FC	Mod	GE	NDI FPN	NDI CON	NDI DMN	NDI SN	NDI DAN	NDI VAN	NDI SMH	NDI VN
density	1											
mean FC	-0.76***	1										
Mod	-0.57***	0.59***	1									
GE	0.95***	-0.62***	-0.51***	1								
NDI FPN	0.17***	-0.17***	-0.34***	0.14**	1							
NDI CON	0.26***	-0.32***	-0.54***	0.20***	0.14**	1						
NDI DMN	0.24***	-0.19***	-0.51***	0.30***	0.21***	0.25***	1					
NDI SN	0.20***	-0.18***	-0.16***	0.22***	0.07	0.15***	0.17***	1				
NDI DAN	0.26***	-0.23***	-0.56***	0.26***	0.17***	0.30***	0.25***	0.13**	1			
NDI VAN	0.43***	-0.38***	-0.35***	0.38***	0.16***	0.14**	0.09	0.11*	0.17***	1		
NDI SMH	0.42***	-0.42***	-0.62***	0.36***	0.16***	0.35***	0.27***	0.13**	0.33***	0.27***	1	
NDI VN	0.16***	-0.23***	-0.48***	0.14**	0.06	0.11*	0.09*	-0.09*	0.26***	0.03	0.12**	1

Correlation values are shown for each brain metric pair. Significance is shown for uncorrected p values: *$p < .05$, **$p < .01$, **$p < .001$. Mod = modularity, GE = global efficiency, NDI = network dissociation index, FPN = fronto-parietal network, CON = cingulo-opercular network, DMN = default mode network, SN = salience network, DAN = dorsal attention network, VAN = ventral attention network, SMH = somatomotor hand network, VN = visual network

APPENDIX 2. CORRELATIONS BETWEEN BRAIN NETWORK ORGANIZATION METRICS DURING THE RESTING STATE (REPLICATION SAMPLE).

	density	mean FC	Mod	GE	NDI FPN	NDI CON	NDI DMN	NDI SN	NDI DAN	NDI VAN	NDI SMH	NDI VN
density	1											
mean FC	-0.77***	1										
Mod	-0.55***	0.57***	1									
GE	0.94***	-0.61***	-0.48***	1								
NDI FPN	0.27***	-0.26***	-0.46***	0.26***	1							
NDI CON	0.18***	-0.30***	-0.55***	0.10*	0.21***	1						
NDI DMN	0.24***	-0.15***	-0.49***	0.28***	0.24***	0.22***	1					
NDI SN	0.20***	-0.17***	-0.31***	0.18***	0.19***	0.20***	0.18***	1				
NDI DAN	0.24***	-0.19***	-0.56***	0.24***	0.24***	0.28***	0.29***	0.17***	1			
NDI VAN	0.43***	-0.40***	-0.46***	0.39***	0.27***	0.22***	0.18***	0.15***	0.30***	1		
NDI SMH	0.43***	-0.44***	-0.64***	0.36***	0.26***	0.37***	0.24***	0.14**	0.35***	0.29***	1	
NDI VN	0.18***	-0.23***	-0.44***	0.18***	0.16***	0.11*	0.10*	0.05	0.13**	0.11**	0.15***	1

Correlation values are shown for each brain metric pair. Significance is shown for uncorrected p values: *$p < .05$, **$p < .01$, **$p < .001$. Mod = modularity, GE = global efficiency, NDI = network dissociation index, FPN = fronto-parietal network, CON = cingulo-opercular network, DMN = default mode network, SN = salience network, DAN = dorsal attention network, VAN = ventral attention network, SMH = somatomotor hand network, VN = visual network

APPENDIX 3: CORRELATIONS BETWEEN BRAIN NETWORK ORGANIZATION METRICS DURING THE SST (DISCOVERY SAMPLE).

	density	mean FC	Mod	GE	NDI FPN	NDI CON	NDI DMN	NDI SN	NDI DAN	NDI VAN	NDI SMH	NDI VN
density	1											
mean FC	-0.74***	1										
Mod	-0.37***	0.45***	1									
GE	0.94***	-0.62***	-0.24***	1								
NDI FPN	0.08	-0.17***	-0.36***	0.05	1							
NDI CON	0.17***	-0.31***	-0.51***	0.11*	0.15***	1						
NDI DMN	0.16***	-0.10*	-0.52***	0.17***	0.23***	0.15***	1					
NDI SN	0.10*	-0.17***	-0.23***	0.11*	0.12**	0.21***	0.17***	1				
NDI DAN	0.30***	-0.31***	-0.52***	0.26***	0.19***	0.28***	0.28***	0.19***	1			
NDI VAN	0.20***	-0.22***	-0.35***	0.14**	0.16***	0.13**	0.14**	0.09	0.24***	1		
NDI SMH	0.30***	-0.34***	-0.53***	0.21***	0.13**	0.34***	0.13**	0.10*	0.29***	0.16***	1	
NDI VN	0.10*	-0.36***	-0.53***	0.01	0.12**	0.23***	0.05	0.11*	0.16***	0.08	0.23***	1

Correlation values are shown for each brain metric pair. Significance is shown for uncorrected p values: *$p < .05$, **$p < .01$, **$p < .001$. Mod = modularity, GE = global efficiency, NDI = network dissociation index, FPN = fronto-parietal network, CON = cingulo-opercular network, DMN = default mode network, SN = salience network, DAN = dorsal attention network, VAN = ventral attention network, SMH = somatomotor hand network, VN = visual network

APPENDIX 4: CORRELATIONS BETWEEN BRAIN NETWORK ORGANIZATION METRICS DURING THE SST (REPLICATION SAMPLE).

	density	mean FC	Mod	GE	NDI FPN	NDI CON	NDI DMN	NDI SN	NDI DAN	NDI VAN	NDI SMH	NDI VN
density	1											
mean FC	-0.81***	1										
Mod	-0.50***	0.53***	1									
GE	0.93***	-0.70***	-0.36***	1								
NDI FPN	0.18***	-0.19***	-0.36***	0.15***	1							
NDI CON	0.20***	-0.33***	-0.54***	0.13**	0.21***	1						
NDI DMN	0.24***	-0.17***	-0.49***	0.26***	0.26***	0.12**	1					
NDI SN	0.06	-0.05	-0.27***	0.06	0.16***	0.22***	0.22***	1				
NDI DAN	0.29***	-0.32***	-0.58***	0.21***	0.24***	0.32***	0.28***	0.17***	1			
NDI VAN	0.23***	-0.28***	-0.42***	0.16***	0.18***	0.22***	0.16***	0.15***	0.32***	1		
NDI SMH	0.37***	-0.42***	-0.57***	0.28***	0.17***	0.37***	0.19***	0.10*	0.36***	0.20***	1	
NDI VN	0.23***	-0.38***	-0.57***	0.15***	0.16***	0.34***	0.09*	0.13**	0.19***	0.18***	0.23***	1

Correlation values are shown for each brain metric pair. Significance is shown for uncorrected p values: *$p < .05$, **$p < .01$, **$p < .001$. Mod = modularity, GE = global efficiency, NDI = network dissociation index, FPN = fronto-parietal network, CON = cingulo-opercular network, DMN = default mode network, SN = salience network, DAN = dorsal attention network, VAN = ventral attention network, SMH = somatomotor hand network, VN = visual network

APPENDIX 5: CORRELATIONS BETWEEN BRAIN NETWORK ORGANIZATION METRICS DURING THE MID (DISCOVERY SAMPLE).

	density	mean FC	Mod	GE	NDI FPN	NDI CON	NDI DMN	NDI SN	NDI DAN	NDI VAN	NDI SMH	NDI VN
density	1											
mean FC	-0.85***	1										
Mod	-0.41***	0.53***	1									
GE	0.93***	-0.74***	-0.30***	1								
NDI FPN	0.03	-0.08	-0.33***	0	1							
NDI CON	0.22***	-0.34***	-0.59***	0.17***	0.16***	1						
NDI DMN	0.10*	-0.18***	-0.50***	0.10*	0.21***	0.29***	1					
NDI SN	0.02	-0.09*	-0.22***	0.03	0.08	0.23***	0.14**	1				
NDI DAN	0.21***	-0.27***	-0.51***	0.16***	0.16***	0.29***	0.27***	0.12**	1			
NDI VAN	0.19***	-0.24***	-0.39***	0.16***	0.14**	0.19***	0.12**	0.08	0.18***	1		
NDI SMH	0.19***	-0.22***	-0.54***	0.13**	0.08	0.31***	0.11*	0.10*	0.29***	0.15***	1	
NDI VN	0.11*	-0.32***	-0.58***	0.09*	0.11*	0.34***	0.19***	0.16***	0.20***	0.17***	0.19***	1

Correlation values are shown for each brain metric pair. Significance is shown for uncorrected p values: *$p < .05$, **$p < .01$, **$p < .001$. Mod = modularity, GE = global efficiency, NDI = network dissociation index, FPN = fronto-parietal network, CON = cingulo-opercular network, DMN = default mode network, SN = salience network, DAN = dorsal attention network, VAN = ventral attention network, SMH = somatomotor hand network, VN = visual network

APPENDIX 6: CORRELATIONS BETWEEN BRAIN NETWORK ORGANIZATION METRICS DURING THE MID (REPLICATION SAMPLE).

	density	mean FC	Mod	GE	NDI FPN	NDI CON	NDI DMN	NDI SN	NDI DAN	NDI VAN	NDI SMH	NDI VN
density	1											
mean FC	-0.88***	1										
Mod	-0.56***	0.60***	1									
GE	0.94***	-0.84***	-0.47***	1								
NDI FPN	0.17***	-0.19***	-0.43***	0.14**	1							
NDI CON	0.27***	-0.32***	-0.62***	0.23***	0.27***	1						
NDI DMN	0.28***	-0.31***	-0.52***	0.28***	0.25***	0.25***	1					
NDI SN	0.10*	-0.12**	-0.25***	0.07	0.23***	0.19***	0.11*	1				
NDI DAN	0.27***	-0.27***	-0.55***	0.23***	0.20***	0.29***	0.32***	0.19***	1			
NDI VAN	0.23***	-0.29***	-0.39***	0.22***	0.24***	0.28***	0.14**	0.09*	0.22***	1		
NDI SMH	0.37***	-0.38***	-0.62***	0.34***	0.21***	0.34***	0.21***	0.10*	0.39***	0.14**	1	
NDI VN	0.27***	-0.38***	-0.61***	0.25***	0.20***	0.39***	0.18***	0.17***	0.20***	0.23***	0.28***	1

Correlation values are shown for each brain metric pair. Significance is shown for uncorrected p values: *$p < .05$, **$p < .01$, **$p < .001$. Mod = modularity, GE = global efficiency, NDI = network dissociation index, FPN = fronto-parietal network, CON = cingulo-opercular network, DMN = default mode network, SN = salience network, DAN = dorsal attention network, VAN = ventral attention network, SMH = somatomotor hand network, VN = visual network

APPENDIX 7: CORRELATIONS BETWEEN BRAIN NETWORK ORGANIZATION METRICS DURING THE EN-BACK (DISCOVERY SAMPLE).

	density	mean FC	Mod	GE	NDI FPN	NDI CON	NDI DMN	NDI SN	NDI DAN	NDI VAN	NDI SMH	NDI VN
density	1											
mean FC	-0.46***	1										
Mod	-0.60***	0.60***	1									
GE	0.94***	-0.27***	-0.45***	1								
NDI FPN	0.04	-0.27***	-0.34***	0	1							
NDI CON	0.34***	-0.38***	-0.61***	0.23***	0.20***	1						
NDI DMN	0.26***	-0.31***	-0.59***	0.19***	0.19***	0.32***	1					
NDI SN	0.22***	-0.19***	-0.24***	0.20***	0.08	0.20***	0.15**	1				
NDI DAN	0.20***	-0.12**	-0.37***	0.19***	0.04	0.10*	0.17***	0.11*	1			
NDI VAN	0.24***	-0.27***	-0.36***	0.18***	0.14**	0.17***	0.14**	0.07	0.08	1		
NDI SMH	0.28***	-0.40***	-0.55***	0.21***	0.20***	0.29***	0.18***	0.14**	0.14**	0.15***	1	
NDI VN	0.30***	-0.37***	-0.54***	0.24***	0.12**	0.26***	0.12**	0.04	0.11*	0.18***	0.17***	1

Correlation values are shown for each brain metric pair. Significance is shown for uncorrected p values: *$p < .05$, **$p < .01$, **$p < .001$. Mod = modularity, GE = global efficiency, NDI = network dissociation index, FPN = fronto-parietal network, CON = cingulo-opercular network, DMN = default mode network, SN = salience network, DAN = dorsal attention network, VAN = ventral attention network, SMH = somatomotor hand network, VN = visual network

APPENDIX 8: CORRELATIONS BETWEEN BRAIN NETWORK ORGANIZATION METRICS DURING THE EN-BACK (REPLICATION SAMPLE).

	density	mean FC	Mod	GE	NDI FPN	NDI CON	NDI DMN	NDI SN	NDI DAN	NDI VAN	NDI SMH	NDI VN
density	1											
mean FC	-0.45***	1										
Mod	-0.59***	0.60***	1									
GE	0.95***	-0.26***	-0.46***	1								
NDI FPN	0.03	-0.16***	-0.27***	0.02	1							
NDI CON	0.29***	-0.34***	-0.60***	0.22***	0.15***	1						
NDI DMN	0.30***	-0.34***	-0.60***	0.24***	0.17***	0.34***	1					
NDI SN	0.05	-0.16***	-0.15***	0.04	0.12**	0.15***	0.09*	1				
NDI DAN	0.07	-0.11*	-0.30***	0.08	0.08	0.10*	0.10*	0.09*	1			
NDI VAN	0.22***	-0.23***	-0.36***	0.18***	0.22***	0.16***	0.12**	0.11*	0.13**	1		
NDI SMH	0.31***	-0.38***	-0.59***	0.23***	0.08	0.22***	0.26***	0.04	0.17***	0.23***	1	
NDI VN	0.32***	-0.39***	-0.57***	0.24***	0.11**	0.25***	0.15***	0.03	-0.01	0.14**	0.22***	1

Correlation values are shown for each brain metric pair. Significance is shown for uncorrected p values: *$p < .05$, **$p < .01$, **$p < .001$. Mod = modularity, GE = global efficiency, NDI = network dissociation index, FPN = fronto-parietal network, CON = cingulo-opercular network, DMN = default mode network, SN = salience network, DAN = dorsal attention network, VAN = ventral attention network, SMH = somatomotor hand network, VN = visual network

APPENDIX 9: DIFFERENCES IN BRAIN NETWORK ORGANIZATION BETWEEN THE RESTING STATE AND TASK STATES WITH BY CORRECTION.

Task 1 (Reference)	*Task 2*	*b*	*β*	*SE*	*t*	*df*	*raw p*	*adjusted-p*
Modularity								
Intercept (Resting state)		0.314	0.715	0.00214	146.632	734.9		
Resting state	Stop Signal task	-0.045	-0.727	0.00131	-34.028	1530.07	1.91E-189***	1.40e-188***
Resting state	Monetary Incentive Delay task	-0.039	-0.63	0.00126	-30.637	1482.41	4.21E-160***	1.24e-159***
Resting state	Emotional N-back task	-0.101	-1.646	0.00215	-47.136	1847.88	3.88e-319***	5.70e-318***
Stop Signal task	Monetary Incentive Delay task	0.006	0.098	0.001	4.69	1500.15	2.96E-06***	7.25e-06***
Stop Signal task	Emotional N-back task	-0.056	-0.919	0.002	-30.56	1793.11	1.76E-165***	6.47e-165***
Monetary Incentive Delay task	Emotional N-back task	-0.063	-1.017	0.002	-30.62	1832.12	1.15E-166***	5.64e-166***
Global efficiency								
Intercept (Resting state)		0.23	0.02	0.00101	227.631	662.37		
Resting state	Stop Signal task	-0.007	-0.285	0.00053	-12.759	1516.57	1.72E-35***	5.06e-35***
Resting state	Monetary Incentive Delay task	-0.013	-0.561	0.00051	-26.202	1478.92	1.29E-124***	6.32e-124***
Resting state	Emotional N-back task	0.016	0.671	0.00089	18.025	1771.75	8.03E-67***	2.95e-66***
Stop Signal task	Monetary Incentive Delay task	-0.007	-0.276	0.001	-12.70	1492.97	3.72E-35***	9.11e-35***
Stop Signal task	Emotional N-back task	0.023	0.956	0.001	29.95	1724.78	4.52E-159***	3.32e-158***
Monetary Incentive	Emotional N-back	0.029	1.232	0.001	34.86	1757.86	7.59E-203***	1.12e-201***

Delay task	task							
NDI of the Fronto-parietal network								
Intercept (Resting state)		0.736	0.132	0.0039	188.775	611.64		
Resting state	Stop Signal task	0.003	0.076	0.00176	1.889	1507.53	0.059^	1.45e-01
Resting state	Monetary Incentive Delay task	-0.012	-0.282	0.00169	-7.321	1478.84	4.04E-13***	1.98e-12***
Resting state	Emotional N-back task	0.018	0.403	0.00298	5.908	1702	4.18E-09***	1.54e-08***
Stop Signal task	Monetary Incentive Delay task	-0.016	-0.359	0.002	-9.15	1489.57	1.87E-19***	1.37e-18***
Stop Signal task	Emotional N-back task	0.014	0.327	0.003	5.60	1665.33	2.44E-08***	7.17e-08***
Monetary Incentive Delay task	Emotional N-back task	0.030	0.685	0.003	10.59	1691.05	1.95E-25***	2.87e-24***
NDI of the Cingulo-opercular network								
Intercept (Resting state)		0.539	-0.634	0.00441	122.354	672.89		
Resting state	Stop Signal task	0.032	0.386	0.00238	13.453	1519.42	4.63E-39***	1.36e-38***
Resting state	Monetary Incentive Delay task	0.037	0.444	0.00228	16.106	1480.45	6.67E-54***	2.45e-53***
Resting state	Emotional N-back task	0.127	1.539	0.00395	32.218	1783.15	7.16E-180***	1.05e-178***
Stop Signal task	Monetary Incentive Delay task	0.005	0.057	0.002	2.05	1494.99	0.04*	9.80e-02^
Stop Signal task	Emotional N-back task	0.095	1.152	0.003	28.13	1734.92	9.81E-144***	7.21e-143***
Monetary Incentive	Emotional N-back	0.091	1.095	0.004	24.15	1768.93	1.43E-111***	7.01e-111***

Delay task	task							
NDI of the Default mode network								
Intercept (Resting state)		0.534	-0.741	0.00399	133.896	697.06		
Resting state	Stop Signal task	0.024	0.333	0.00227	10.689	1524.01	9.18E-26***	2.70e-25***
Resting state	Monetary Incentive Delay task	0.036	0.5	0.00218	16.699	1481.55	1.72E-57***	6.32e-57***
Resting state	Emotional N-back task	0.126	1.735	0.00375	33.669	1810.11	2.20E-193***	3.23e-192***
Stop Signal task	Monetary Incentive Delay task	0.012	0.167	0.002	5.48	1497.38	4.91E-08***	1.20e-07***
Stop Signal task	Emotional N-back task	0.102	1.402	0.003	31.66	1758.79	1.64E-174***	1.21e-173***
Monetary Incentive Delay task	Emotional N-back task	0.090	1.235	0.004	25.23	1795.09	1.93E-120***	9.46e-120***
NDI of the Salience network								
Intercept (Resting state)		0.897	-0.228	0.00322	278.906	751.38		
Resting state	Stop Signal task	0.01	0.236	0.00203	4.788	1531.76	1.85E-06***	5.44e-06***
Resting state	Monetary Incentive Delay task	0.014	0.337	0.00196	7.1	1481.78	1.92E-12***	9.41e-12***
Resting state	Emotional N-back task	0.036	0.868	0.00331	10.838	1863.15	1.38E-26***	2.03e-25***
Stop Signal task	Monetary Incentive Delay task	0.004	0.101	0.002	2.09	1500.37	0.04*	9.80e-02^
Stop Signal task	Emotional N-back task	0.026	0.632	0.003	9.16	1807.33	1.38E-19***	1.01e-18***
Monetary Incentive Delay task	Emotional N-back task	0.022	0.532	0.003	6.98	1847.25	4.13E-12***	1.52e-11***

NDI of the Dorsal attention network								
Intercept (Resting state)		0.624	-0.584	0.00425	146.906	684.45		
Resting state	Stop Signal task	0.025	0.399	0.00235	10.507	1521.82	5.58E-25***	2.05e-24***
Resting state	Monetary Incentive Delay task	0.046	0.742	0.00225	20.339	1481.21	2.66E-81***	3.91e-80***
Resting state	Emotional N-back task	0.076	1.228	0.00389	19.491	1796.13	6.63E-77***	4.87e-76***
Stop Signal task	Monetary Incentive Delay task	0.021	0.342	0.002	9.25	1496.35	7.60E-20***	2.23e-19***
Stop Signal task	Emotional N-back task	0.051	0.829	0.003	15.32	1746.39	8.11E-50***	3.97e-49***
Monetary Incentive Delay task	Emotional N-back task	0.030	0.486	0.004	8.13	1781.51	8.26E-16***	2.02e-15***
NDI of the Ventral attention network								
Intercept (Resting state)		0.741	-0.46	0.00366	202.492	667.37		
Resting state	Stop Signal task	0.033	0.603	0.00195	16.954	1518.67	3.52E-59***	1.72e-58***
Resting state	Monetary Incentive Delay task	0.011	0.204	0.00187	5.98	1480.64	2.79E-09***	6.84e-09***
Resting state	Emotional N-back task	0.063	1.153	0.00324	19.453	1776.16	1.45E-76***	2.13e-75***
Stop Signal task	Monetary Incentive Delay task	-0.022	-0.399	0.002	-11.52	1494.83	1.70E-29***	6.25e-29***
Stop Signal task	Emotional N-back task	0.030	0.549	0.003	10.81	1728.88	2.02E-26***	5.94e-26***
Monetary Incentive Delay task	Emotional N-back task	0.052	0.949	0.003	16.86	1762.19	2.92E-59***	1.72e-58***

NDI of the Dorsal somatomotor network								
Intercept (Resting state)		0.452	-0.324	0.00545	82.959	682.05		
Resting state	Stop Signal task	0.007	0.07	0.00301	2.26	1520.33	0.02*	7.35e-02^
Resting state	Monetary Incentive Delay task	0.006	0.06	0.00289	2.018	1479.71	0.04*	1.18e-01
Resting state	Emotional N-back task	0.109	1.131	0.00499	21.927	1794.89	1.27E-94***	9.33e-94***
Stop Signal task	Monetary Incentive Delay task	-0.001	-0.010	0.003	-0.33	1494.86	0.74	1.00e+00
Stop Signal task	Emotional N-back task	0.103	1.061	0.004	23.96	1745.06	6.56E-110***	9.64e-109***
Monetary Incentive Delay task	Emotional N-back task	0.104	1.071	0.005	21.86	1780.24	5.06E-94***	2.48e-93***
NDI of the Visual network								
Intercept (Resting state)		0.297	-0.6	0.00525	56.647	768.17		
Resting state	Stop Signal task	0.088	0.709	0.00341	25.897	1534.82	5.48E-123***	2.01e-122***
Resting state	Monetary Incentive Delay task	0.062	0.502	0.00328	19.061	1483.03	1.26E-72***	3.70e-72***
Resting state	Emotional N-back task	0.216	1.739	0.00551	39.268	1875.79	1.15E-246***	1.69e-245***
Stop Signal task	Monetary Incentive Delay task	-0.026	-0.207	0.003	-7.74	1502.28	1.87E-14***	4.58e-14 ***
Stop Signal task	Emotional N-back task	0.128	1.030	0.005	26.97	1819.68	4.72E-135***	2.31e-134***
Monetary Incentive Delay task	Emotional N-back task	0.154	1.237	0.005	29.36	1859.97	4.82E-156***	3.54e-155***

The tests are reported for the difference between Task 2 from the Intercept (Task 1) in each model. Significance is indicated with: ^$p < .10$, *$p < .05$, **$p < .01$, ***$p < .001$

APPENDIX 10: REPLICATION OF DIFFERENCES IN BRAIN NETWORK ORGANIZATION BETWEEN THE RESTING STATE AND TASK STATES WITH BY CORRECTION.

Fixed Effects		*b*	*β*	*SE*	*t*	*df*	*raw p*	*adjusted-p*
Modularity								
Intercept (Resting state)		0.318	0.748	0.00225	141.41	693.87		
Resting state	Stop Signal task	-0.047	-0.750	0.00122	-38.33	1566.07	2.73E-227***	2.01e-22***
Resting state	Monetary Incentive Delay task	-0.039	-0.628	0.00118	-33.05	1529.01	3.21E-181***	9.44e-181***
Resting state	Emotional N-back task	-0.105	-1.678	0.00191	-54.84	1880.73	0***	0.00e+00***
Stop Signal task	Monetary Incentive Delay task	0.008	0.123	0.001	6.36	1548.59	2.63E-10***	6.44e-10***
Stop Signal task	Emotional N-back task	-0.058	-0.927	0.002	-34.48	1825.50	4.37E-201***	1.61e-200***
Monetary Incentive Delay task	Emotional N-back task	-0.066	-1.050	0.002	-35.49	1868.42	2.72E-211***	1.33e-210***
Global efficiency								
Intercept (Resting state)		0.227	-0.089	0.00102	222.51	653.02		
Resting state	Stop Signal task	-0.006	-0.254	0.00051	-12.22	1553.31	7.86E-33***	1.93e-32***
Resting state	Monetary Incentive Delay task	-0.012	-0.507	0.00049	-25.19	1520.10	2.50E-117***	1.23e-116***
Resting state	Emotional N-back task	0.018	0.745	0.00081	22.69	1837.46	1.06E-100***	3.90e-100***
Stop Signal task	Monetary Incentive Delay task	-0.006	-0.253	0.001	-12.38	1537.66	1.24E-33***	3.65e-33***
Stop Signal task	Emotional N-back task	0.025	0.998	0.001	34.68	1786.08	5.89E-202***	4.33e-201***
Monetary Incentive	Emotional N-back task	0.031	1.252	0.001	39.46	1825.86	8.57E-247***	1.26e-245***

Delay task								
NDI of the Fronto-parietal network								
Intercept (Resting state)		0.737	0.130	0.00404	182.18	605.70		
Resting state	Stop Signal task	0.004	0.082	0.00165	2.20	1551.36	0.02*	4.90e-02*
Resting state	Monetary Incentive Delay task	-0.015	-0.335	0.00160	-9.32	1527.84	3.82E-20***	1.87e-19***
Resting state	Emotional N-back task	0.020	0.446	0.00266	7.47	1751.44	1.25E-13***	4.59e-13***
Stop Signal task	Monetary Incentive Delay task	-0.019	-0.416	0.002	-11.40	1540.30	5.80E-29***	4.26e-28***
Stop Signal task	Emotional N-back task	0.016	0.365	0.002	6.98	1714.29	4.16E-12***	1.22e-11***
Monetary Incentive Delay task	Emotional N-back task	0.035	0.781	0.003	13.53	1742.94	9.65E-40***	1.42e-38***
NDI of the Cingulo-opercular network								
Intercept (Resting state)		0.550	-0.479	0.00467	117.77	657.07		
Resting state	Stop Signal task	0.034	0.415	0.00230	14.89	1560.64	5.76E-47***	1.69e-46***
Resting state	Monetary Incentive Delay task	0.038	0.457	0.00222	16.92	1528.78	5.70E-59***	2.09e-58***
Resting state	Emotional N-back task	0.124	1.502	0.00363	34.05	1832.45	2.51E-197***	3.69e-196***
Stop Signal task	Monetary Incentive Delay task	0.003	0.042	0.002	1.52	1545.63	0.13	3.19e-01***
Stop Signal task	Emotional N-back task	0.090	1.087	0.003	28.10	1783.21	3.75E-144***	2.76e-143***

Monetary Incentive Delay task	Emotional N-back task	0.086	1.045	0.004	24.51	1821.31	6.78E-115***	3.32e-114***
NDI of the Default mode network								
Intercept (Resting state)		0.533	-0.741	0.00402	132.78	678.54		
Resting state	Stop Signal task	0.024	0.333	0.00210	11.45	1563.83	3.29E-29***	9.67e-29***
Resting state	Monetary Incentive Delay task	0.039	0.535	0.00204	18.97	1528.82	2.99E-72***	1.10e-71***
Resting state	Emotional N-back task	0.122	1.695	0.00330	37.11	1861.78	3.85E-226***	5.66e-225***
Stop Signal task	Monetary Incentive Delay task	0.015	0.202	0.002	7.05	1547.33	2.75E-12***	6.74e-12***
Stop Signal task	Emotional N-back task	0.098	1.362	0.003	33.96	1808.72	5.99E-196***	4.40e-195***
Monetary Incentive Delay task	Emotional N-back task	0.084	1.160	0.003	26.27	1849.87	1.65E-129***	8.09e-129***
NDI of the Salience network								
Intercept (Resting state)		0.897	-0.220	0.00344	260.87	712.55		
Resting state	Stop Signal task	0.007	0.179	0.00195	3.79	1568.66	0.00016***	4.70e-04***
Resting state	Monetary Incentive Delay task	0.012	0.285	0.00189	6.21	1529.26	6.99E-10***	2.57e-09***
Resting state	Emotional N-back task	0.035	0.842	0.00303	11.47	1901.78	1.76E-29***	2.59e-28***
Stop Signal task	Monetary Incentive Delay task	0.004	0.106	0.002	2.27	1550.06	0.02*	4.90e-02
Stop Signal task	Emotional N-back task	0.027	0.663	0.003	10.26	1844.51	4.80E-24***	3.53e-23*
Monetary	Emotional	0.023	0.557	0.003	7.84	1889.15	7.34E-	3.60e-

Incentive Delay task	N-back task						15***	14***
NDI of the Dorsal attention network								
Intercept (Resting state)		0.617	-0.686	0.00477	129.21	652.12		
Resting state	Stop Signal task	0.025	0.385	0.00231	10.79	1559.79	3.08E-26***	1.13e-25***
Resting state	Monetary Incentive Delay task	0.048	0.742	0.00224	21.46	1528.65	1.72E-89***	1.26e-88***
Resting state	Emotional N-back task	0.084	1.300	0.00367	22.97	1825.41	8.22E-103***	1.21e-101***
Stop Signal task	Monetary Incentive Delay task	0.023	0.357	0.002	10.14	1545.12	1.89E-23***	4.63e-23***
Stop Signal task	Emotional N-back task	0.059	0.915	0.003	18.44	1777.13	1.29E-69***	6.32e-69***
Monetary Incentive Delay task	Emotional N-back task	0.036	0.558	0.004	10.20	1814.47	8.28E-24***	2.43e-23***
NDI of the Ventral attention network								
Intercept (Resting state)		0.738	-0.441	0.00413	178.71	637.82		
Resting state	Stop Signal task	0.033	0.578	0.00191	17.27	1557.11	2.80E-61***	1.37e-60***
Resting state	Monetary Incentive Delay task	0.013	0.227	0.00185	7.01	1528.12	3.52E-12***	8.62e-12***
Resting state	Emotional N-back task	0.065	1.137	0.00305	21.35	1804.42	2.20E-90***	3.23e-89***
Stop Signal task	Monetary Incentive Delay task	-0.020	-0.351	0.002	-10.65	1543.46	1.36E-25***	4.00e-25***
Stop Signal task	Emotional N-back task	0.032	0.560	0.003	12.00	1759.10	6.21E-32***	2.28e-31***
Monetary Incentive	Emotional N-back task	0.052	0.910	0.003	17.68	1794.12	1.23E-64***	9.04e-64***

Delay task								
NDI of the Dorsal somatomotor network								
Intercept (Resting state)		0.444	-0.388	0.00561	79.15	683.47		
Resting state	Stop Signal task	0.006	0.065	0.00297	2.16	1564.26	0.03*	8.82e-02^
Resting state	Monetary Incentive Delay task	0.008	0.078	0.00288	2.70	1528.50	0.007**	2.57e-02*
Resting state	Emotional N-back task	0.110	1.112	0.00466	23.66	1868.49	1.90E-108***	1.40e-107***
Stop Signal task	Monetary Incentive Delay task	0.001	0.014	0.003	0.46	1547.40	0.64	1.00e+00
Stop Signal task	Emotional N-back task	0.104	1.048	0.004	25.36	1814.57	1.05E-121***	1.54e-120***
Monetary Incentive Delay task	Emotional N-back task	0.103	1.034	0.005	22.74	1856.42	3.78E-101***	1.85e-100***
NDI of the Visual network								
Intercept (Resting state)		0.290	-0.660	0.00531	54.71	774.53		
Resting state	Stop Signal task	0.095	0.749	0.00340	27.86	1575.94	3.05E-139***	1.12e-138***
Resting state	Monetary Incentive Delay task	0.060	0.472	0.00330	18.05	1529.97	3.79E-66***	1.11e-65***
Resting state	Emotional N-back task	0.224	1.772	0.00517	43.33	1956.72	3.86E-288***	5.67e-287***
Stop Signal task	Monetary Incentive Delay task	-0.035	-0.277	0.003	-10.45	1554.20	9.75E-25***	2.39e-24***
Stop Signal task	Emotional N-back task	0.129	1.023	0.005	28.30	1896.99	3.03E-147***	1.48e-146***
Monetary Incentive Delay task	Emotional N-back task	0.164	1.300	0.005	32.82	1944.16	2.15E-188***	1.58e-187***

The tests are reported for the difference between Task 2 from the Intercept (Task 1) in each model. Significance is indicated with: ^$p < .10$, *$p < .05$, **$p < .01$, ***$p < .001$

APPENDIX 11: RELATIONSHIPS BETWEEN BRAIN ORGANIZATION AND TASK PERFORMANCE ON THE SST WITH BY CORRECTION.

Fixed Effects	*b*	*β*	*SE*	*t*	*raw p*	*adjusted-p*
Modularity						
Resting state	20.293	0.010	118.320	0.172	0.86	1.00
Stop Signal Task (SST)	234.167	0.115	101.526	2.306	0.02	0.26
Global efficiency						
Resting state	14.523	0.004	250.204	0.058	0.95	1.00
Stop Signal Task (SST)	629.076	0.144	256.943	2.448	0.01	0.26
NDI of the Fronto-parietal network						
Resting state	-22.236	-0.015	67.015	-0.332	0.74	1.00
Stop Signal Task (SST)	-60.973	-0.040	69.897	-0.872	0.38	1.00
NDI of the Cingulo-opercular network						
Resting state	123.858	0.103	57.436	2.156	0.03	0.92
Stop Signal Task (SST)	56.389	0.045	58.534	0.963	0.34	1.00
NDI of the Default mode network						
Resting state	-62.374	-0.045	64.826	-0.962	0.34	1.00
Stop Signal Task (SST)	-134.155	-0.100	60.365	-2.222	0.03	0.26
NDI of the Salience network						
Resting state	14.618	0.009	71.710	0.204	0.84	1.00
Stop Signal Task (SST)	-36.915	-0.023	71.070	-0.519	0.60	1.00
NDI of the Dorsal attention network						
Resting state	28.350	0.024	53.910	0.526	0.60	1.00
Stop Signal Task (SST)	-94.489	-0.068	65.073	-1.452	0.15	1.00
NDI of the Ventral attention network						
Resting state	-38.766	-0.028	67.408	-0.575	0.57	1.00
Stop Signal Task (SST)	-86.704	-0.060	66.566	-1.303	0.19	1.00

NDI of the Dorsal somatomotor network						
Resting state	-57.426	-0.063	45.408	-1.265	0.21	1.00
Stop Signal Task (SST)	-7.148	-0.008	44.760	-0.160	0.87	1.00
NDI of the Visual network						
Resting state	16.188	0.014	54.272	0.298	0.77	1.00
Stop Signal Task (SST)	-30.910	-0.036	42.363	-0.730	0.47	1.00

Tests are reported from separate models for the resting state and the SST. Significance is indicated with: ^$p < .10$, *$p < .05$, **$p < .01$, ***$p < .001$

APPENDIX 12: RELATIONSHIPS BETWEEN BRAIN ORGANIZATION AND TASK PERFORMANCE ON THE MID WITH BY CORRECTION.

Fixed Effects	b	*β*	SE	t	*raw p*	*adjusted-p*
Modularity						
Resting state	5.703	0.028	11.762	0.485	0.63	1.00
Monetary Incentive Delay (MID) Task	2.781	0.014	11.081	0.251	0.80	1.00
Global efficiency						
Resting state	-11.928	-0.031	24.872	-0.480	0.63	1.00
Monetary Incentive Delay (MID) Task	-101.498	-0.213	32.730	-3.101	0.002	0.06^
NDI of the Fronto-parietal network						
Resting state	-2.258	-0.016	6.663	-0.339	0.73	1.00
Monetary Incentive Delay (MID) Task	-2.090	-0.014	6.726	-0.311	0.76	1.00
NDI of the Cingulo-opercular network						
Resting state	-5.387	-0.046	5.733	-0.940	0.35	1.00
Monetary Incentive Delay (MID) Task	-5.957	-0.055	5.488	-1.086	0.28	1.00
NDI of the Default mode network						
Resting state	1.778	0.013	6.452	0.276	0.78	1.00
Monetary Incentive Delay (MID) Task	-0.898	-0.007	6.388	-0.141	0.89	1.00
NDI of the Salience network						
Resting state	-16.176	-0.106	7.092	-2.281	0.02	0.67
Monetary Incentive Delay (MID) Task	-10.995	-0.080	6.338	-1.735	0.08	1.00
NDI of the Dorsal attention network						
Resting state	4.705	0.042	5.358	0.878	0.38	1.00

Monetary Incentive Delay (MID) Task	-0.422	-0.003	6.218	-0.068	0.95	1.00
NDI of the Ventral attention network						
Resting state	-4.296	-0.032	6.702	-0.641	0.52	1.00
Monetary Incentive Delay (MID) Task	3.974	0.029	6.469	0.614	0.54	1.00
NDI of the Dorsal somatomotor network						
Resting state	3.216	0.037	4.520	0.711	0.48	1.00
Monetary Incentive Delay (MID) Task	2.621	0.026	4.863	0.539	0.59	1.00
NDI of the Visual network						
Resting state	-7.146	-0.063	5.387	-1.327	0.19	1.00
Monetary Incentive Delay (MID) Task	-3.651	-0.044	4.254	-0.858	0.39	1.00

Tests are reported from separate models for the resting state and the MID task. Significance is indicated with: ^$p <$ .10, *$p <$ .05, **$p <$ .01, ***$p <$ .001

APPENDIX 13: RELATIONSHIPS BETWEEN BRAIN ORGANIZATION AND TASK PERFORMANCE ON THE EN-BACK WITH BY CORRECTION.

Fixed Effects	**b**	***β***	**SE**	**t**	***raw p***	***adjusted-p***
Modularity						
Resting state	0.072	0.025	0.156	0.462	0.64	1.00
Emotional N-back (EN-back) Task	-0.337	-0.107	0.166	-2.027	0.04	0.32
Global efficiency						
Resting state	-0.574	-0.102	0.330	-1.742	0.08	1.00
Emotional N-back (EN-back) Task	-0.455	-0.071	0.284	-1.602	0.11	0.64
NDI of the Fronto-parietal network						
Resting state	-0.068	-0.033	0.089	-0.773	0.44	1.00
Emotional N-back (EN-back) Task	0.036	0.017	0.093	0.388	0.70	1.00
NDI of the Cingulo-opercular network						
Resting state	-0.090	-0.054	0.076	-1.188	0.24	1.00
Emotional N-back (EN-back) Task	0.168	0.099	0.077	2.175	0.03	0.32
NDI of the Default mode network						
Resting state	-0.005	-0.003	0.086	-0.060	0.95	1.00
Emotional N-back (EN-back) Task	0.085	0.048	0.080	1.068	0.29	1.00
NDI of the Salience network						
Resting state	0.048	0.022	0.095	0.504	0.61	1.00
Emotional N-back (EN-back) Task	-0.140	-0.044	0.136	-1.030	0.30	1.00
NDI of the Dorsal attention network						
Resting state	-0.002	-0.001	0.071	-0.033	0.97	1.00

Emotional N-back (EN-back) Task	-0.198	-0.115	0.074	-2.664	0.008	0.23
NDI of the Ventral attention network						
Resting state	-0.135	-0.070	0.089	-1.514	0.13	1.00
Emotional N-back (EN-back) Task	-0.234	-0.094	0.109	-2.142	0.03	0.32
NDI of the Dorsal somatomotor network						
Resting state	-0.034	-0.027	0.060	-0.559	0.58	1.00
Emotional N-back (EN-back) Task	0.091	0.067	0.062	1.456	0.15	0.71
NDI of the Visual network						
Resting state	0.092	0.056	0.072	1.282	0.20	1.00
Emotional N-back (EN-back) Task	-0.031	-0.024	0.058	-0.529	0.60	1.00

Tests are reported from separate models for the resting state and the EN-back task. Significance is indicated with: ^p < .10, *p< .05, **p< .01, ***p< .001

APPENDIX 14: REPLICATION OF RELATIONSHIPS BETWEEN BRAIN ORGANIZATION AND TASK PERFORMANCE ON THE SST WITH BY CORRECTION.

Fixed Effects	b	*β*	SE	t	*raw p*	*adjusted-p*
Modularity						
Resting state	52.642	0.023	122.851	0.428	0.668	1.00
Stop Signal Task (SST)	152.656	0.074	109.557	1.393	0.164	1.00
Global efficiency						
Resting state	-34.005	-0.008	270.006	-0.126	0.900	1.00
Stop Signal Task (SST)	674.552	0.154	282.755	2.386	0.017	0.51
NDI of the Fronto-parietal network						
Resting state	-7.566	-0.005	73.268	-0.103	0.918	1.00
Stop Signal Task (SST)	-9.454	-0.006	74.131	-0.128	0.899	1.00
NDI of the Cingulo-opercular network						
Resting state	3.448	0.003	60.289	0.057	0.954	1.00
Stop Signal Task (SST)	-71.373	-0.058	62.007	-1.151	0.250	1.00
NDI of the Default mode network						
Resting state	186.216	0.120	71.338	2.610	0.009	0.27
Stop Signal Task (SST)	22.995	0.016	66.941	0.344	0.731	1.00
NDI of the Salience network						
Resting state	99.805	0.059	76.746	1.300	0.194	1.00
Stop Signal Task (SST)	71.202	0.045	71.804	0.992	0.322	1.00
NDI of the Dorsal attention network						
Resting state	-44.543	-0.037	54.423	-0.818	0.413	1.00

Stop Signal Task (SST)	-53.430	-0.041	60.787	-0.879	0.380	1.00
NDI of the Ventral attention network						
Resting state	35.955	0.027	64.847	0.554	0.580	1.00
Stop Signal Task (SST)	-63.968	-0.046	64.199	-0.996	0.320	1.00
NDI of the Dorsal somatomotor network						
Resting state	20.934	0.022	46.916	0.446	0.656	1.00
Stop Signal Task (SST)	17.389	0.018	47.455	0.366	0.714	1.00
NDI of the Visual network						
Resting state	-62.983	-0.047	61.337	-1.027	0.305	1.00
Stop Signal Task (SST)	-40.976	-0.048	41.940	-0.977	0.329	1.00

Tests are reported from separate models for the resting state and the SST. Significance is indicated with: ^$p < .10$, *$p < .05$, **$p < .01$, ***$p < .001$

APPENDIX 15: REPLICATION OF RELATIONSHIPS BETWEEN BRAIN ORGANIZATION AND TASK PERFORMANCE ON THE MID WITH BY CORRECTION.

Fixed Effects	*b*	*β*	*SE*	*t*	*raw p*	*adjusted-p*
Modularity						
Resting state	32.195	0.145	11.977	2.688	0.007	0.11
Monetary Incentive Delay (MID) Task	23.414	0.121	11.163	2.097	0.036	0.27
Global efficiency						
Resting state	34.352	0.077	26.465	1.298	0.195	0.95
Monetary Incentive Delay (MID) Task	-42.202	-0.096	36.141	-1.168	0.243	1.00
NDI of the Fronto-parietal network						
Resting state	2.820	0.018	7.193	0.392	0.695	1.00
Monetary Incentive Delay (MID) Task	5.144	0.035	6.722	0.765	0.445	1.00
NDI of the Cingulo-opercular network						
Resting state	-13.995	-0.112	5.886	-2.378	0.018	0.13
Monetary Incentive Delay (MID) Task	-12.332	-0.108	5.496	-2.244	0.025	0.25
NDI of the Default mode network						
Resting state	-0.334	-0.002	7.052	-0.047	0.962	1.00
Monetary Incentive Delay (MID) Task	4.365	0.031	6.611	0.660	0.509	1.00
NDI of the Salience network						
Resting state	-2.567	-0.015	7.547	-0.340	0.734	1.00
Monetary Incentive Delay (MID) Task	-2.735	-0.020	6.348	-0.431	0.667	1.00
NDI of the Dorsal attention network						
Resting state	-2.669	-0.023	5.346	-0.499	0.618	1.00

Monetary Incentive Delay (MID) Task	-0.886	-0.007	5.943	-0.149	0.882	1.00
NDI of the Ventral attention network						
Resting state	-15.111	-0.115	6.332	-2.386	0.017	0.13
Monetary Incentive Delay (MID) Task	-9.818	-0.072	6.222	-1.578	0.115	0.67
NDI of the Dorsal somatomotor network						
Resting state	-15.652	-0.170	4.553	-3.438	0.001	0.02*
Monetary Incentive Delay (MID) Task	-13.949	-0.139	4.821	-2.894	0.004	0.12
NDI of the Visual network						
Resting state	-10.745	-0.082	6.009	-1.788	0.074	0.44
Monetary Incentive Delay (MID) Task	-9.897	-0.114	4.410	-2.244	0.025	0.25

Tests are reported from separate models for the resting state and the MID task. Significance is indicated with: ^p < .10, *p< .05, **p< .01, ***p< .001

APPENDIX 16: REPLICATION OF RELATIONSHIPS BETWEEN BRAIN ORGANIZATION AND TASK PERFORMANCE ON THE EN-BACK WITH BY CORRECTION.

Fixed Effects	*b*	*β*	*SE*	*t*	*raw p*	*adjusted-p*
Modularity						
Resting state	0.298	0.101	0.152	1.956	0.051	0.50
Emotional N-back (EN-back) Task	-0.278	-0.088	0.169	-1.642	0.101	0.74
Global efficiency						
Resting state	0.244	0.041	0.336	0.725	0.469	1.00
Emotional N-back (EN-back) Task	0.049	0.008	0.274	0.181	0.857	1.00
NDI of the Fronto-parietal network						
Resting state	-0.056	-0.027	0.091	-0.613	0.540	1.00
Emotional N-back (EN-back) Task	-0.034	-0.016	0.090	-0.377	0.707	1.00
NDI of the Cingulo-opercular network						
Resting state	-0.151	-0.091	0.075	-2.021	0.044	0.50
Emotional N-back (EN-back) Task	0.213	0.131	0.073	2.896	0.004	0.12
NDI of the Default mode network						
Resting state	-0.052	-0.025	0.089	-0.582	0.561	1.00
Emotional N-back (EN-back) Task	0.168	0.095	0.080	2.087	0.037	0.37
NDI of the Salience network						
Resting state	0.008	0.003	0.096	0.081	0.935	1.00
Emotional N-back (EN-back) Task	-0.198	-0.064	0.131	-1.506	0.133	0.78
NDI of the Dorsal attention network						
Resting state	-0.071	-0.045	0.068	-1.050	0.294	1.00

Emotional N-back (EN-back) Task	-0.180	-0.110	0.072	-2.518	0.012	0.18
NDI of the Ventral attention network						
Resting state	0.033	0.019	0.081	0.413	0.680	1.00
Emotional N-back (EN-back) Task	0.060	0.024	0.109	0.557	0.578	1.00
NDI of the Dorsal somatomotor network						
Resting state	-0.160	-0.131	0.058	-2.762	0.006	0.17
Emotional N-back (EN-back) Task	-0.074	-0.056	0.062	-1.187	0.236	1.00
NDI of the Visual network						
Resting state	0.074	0.042	0.076	0.968	0.334	1.00
Emotional N-back (EN-back) Task	0.024	0.020	0.057	0.416	0.677	1.00

Tests are reported from separate models for the resting state and the EN-back task. Significance is indicated with: ^p < .10, *p< .05, **p< .01, ***p< .001

APPENDIX 17: DIFFERENCES IN BRAIN-TASK PERFORMANCE RELATIONSHIPS BETWEEN THE RESTING STATE AND THE SST STATE WITH BY CORRECTION.

Fixed Effects	**Task Performance Metric**	*b*	*β*	*SE*	*t*	*df*	*raw p*	*adjusted-p*
Modularity	**SSRT**							
Intercept (Resting state)		0.315	0.502	0.00261	120.64	609.45		
Stop Signal Task (SST)		0.00006	0.083	0.00002	2.74	492.47	0.0064**	0.13
Global efficiency	**SSRT**							
Intercept (Resting state)		0.230	0.152	0.00115	199.25	586.52		
Stop Signal Task (SST)		0.00002	0.081	0.00001	2.64	491.84	0.0086**	0.13
NDI of the Fronto-parietal network	**SSRT**							
Intercept (Resting state)		0.734	0.080	0.00434	169.31	575.78		
Stop Signal Task (SST)		-0.00002	-0.028	0.00003	-0.71	488.08	0.48	1.00
NDI of the Cingulo-opercular network	**SSRT**							
Intercept (Resting state)		0.533	-0.463	0.00501	106.37	590.90		

Stop Signal Task (SST)		-0.00005	-0.058	0.00003	-1.55	491.79	0.12	0.72
NDI of the Default mode network	**SSRT**							
Intercept (Resting state)		0.531	-0.462	0.00465	114.06	590.96		
Stop Signal Task (SST)		-0.00006	-0.075	0.00003	-1.88	492.41	0.06^	0.59
NDI of the Salience network	**SSRT**							
Intercept (Resting state)		0.900	0.049	0.00397	226.75	611.25		
Stop Signal Task (SST)		-0.00002	-0.027	0.00003	-0.56	492.54	0.58	1.00
NDI of the Dorsal attention network	**SSRT**							
Intercept (Resting state)		0.623	-0.244	0.00496	125.50	591.55		
Stop Signal Task (SST)		-0.00006	-0.068	0.00003	-1.72	492.00	0.08^	0.63
NDI of the Ventral attention network	**SSRT**							
Intercept (Resting state)		0.739	-0.368	0.00437	169.23	590.01		

Stop Signal Task (SST)		-0.00003	-0.042	0.00003	-1.15	491.23	0.25	1.00
NDI of the Dorsal somatomotor network	**SSRT**							
Intercept (Resting state)		0.460	0.032	0.00634	72.65	605.55		
Stop Signal Task (SST)		0.00003	0.030	0.00005	0.68	489.61	0.50	1.00
NDI of the Visual network	**SSRT**							
Intercept (Resting state)		0.295	-0.355	0.00589	50.07	625.22		
Stop Signal Task (SST)		-0.00001	-0.009	0.00005	-0.23	490.52	0.82	1.00

Estimates for the SST above are the tests of the interaction term. Significance is indicated with: ^$p < .10$, *$p < .05$,

**$p < .01$, ***$p < .001$

APPENDIX 18: DIFFERENCES IN BRAIN-TASK PERFORMANCE RELATIONSHIPS BETWEEN THE RESTING STATE AND THE MID STATE WITH BY CORRECTION.

Fixed Effects	**Task Performance Metric**	*b*	*β*	*SE*	*t*	*df*	*raw p*	*adjusted-p*
Modularity	**Monetary value won**							
Intercept (Resting state)		0.313	0.438	0.00248	126.17	624.14		
Monetary Incentive Delay (MID) Task		0.0000	-0.001	0.00022	-0.02	490.71	0.99	1.00
Global efficiency	**Monetary value won**							
Intercept (Resting state)		0.230	0.388	0.00101	226.93	616.39		
Monetary Incentive Delay (MID) Task		-0.0002	-0.084	0.00008	-2.55	488.46	0.01*	0.33
NDI of the Fronto-parietal network	**Monetary value won**							
Intercept (Resting state)		0.731	0.257	0.00443	164.84	580.10		
Monetary Incentive Delay (MID) Task		-0.0001	-0.008	0.00027	-0.20	489.73	0.84	1.00
NDI of the Cingulo-opercular network	**Monetary value won**							
Intercept (Resting state)		0.539	-0.397	0.00514	104.88	601.89		
Monetary Incentive Delay (MID) Task		-0.0002	-0.025	0.00038	-0.63	490.13	0.53	1.00
NDI of the Default mode network	**Monetary value won**							

Intercept (Resting state)		0.534	-0.533	0.00447	119.43	607.40		
Monetary Incentive Delay (MID) Task		-0.0001	-0.016	0.00034	-0.38	490.65	0.70	1.00
NDI of the Salience network	**Monetary value won**							
Intercept (Resting state)		0.895	-0.074	0.00415	215.89	622.08		
Monetary Incentive Delay (MID) Task		0.00001	0.002	0.00036	0.04	490.10	0.97	1.00
NDI of the Dorsal attention network	**Monetary value won**							
Intercept (Resting state)		0.624	-0.406	0.00496	125.74	610.50		
Monetary Incentive Delay (MID) Task		-0.0005	-0.052	0.00039	-1.24	490.61	0.21	1.00
NDI of the Ventral attention network	**Monetary value won**							
Intercept (Resting state)		0.742	-0.102	0.00437	169.65	606.95		
Monetary Incentive Delay (MID) Task		0.0003	0.040	0.00033	0.89	490.64	0.37	1.00
NDI of the Dorsal somatomotor network	**Monetary value won**							
Intercept (Resting state)		0.446	-0.102	0.00609	73.16	619.35		
Monetary Incentive Delay (MID) Task		-0.0002	-0.022	0.00051	-0.47	489.90	0.64	1.00

NDI of the Visual network	**Monetary value won**							
Intercept (Resting state)		0.295	-0.189	0.00580	50.88	636.46		
Monetary Incentive Delay (MID) Task		-0.0002	-0.015	0.00056	-0.33	489.38	0.74	1.00

Estimates for the MID above are the tests of the interaction term. Significance is indicated with: ^$p < .10$, *$p < .05$, **$p < .01$, ***$p < .001$

APPENDIX 19: DIFFERENCES IN BRAIN-TASK PERFORMANCE RELATIONSHIPS BETWEEN THE RESTING STATE AND THE EN-BACK STATE WITH BY CORRECTION.

Fixed Effects	**Task Performance Metric**	***b***	***β***	***SE***	***t***	***df***	***raw p***	***adjusted-p***
Modularity	**2-back percent accuracy**							
Intercept (Resting state)		0.309	0.517	0.00229	135.21	676.83		
Emotional N-back (EN-back) Task		-0.024	-0.025	0.01507	-1.61	490.57	0.11	0.72
Global efficiency	**2-back percent accuracy**							
Intercept (Resting state)		0.230	-0.356	0.00126	182.15	651.33		
Emotional N-back (EN-back) Task		-0.002	-0.008	0.00707	-0.32	490.88	0.75	1.00
NDI of the Fronto-parietal network	**2-back percent accuracy**							
Intercept (Resting state)		0.739	0.079	0.00427	173.03	639.03		
Emotional N-back (EN-back) Task		0.041	0.077	0.02240	1.84	490.05	0.067^	0.65
NDI of the Cingulo-opercular network	**2-back percent accuracy**							
Intercept (Resting state)		0.541	-0.628	0.00489	110.69	663.29		
Emotional N-back (EN-back) Task		0.081	0.067	0.02953	2.73	490.88	0.0065**	0.09^
NDI of the Default mode network	**2-back percent accuracy**							

Intercept (Resting state)		0.539	-0.721	0.00448	120.16	676.54		
Emotional N-back (EN-back) Task		0.026	0.025	0.02951	0.90	490.40	0.37	1.00
NDI of the Salience network	**2-back percent accuracy**							
Intercept (Resting state)		0.898	-0.250	0.00336	267.10	671.78		
Emotional N-back (EN-back) Task		-0.025	-0.049	0.02175	-1.13	488.10	0.26	0.95
NDI of the Dorsal attention network	**2-back percent accuracy**							
Intercept (Resting state)		0.625	-0.493	0.00511	122.22	666.59		
Emotional N-back (EN-back) Task		-0.114	-0.127	0.03152	-3.62	490.77	0.0003***	0.01*
NDI of the Ventral attention network	**2-back percent accuracy**							
Intercept (Resting state)		0.747	-0.347	0.00387	193.14	655.84		
Emotional N-back (EN-back) Task		-0.034	-0.046	0.02232	-1.54	490.92	0.12	0.72
NDI of the Dorsal somatomotor network	**2-back percent accuracy**							
Intercept (Resting state)		0.460	-0.393	0.00615	74.76	662.00		
Emotional N-back (EN-back) Task		0.047	0.035	0.03684	1.28	490.90	0.20	0.84
NDI of the Visual network	**2-back percent accuracy**							
Intercept (Resting		0.295	-0.607	0.00580	50.86	678.24		

state)							
Emotional N-back (EN-back) Task	-0.050	-0.027	0.03853	-1.31	490.76	0.19	0.84

Estimates for the EN-back task above are the tests of the interaction term. Significance is indicated with: ^$p < .10$, *$p < .05$, **$p < .01$, ***$p < .001$

APPENDIX 20: REPLICATION OF DIFFERENCES IN BRAIN-TASK PERFORMANCE RELATIONSHIPS BETWEEN THE RESTING STATE AND THE SST TASK WITH BY CORRECTION.

Fixed Effects	**Task Performance Metric**	*b*	*β*	*SE*	*t*	*df*		*adjusted-p*
Modularity	**SSRT**							
Intercept (Resting state)		0.318	0.557	0.0027	117.94	620.61		
Stop Signal Task (SST)		0.00003	0.042	0.0000	1.50	507.00	0.13	0.98
Global efficiency	**SSRT**							
Intercept (Resting state)		0.227	0.086	0.0012	196.30	596.50		
Stop Signal Task (SST)		0.00002	0.089	0.0000	3.01	501.20	0.0028**	0.08^
NDI of the Fronto-parietal network	**SSRT**							
Intercept (Resting state)		0.738	0.168	0.0044	168.41	596.04		
Stop Signal Task (SST)		-0.000003	-0.004	0.0000	-0.11	507.39	0.91	1.00
NDI of the Cingulo-opercular network	**SSRT**							
Intercept (Resting state)		0.549	-0.148	0.0052	106.40	615.12		
Stop Signal Task (SST)		-0.00004	-0.050	0.0000	-1.33	507.66	0.18	1.00
NDI of the Default mode network	**SSRT**							
Intercept (Resting state)		0.525	-0.558	0.0046	114.17	603.35		

Stop Signal Task (SST)		-0.00007	-0.091	0.0000	-2.43	505.92	0.016*	0.23
NDI of the Salience network	**SSRT**							
Intercept (Resting state)		0.899	0.052	0.0042	215.06	625.23		
Stop Signal Task (SST)		-0.00002	-0.032	0.0000	-0.68	507.92	0.50	1.00
NDI of the Dorsal attention network	**SSRT**							
Intercept (Resting state)		0.621	-0.272	0.0056	111.41	603.36		
Stop Signal Task (SST)		-0.00001	-0.007	0.0000	-0.17	507.44	0.86	1.00
NDI of the Ventral attention network	**SSRT**							
Intercept (Resting state)		0.735	-0.353	0.0050	147.50	599.01		
Stop Signal Task (SST)		-0.00006	-0.079	0.0000	-2.23	504.60	0.02*	0.26
NDI of the Dorsal somatomotor network	**SSRT**							
Intercept (Resting state)		0.455	-0.023	0.0067	68.18	618.63		
Stop Signal Task (SST)		-0.00001	-0.012	0.0000	-0.28	507.56	0.78	1.00
NDI of the Visual network	**SSRT**							
Intercept (Resting state)		0.289	-0.443	0.0060	48.45	652.54		
Stop Signal Task (SST)		-0.000004	-0.003	0.0001	-0.08	506.83	0.94	1.00

Estimates for the SST above are the tests of the interaction term. Significance is indicated with: ^$p < .10$, *$p < .05$,

**$p < .01$, ***$p < .001$

APPENDIX 21: REPLICATION OF DIFFERENCES IN BRAIN-TASK PERFORMANCE RELATIONSHIPS BETWEEN THE RESTING STATE AND THE MID TASK WITH BY CORRECTION.

Fixed Effects	**Task Performance Metric**	*b*	*β*	*SE*	*t*	*df*	*raw p*	*adjusted-p*
Modularity	**Monetary value won**							
Intercept (Resting state)		0.317	0.481	0.0026	121.70	604.62		
Monetary Incentive Delay (MID) Task		0.00005	0.008	0.0002	0.26	508.29	0.80	1.00
Global efficiency	**Monetary value won**							
Intercept (Resting state)		0.228	0.324	0.0010	228.41	602.18		
Monetary Incentive Delay (MID) Task		-0.00021	-0.087	0.0001	-2.97	504.48	0.0032**	0.09^
NDI of the Fronto-parietal network	**Monetary value won**							
Intercept (Resting state)		0.738	0.378	0.0045	163.21	578.95		
Monetary Incentive Delay (MID) Task		0.00007	0.010	0.0002	0.27	507.67	0.79	1.00
NDI of the Cingulo-opercular network	**Monetary value won**							
Intercept (Resting state)		0.544	-0.255	0.0054	101.38	592.03		
Monetary Incentive Delay (MID) Task		0.00003	0.003	0.0003	0.09	508.34	0.93	1.00
NDI of the Default	**Monetary value won**							

mode network								
Intercept (Resting state)		0.534	-0.539	0.0045	119.09	597.37		
Monetary Incentive Delay (MID) Task		0.00005	0.006	0.0003	0.15	507.89	0.89	1.00
NDI of the Salience network	**Monetary value won**							
Intercept (Resting state)		0.897	-0.057	0.0044	205.98	609.34		
Monetary Incentive Delay (MID) Task		-0.00013	-0.020	0.0003	-0.41	507.56	0.69	1.00
NDI of the Dorsal attention network	**Monetary value won**							
Intercept (Resting state)		0.616	-0.532	0.0055	112.80	596.31		
Monetary Incentive Delay (MID) Task		0.00006	0.007	0.0004	0.17	508.38	0.87	1.00
NDI of the Ventral attention network	**Monetary value won**							
Intercept (Resting state)		0.737	-0.133	0.0049	150.14	590.90		
Monetary Incentive Delay (MID) Task		0.00017	0.022	0.0003	0.56	507.76	0.58	1.00
NDI of the Dorsal somatomotor network	**Monetary value won**							
Intercept (Resting state)		0.445	-0.125	0.0063	70.26	609.10		
Monetary Incentive		0.00016	0.015	0.0005	0.34	507.48	0.74	1.00

Delay (MID) Task								
NDI of the Visual network	**Monetary value won**							
Intercept (Resting state)		0.289	-0.237	0.0057	50.69	627.95		
Monetary Incentive Delay (MID) Task		-0.00078	-0.071	0.0005	-1.60	508.50	0.11	1.00

Estimates for the MID above are the tests of the interaction term. Significance is indicated with: ^$p < .10$, *$p < .05$, **$p < .01$, ***$p < .001$

APPENDIX 22: REPLICATION OF DIFFERENCES IN BRAIN-TASK PERFORMANCE RELATIONSHIPS BETWEEN THE RESTING STATE AND THE EN-BACK TASK WITH BY CORRECTION.

Fixed Effects	**Task Performance Metric**	*b*	*β*	*SE*	*t*	*df*	*raw p*	*adjusted-p*
Modularity	**2-back percent accuracy**							
Intercept (Resting state)		0.316	0.599	0.0023	136.14	669.03		
Emotional N-back (EN-back) Task		-0.036	-0.036	0.0145	-2.46	507.89	0.014*	0.14
Global efficiency	**2-back percent accuracy**							
Intercept (Resting state)		0.225	-0.517	0.0013	176.22	654.41		
Emotional N-back (EN-back) Task		-0.008	-0.026	0.0072	-1.10	507.73	0.27	1.00
NDI of the Fronto-parietal network	**2-back percent accuracy**							
Intercept (Resting state)		0.739	0.049	0.0044	169.18	628.55		
Emotional N-back (EN-back) Task		-0.006	-0.011	0.0209	-0.30	507.66	0.77	1.00
NDI of the Cingulo-opercular network	**2-back percent accuracy**							
Intercept (Resting state)		0.548	-0.531	0.0051	107.40	654.93		
Emotional N-back (EN-back) Task		0.149	0.122	0.0291	5.12	507.36	4.33E-07***	0.000013***
NDI of the Default mode network	**2-back percent accuracy**							

Intercept (Resting state)		0.536	-0.733	0.0045	120.39	666.98		
Emotional N-back (EN-back) Task		0.063	0.058	0.0275	2.27	507.60	0.02*	0.17
NDI of the Salience network	**2-back percent accuracy**							
Intercept (Resting state)		0.899	-0.248	0.0034	265.04	669.55		
Emotional N-back (EN-back) Task		-0.031	-0.064	0.0213	-1.46	507.87	0.15	0.85
NDI of the Dorsal attention network	**2-back percent accuracy**							
Intercept (Resting state)		0.614	-0.654	0.0055	111.45	649.07		
Emotional N-back (EN-back) Task		-0.082	-0.088	0.0303	-2.72	506.99	0.0067**	0.10
NDI of the Ventral attention network	**2-back percent accuracy**							
Intercept (Resting state)		0.744	-0.332	0.0042	175.80	647.80		
Emotional N-back (EN-back) Task		-0.022	-0.029	0.0230	-0.98	507.75	0.33	1.00
NDI of the Dorsal somatomotor network	**2-back percent accuracy**							
Intercept (Resting state)		0.449	-0.478	0.0063	71.33	661.92		
Emotional N-back (EN-back) Task		0.035	0.026	0.0375	0.95	507.85	0.34	1.00
NDI of the Visual network	**2-back percent accuracy**							
Intercept (Resting		0.284	-0.686	0.0057	49.50	682.97		

state)							
Emotional N-back (EN-back) Task	-0.020	-0.011	0.0394	-0.52	507.66	0.60	1.00

Estimates for the EN-back task above are the tests of the interaction term. Significance is indicated with: ^$p < .10$, *$p < .05$, **$p < .01$, ***$p < .001$

REFERENCES

Adepeju, M., Langton, S., & Bannister, J. (2020). *akmedoids: Anchored Kmedoids for Longitudinal Data Clustering* (R package version 0.1.5) [Computer software]. https://CRAN.R-project.org/package=akmedoids

Afek, A., Ben-Avraham, R., Davidov, A., Berezin Cohen, N., Ben Yehuda, A., Gilboa, Y., & Nahum, M. (2021). Psychological Resilience, Mental Health, and Inhibitory Control Among Youth and Young Adults Under Stress. *Frontiers in Psychiatry*, *11*. https://doi.org/10.3389/fpsyt.2020.608588

Angelides, N. H., Gupta, J., & Vickery, T. J. (2017). Associating resting-state connectivity with trait impulsivity. *Social Cognitive and Affective Neuroscience*, *12*(6), 1001–1008. https://doi.org/10.1093/scan/nsx031

Arnsten, A. F. T., & Rubia, K. (2012). Neurobiological Circuits Regulating Attention, Cognitive Control, Motivation, and Emotion: Disruptions in Neurodevelopmental Psychiatric Disorders. *Journal of the American Academy of Child & Adolescent Psychiatry*, *51*(4), 356–367. https://doi.org/10.1016/j.jaac.2012.01.008

Aron, A. R., & Poldrack, R. A. (2006). Cortical and Subcortical Contributions to Stop Signal Response Inhibition: Role of the Subthalamic Nucleus. *Journal of Neuroscience*, *26*(9), 2424–2433. https://doi.org/10.1523/JNEUROSCI.4682-05.2006

Aron, A. R., Robbins, T. W., & Poldrack, R. A. (2014). Inhibition and the right inferior frontal cortex: One decade on. *Trends in Cognitive Sciences*, *18*(4), 177–185. https://doi.org/10.1016/j.tics.2013.12.003

Bahlmann, J., Aarts, E., & D'Esposito, M. (2015). Influence of Motivation on Control Hierarchy in the Human Frontal Cortex. *Journal of Neuroscience*, *35*(7), 3207–3217. https://doi.org/10.1523/JNEUROSCI.2389-14.2015

Barber, A. D., Caffo, B. S., Pekar, J. J., & Mostofsky, S. H. (2013). Developmental changes in within- and between-network connectivity between late childhood and adulthood. *Neuropsychologia*, *51*(1), 156–167. https://doi.org/10.1016/j.neuropsychologia.2012.11.011

Barch, D. M., Burgess, G. C., Harms, M. P., Petersen, S. E., Schlaggar, B. L., Corbetta, M., Glasser, M. F., Curtiss, S., Dixit, S., Feldt, C., Nolan, D., Bryant, E., Hartley, T., Footer, O., Bjork, J. M., Poldrack, R., Smith, S., Johansen-Berg, H., Snyder, A. Z., & Van Essen, D. C. (2013). Function in the human connectome: Task-fMRI and individual differences in behavior. *NeuroImage*, *80*, 169–189. https://doi.org/10.1016/j.neuroimage.2013.05.033

Barnes, J. J., Nobre, A. C., Woolrich, M. W., Baker, K., & Astle, D. E. (2016). Training Working Memory in Childhood Enhances Coupling between Frontoparietal Control Network and Task-Related Regions. *Journal of Neuroscience*, *36*(34), 9001–9011. https://doi.org/10.1523/JNEUROSCI.0101-16.2016

Bates, D., Mächler, M., Bolker, B., & Walker, S. (2015). Fitting Linear Mixed-Effects Models Using lme4. *Journal of Statistical Software*, *67*(1), 1–48. https://doi.org/10.18637/jss.v067.i01

Benjamini, Y., & Hochberg, Y. (1995). Controlling the False Discovery Rate: A Practical and Powerful Approach to Multiple Testing. *Journal of the Royal Statistical Society: Series B (Methodological)*, *57*(1), 289–300. https://doi.org/10.1111/j.2517-6161.1995.tb02031.x

Benjamini, Y., & Yekutieli, D. (2001). The control of the false discovery rate in multiple testing under dependency. *The Annals of Statistics*, *29*(4). https://doi.org/10.1214/aos/1013699998

Best, J. R., & Miller, P. H. (2010). A Developmental Perspective on Executive Function: Development of Executive Functions. *Child Development*, *81*(6), 1641–1660. https://doi.org/10.1111/j.1467-8624.2010.01499.x

Betzel, R. F., Byrge, L., He, Y., Goñi, J., Zuo, X.-N., & Sporns, O. (2014). Changes in structural and functional connectivity among resting-state networks across the human lifespan. *NeuroImage*, *102*, 345–357. https://doi.org/10.1016/j.neuroimage.2014.07.067

Bissett, P. G., Hagen, M. P., Jones, H. M., & Poldrack, R. A. (2021). Design issues and solutions for stop-signal data from the Adolescent Brain Cognitive Development (ABCD) study. *ELife*, *10*. https://doi.org/10.7554/eLife.60185

Biswal, B., Yetkin, F. Z., Haughton, V. M., & Hyde, J. S. (1995). Functional connectivity in the motor cortex of resting human brain using echo-planar mri. *Magnetic Resonance in Medicine*, *34*(4), 537–541. https://doi.org/10.1002/mrm.1910340409

Bjork, J. M., & Pardini, D. A. (2015). Who are those "risk-taking adolescents"? Individual differences in developmental neuroimaging research. *Developmental Cognitive Neuroscience*, *11*, 56–64. https://doi.org/10.1016/j.dcn.2014.07.008

Black, W. R., Lepping, R. J., Bruce, A. S., Powell, J. N., Bruce, J. M., Martin, L. E., Davis, A. M., Brooks, W. M., Savage, C. R., & Simmons, W. K. (2014). Tonic hyper-connectivity of reward neurocircuitry in obese children. *Obesity*, *22*(7), 1590–1593. https://doi.org/10.1002/oby.20741

Boehler, C. N., Schevernels, H., Hopf, J.-M., Stoppel, C. M., & Krebs, R. M. (2014). Reward prospect rapidly speeds up response inhibition via reactive control. *Cognitive, Affective, & Behavioral Neuroscience*, *14*(2), 593–609. https://doi.org/10.3758/s13415-014-0251-5

Bosch, G. E. van den, Marroun, H. E., Schmidt, M. N., Tibboel, D., Manoach, D. S., Calhoun, V. D., & White, T. J. H. (2014). Brain connectivity during verbal working memory in children and adolescents. *Human Brain Mapping*, *35*(2), 698–711. https://doi.org/10.1002/hbm.22193

Botvinick, M., & Braver, T. (2015). Motivation and Cognitive Control: From Behavior to Neural Mechanism. *Annual Review of Psychology*, *66*(1), 83–113. https://doi.org/10.1146/annurev-psych-010814-015044

Braun, U., Schäfer, A., Walter, H., Erk, S., Romanczuk-Seiferth, N., Haddad, L., Schweiger, J. I., Grimm, O., Heinz, A., Tost, H., Meyer-Lindenberg, A., & Bassett, D. S. (2015). Dynamic reconfiguration of frontal brain networks during executive cognition in humans. *Proceedings of the National Academy of Sciences*, *112*(37), 11678–11683. https://doi.org/10.1073/pnas.1422487112

Bullmore, E. T., & Bassett, D. S. (2011). Brain Graphs: Graphical Models of the Human Brain Connectome. *Annual Review of Clinical Psychology*, *7*(1), 113–140. https://doi.org/10.1146/annurev-clinpsy-040510-143934

Camacho, M. C., Quiñones-Camacho, L. E., & Perlman, S. B. (2020). Does the child brain rest?: An examination and interpretation of resting cognition in developmental cognitive neuroscience. *NeuroImage*, *212*, 116688. https://doi.org/10.1016/j.neuroimage.2020.116688

Camara, E., Rodriguez-Fornells, A., & Münte, T. F. (2009). Functional connectivity of reward processing in the brain. *Frontiers in Human Neuroscience*, *2*. https://doi.org/10.3389/neuro.09.019.2008

Cao, Z., Bennett, M., Orr, C., Icke, I., Banaschewski, T., Barker, G. J., Bokde, A. L. W., Bromberg, U., Büchel, C., Quinlan, E. B., Desrivières, S., Flor, H., Frouin, V., Garavan, H., Gowland, P., Heinz, A., Ittermann, B., Martinot, J.-L., Nees, F., … Whelan, R. (2019). Mapping adolescent reward anticipation, receipt, and prediction error during the monetary incentive delay task. *Human Brain Mapping*, *40*(1), 262–283. https://doi.org/10.1002/hbm.24370

Cary, R. P., Ray, S., Grayson, D. S., Painter, J., Carpenter, S., Maron, L., Sporns, O., Stevens, A. A., Nigg, J. T., & Fair, D. A. (2016). Network Structure among Brain Systems in Adult ADHD is Uniquely Modified by Stimulant Administration. *Cerebral Cortex*, cercor;bhw209v1. https://doi.org/10.1093/cercor/bhw209

Casey, B. J. (2015). Beyond Simple Models of Self-Control to Circuit-Based Accounts of Adolescent Behavior. *Annual Review of Psychology*, *66*(1), 295–319. https://doi.org/10.1146/annurev-psych-010814-015156

Casey, B. J., Cannonier, T., Conley, M. I., Cohen, A. O., Barch, D. M., Heitzeg, M. M., Soules, M. E., Teslovich, T., Dellarco, D. V., Garavan, H., Orr, C. A., Wager, T. D., Banich, M. T., Speer, N. K., Sutherland, M. T., Riedel, M. C., Dick, A. S., Bjork, J. M., Thomas, K. M., … Dale, A. M. (2018). The Adolescent Brain Cognitive Development (ABCD) study: Imaging acquisition across 21 sites. *Developmental Cognitive Neuroscience*, *32*, 43–54. https://doi.org/10.1016/j.dcn.2018.03.001

Casey, B. J., Getz, S., & Galvan, A. (2008). The adolescent brain. *Developmental Review*, *28*(1), 62–77. https://doi.org/10.1016/j.dr.2007.08.003

Chau, D. T., Roth, R. M., & Green, A. I. (2004). The neural circuitry of reward and its relevance to psychiatric disorders. *Current Psychiatry Reports*, *6*(5), 391–399. https://doi.org/10.1007/s11920-004-0026-8

Chen, M., & Deem, M. W. (2015). Development of modularity in the neural activity of children's brains. *Physical Biology*, *12*(1), 016009. https://doi.org/10.1088/1478-3975/12/1/016009

Cho, Y. T., Fromm, S., Guyer, A. E., Detloff, A., Pine, D. S., Fudge, J. L., & Ernst, M. (2013). Nucleus accumbens, thalamus and insula connectivity during incentive anticipation in typical adults and adolescents. *NeuroImage*, *66*, 508–521. https://doi.org/10.1016/j.neuroimage.2012.10.013

Clark, L., Boileau, I., & Zack, M. (2019). Neuroimaging of reward mechanisms in Gambling disorder: An integrative review. *Molecular Psychiatry*, *24*(5), 674–693. https://doi.org/10.1038/s41380-018-0230-2

Cohen, A. O., Breiner, K., Steinberg, L., Bonnie, R. J., Scott, E. S., Taylor-Thompson, K., Rudolph, M. D., Chein, J., Richeson, J. A., Heller, A. S., Silverman, M. R., Dellarco, D. V., Fair, D. A., Galván, A., & Casey, B. J. (2016). When Is an Adolescent an Adult? Assessing Cognitive Control in Emotional and Nonemotional Contexts. *Psychological Science*, *27*(4), 549–562. https://doi.org/10.1177/0956797615627625

Cohen, J. R., & D'Esposito, M. (2016). The Segregation and Integration of Distinct Brain Networks and Their Relationship to Cognition. *Journal of Neuroscience*, *36*(48), 12083–12094. https://doi.org/10.1523/JNEUROSCI.2965-15.2016

Cohen, J. R., Sreenivasan, K. K., & D'Esposito, M. (2014). Correspondence Between Stimulus Encoding- and Maintenance-Related Neural Processes Underlies Successful Working Memory. *Cerebral Cortex*, *24*(3), 593–599. https://doi.org/10.1093/cercor/bhs339

Cole, M. W., Bassett, D. S., Power, J. D., Braver, T. S., & Petersen, S. E. (2014). Intrinsic and Task-Evoked Network Architectures of the Human Brain. *Neuron*, *83*(1), 238–251. https://doi.org/10.1016/j.neuron.2014.05.014

Cole, M. W., Ito, T., Schultz, D., Mill, R., Chen, R., & Cocuzza, C. (2019). Task activations produce spurious but systematic inflation of task functional connectivity estimates. *NeuroImage*, *189*, 1–18. https://doi.org/10.1016/j.neuroimage.2018.12.054

Conley, M. I., Dellarco, D. V., Rubien-Thomas, E., Cohen, A. O., Cervera, A., Tottenham, N., & Casey, B. (2018). The racially diverse affective expression (RADIATE) face stimulus set. *Psychiatry Research*, *270*, 1059–1067. https://doi.org/10.1016/j.psychres.2018.04.066

Corbetta, M., & Shulman, G. L. (2002). Control of goal-directed and stimulus-driven attention in the brain. *Nature Reviews Neuroscience*, *3*(3), 201–215. https://doi.org/10.1038/nrn755

Crane, N. A., Gorka, S. M., Weafer, J., Langenecker, S. A., de Wit, H., & Phan, K. L. (2017). Preliminary Evidence for Disrupted Nucleus Accumbens Reactivity and Connectivity to

Reward in Binge Drinkers. *Alcohol and Alcoholism*, *52*(6), 647–654. https://doi.org/10.1093/alcalc/agx062

Csardi, G., & Nepusz, T. (2006). *The igraph software package for complex network research*. *Complex Systems*, 1695.

Cubillo, A., Makwana, A. B., & Hare, T. A. (2019). Differential modulation of cognitive control networks by monetary reward and punishment. *Social Cognitive and Affective Neuroscience*, *14*(3), 305–317. https://doi.org/10.1093/scan/nsz006

Dehaene, S., Kerszberg, M., & Changeux, J.-P. (1998). A neuronal model of a global workspace in effortful cognitive tasks. *Proceedings of the National Academy of Sciences*, *95*(24), 14529–14534. https://doi.org/10.1073/pnas.95.24.14529

Demetriou, E. A., Lampit, A., Quintana, D. S., Naismith, S. L., Song, Y. J. C., Pye, J. E., Hickie, I., & Guastella, A. J. (2018). Autism spectrum disorders: A meta-analysis of executive function. *Molecular Psychiatry*, *23*(5), 1198–1204. https://doi.org/10.1038/mp.2017.75

Di Martino, A., Fair, D. A., Kelly, C., Satterthwaite, T. D., Castellanos, F. X., Thomason, M. E., Craddock, R. C., Luna, B., Leventhal, B. L., Zuo, X.-N., & Milham, M. P. (2014). Unraveling the miswired connectome: A developmental perspective. *Neuron*, *83*(6), 1335–1353. https://doi.org/10.1016/j.neuron.2014.08.050

Diamond, A. (2013). Executive Functions. *Annual Review of Psychology*, *64*(1), 135–168. https://doi.org/10.1146/annurev-psych-113011-143750

Dixon, M. L., & Christoff, K. (2012). The Decision to Engage Cognitive Control Is Driven by Expected Reward-Value: Neural and Behavioral Evidence. *PLoS ONE*, *7*(12), e51637. https://doi.org/10.1371/journal.pone.0051637

Dosenbach, N. U. F., Fair, D. A., Cohen, A. L., Schlaggar, B. L., & Petersen, S. E. (2008). A dual-networks architecture of top-down control. *Trends in Cognitive Sciences*, *12*(3), 99–105. https://doi.org/10.1016/j.tics.2008.01.001

Dosenbach, N. U. F., Fair, D. A., Miezin, F. M., Cohen, A. L., Wenger, K. K., Dosenbach, R. A. T., Fox, M. D., Snyder, A. Z., Vincent, J. L., Raichle, M. E., Schlaggar, B. L., & Petersen, S. E. (2007). Distinct brain networks for adaptive and stable task control in humans. *Proceedings of the National Academy of Sciences*, *104*(26), 11073–11078. https://doi.org/10.1073/pnas.0704320104

Dosenbach, N. U. F., Visscher, K. M., Palmer, E. D., Miezin, F. M., Wenger, K. K., Kang, H. C., Burgund, E. D., Grimes, A. L., Schlaggar, B. L., & Petersen, S. E. (2006). A Core System for the Implementation of Task Sets. *Neuron*, *50*(5), 799–812. https://doi.org/10.1016/j.neuron.2006.04.031

Duffy, K. A., Rosch, K. S., Nebel, M. B., Seymour, K. E., Lindquist, M. A., Pekar, J. J., Mostofsky, S. H., & Cohen, J. R. (2021). Increased integration between default mode and task-relevant networks in children with ADHD is associated with impaired response

control. *Developmental Cognitive Neuroscience*, *50*, 100980. https://doi.org/10.1016/j.dcn.2021.100980

Dwyer, D. B., Harrison, B. J., Yucel, M., Whittle, S., Zalesky, A., Pantelis, C., Allen, N. B., & Fornito, A. (2014). Large-Scale Brain Network Dynamics Supporting Adolescent Cognitive Control. *Journal of Neuroscience*, *34*(42), 14096–14107. https://doi.org/10.1523/JNEUROSCI.1634-14.2014

Engelhardt, L. E., Harden, K. P., Tucker-Drob, E. M., & Church, J. A. (2019). The neural architecture of executive functions is established by middle childhood. *NeuroImage*, *185*, 479–489. https://doi.org/10.1016/j.neuroimage.2018.10.024

Enticott, P. G., Ogloff, J. R. P., & Bradshaw, J. L. (2008). Response inhibition and impulsivity in schizophrenia. *Psychiatry Research*, *157*(1), 251–254. https://doi.org/10.1016/j.psychres.2007.04.007

Ernst, M. (2014). The triadic model perspective for the study of adolescent motivated behavior. *Brain and Cognition*, *89*, 104–111. https://doi.org/10.1016/j.bandc.2014.01.006

Fair, D. A., Miranda-Dominguez, O., Snyder, A. Z., Perrone, A., Earl, E. A., Van, A. N., Koller, J. M., Feczko, E., Tisdall, M. D., van der Kouwe, A., Klein, R. L., Mirro, A. E., Hampton, J. M., Adeyemo, B., Laumann, T. O., Gratton, C., Greene, D. J., Schlaggar, B. L., Hagler, D. J., … Dosenbach, N. U. F. (2020). Correction of respiratory artifacts in MRI head motion estimates. *NeuroImage*, *208*, 116400. https://doi.org/10.1016/j.neuroimage.2019.116400

Fareri, D. S., Gabard-Durnam, L., Goff, B., Flannery, J., Gee, D. G., Lumian, D. S., Caldera, C., & Tottenham, N. (2015). Normative development of ventral striatal resting state connectivity in humans. *NeuroImage*, *118*, 422–437. https://doi.org/10.1016/j.neuroimage.2015.06.022

Feczko, E., Earl, E., Perrone, A., & Fair, D. (2020). *ABCD Reproducible Matched Samples (ARMS) software*. osf.io/7xn4f

Follmer, D. J. (2018). Executive Function and Reading Comprehension: A Meta-Analytic Review. *Educational Psychologist*, *53*(1), 42–60. https://doi.org/10.1080/00461520.2017.1309295

Friston, K. J. (1994). Functional and effective connectivity in neuroimaging: A synthesis. *Human Brain Mapping*, *2*(1–2), 56–78. https://doi.org/10.1002/hbm.460020107

Galvan. (2010). Adolescent development of the reward system. *Frontiers in Human Neuroscience*. https://doi.org/10.3389/neuro.09.006.2010

Galvan, A., Hare, T. A., Parra, C. E., Penn, J., Voss, H., Glover, G., & Casey, B. J. (2006). Earlier Development of the Accumbens Relative to Orbitofrontal Cortex Might Underlie Risk-Taking Behavior in Adolescents. *Journal of Neuroscience*, *26*(25), 6885–6892. https://doi.org/10.1523/JNEUROSCI.1062-06.2006

Gao, S., Greene, A. S., Constable, R. T., & Scheinost, D. (2019). Combining multiple connectomes improves predictive modeling of phenotypic measures. *NeuroImage*, *201*, 116038. https://doi.org/10.1016/j.neuroimage.2019.116038

Garavan, H., Hahn, S., Chaarani, B., Juliano, A., Allgaier, N., Yuan, D., Weigard, A., Orr, C., Watts, R., Wager, T., Ruiz de Leon, O., Hagler, D., & Potter, A. (2020). *The ABCD Stop Signal Data: Response to Bissett et al.* [Preprint]. Neuroscience. https://doi.org/10.1101/2020.07.27.223057

García-García, I., Jurado, M. A., Garolera, M., Segura, B., Marqués-Iturria, I., Pueyo, R., Vernet-Vernet, M., Sender-Palacios, M. J., Sala-Llonch, R., Ariza, M., Narberhaus, A., & Junqué, C. (2013). Functional connectivity in obesity during reward processing. *NeuroImage*, *66*, 232–239. https://doi.org/10.1016/j.neuroimage.2012.10.035

Geier, C. F., & Luna, B. (2009). The maturation of incentive processing and cognitive control. *Pharmacology Biochemistry and Behavior*, *93*(3), 212–221. https://doi.org/10.1016/j.pbb.2009.01.021

Geier, C. F., Terwilliger, R., Teslovich, T., Velanova, K., & Luna, B. (2010). Immaturities in Reward Processing and Its Influence on Inhibitory Control in Adolescence. *Cerebral Cortex*, *20*(7), 1613–1629. https://doi.org/10.1093/cercor/bhp225

Glasser, M. F., Sotiropoulos, S. N., Wilson, J. A., Coalson, T. S., Fischl, B., Andersson, J. L., Xu, J., Jbabdi, S., Webster, M., Polimeni, J. R., Van Essen, D. C., & Jenkinson, M. (2013). The minimal preprocessing pipelines for the Human Connectome Project. *NeuroImage*, *80*, 105–124. https://doi.org/10.1016/j.neuroimage.2013.04.127

Gohier, B., Ferracci, L., Surguladze, S. A., Lawrence, E., El Hage, W., Kefi, M. Z., Allain, P., Garre, J.-B., & Le Gall, D. (2009). Cognitive inhibition and working memory in unipolar depression. *Journal of Affective Disorders*, *116*(1), 100–105. https://doi.org/10.1016/j.jad.2008.10.028

Gordon, E. M., Devaney, J. M., Bean, S., & Vaidya, C. J. (2015). Resting-State Striato-Frontal Functional Connectivity is Sensitive to DAT1 Genotype and Predicts Executive Function. *Cerebral Cortex*, *25*(2), 336–345. https://doi.org/10.1093/cercor/bht229

Gordon, E. M., Laumann, T. O., Adeyemo, B., Huckins, J. F., Kelley, W. M., & Petersen, S. E. (2016). Generation and Evaluation of a Cortical Area Parcellation from Resting-State Correlations. *Cerebral Cortex (New York, N.Y.: 1991)*, *26*(1), 288–303. https://doi.org/10.1093/cercor/bhu239

Gracia-Tabuenca, Z., Moreno, M. B., Barrios, F. A., & Alcauter, S. (2021). Development of the brain functional connectome follows puberty-dependent nonlinear trajectories. *NeuroImage*, *229*, 117769. https://doi.org/10.1016/j.neuroimage.2021.117769

Gratton, C., Laumann, T. O., Nielsen, A. N., Greene, D. J., Gordon, E. M., Gilmore, A. W., Nelson, S. M., Coalson, R. S., Snyder, A. Z., Schlaggar, B. L., Dosenbach, N. U. F., & Petersen, S. E. (2018). Functional Brain Networks Are Dominated by Stable Group and

Individual Factors, Not Cognitive or Daily Variation. *Neuron*, *98*(2), 439-452.e5. https://doi.org/10.1016/j.neuron.2018.03.035

Grayson, D. S., & Fair, D. A. (2017). Development of large-scale functional networks from birth to adulthood: A guide to the neuroimaging literature. *NeuroImage*, *160*, 15–31. https://doi.org/10.1016/j.neuroimage.2017.01.079

Grayson, D. S., Ray, S., Carpenter, S., Iyer, S., Dias, T. G. C., Stevens, C., Nigg, J. T., & Fair, D. A. (2014). Structural and Functional Rich Club Organization of the Brain in Children and Adults. *PLOS ONE*, *9*(2), e88297. https://doi.org/10.1371/journal.pone.0088297

Greene, A. S., Gao, S., Noble, S., Scheinost, D., & Constable, R. T. (2020). How Tasks Change Whole-Brain Functional Organization to Reveal Brain-Phenotype Relationships. *Cell Reports*, *32*(8), 108066. https://doi.org/10.1016/j.celrep.2020.108066

Greene, A. S., Gao, S., Scheinost, D., & Constable, R. T. (2018). Task-induced brain state manipulation improves prediction of individual traits. *Nature Communications*, *9*(1), 2807. https://doi.org/10.1038/s41467-018-04920-3

Greene, C. M., & Soto, D. (2014). Functional connectivity between ventral and dorsal frontoparietal networks underlies stimulus-driven and working memory-driven sources of visual distraction. *NeuroImage*, *84*, 290–298. https://doi.org/10.1016/j.neuroimage.2013.08.060

Gu, S., Satterthwaite, T. D., Medaglia, J. D., Yang, M., Gur, R. E., Gur, R. C., & Bassett, D. S. (2015). Emergence of system roles in normative neurodevelopment. *Proceedings of the National Academy of Sciences*, *112*(44), 13681–13686. https://doi.org/10.1073/pnas.1502829112

Gusnard, D. A., & Raichle, M. E. (2001). Searching for a baseline: Functional imaging and the resting human brain. *Nature Reviews Neuroscience*, *2*(10), 685–694. https://doi.org/10.1038/35094500

Hagler, D. J., Hatton, SeanN., Cornejo, M. D., Makowski, C., Fair, D. A., Dick, A. S., Sutherland, M. T., Casey, B. J., Barch, D. M., Harms, M. P., Watts, R., Bjork, J. M., Garavan, H. P., Hilmer, L., Pung, C. J., Sicat, C. S., Kuperman, J., Bartsch, H., Xue, F., … Dale, A. M. (2019). Image processing and analysis methods for the Adolescent Brain Cognitive Development Study. *NeuroImage*, *202*, 116091. https://doi.org/10.1016/j.neuroimage.2019.116091

Hallquist, M. N., Geier, C. F., & Luna, B. (2018). Incentives facilitate developmental improvement in inhibitory control by modulating control-related networks. *NeuroImage*, *172*, 369–380. https://doi.org/10.1016/j.neuroimage.2018.01.045

Hallquist, M. N., & Hillary, F. G. (2019). Graph theory approaches to functional network organization in brain disorders: A critique for a brave new small-world. *Network Neuroscience*, *3*(1), 1–26. https://doi.org/10.1162/netn_a_00054

Hampson, M., Driesen, N. R., Skudlarski, P., Gore, J. C., & Constable, R. T. (2006). Brain Connectivity Related to Working Memory Performance. *Journal of Neuroscience*, *26*(51), 13338–13343. https://doi.org/10.1523/JNEUROSCI.3408-06.2006

Hampson, M., Driesen, N., Roth, J. K., Gore, J. C., & Constable, R. T. (2010). Functional connectivity between task-positive and task-negative brain areas and its relation to working memory performance. *Magnetic Resonance Imaging*, *28*(8), 1051–1057. https://doi.org/10.1016/j.mri.2010.03.021

Hearne, L. J., Cocchi, L., Zalesky, A., & Mattingley, J. B. (2017). Reconfiguration of Brain Network Architectures between Resting-State and Complexity-Dependent Cognitive Reasoning. *The Journal of Neuroscience*, *37*(35), 8399–8411. https://doi.org/10.1523/JNEUROSCI.0485-17.2017

Heitzeg, M. M., Cope, L. M., Martz, M. E., & Hardee, J. E. (2015). Neuroimaging Risk Markers for Substance Abuse: Recent Findings on Inhibitory Control and Reward System Functioning. *Current Addiction Reports*, *2*(2), 91–103. https://doi.org/10.1007/s40429-015-0048-9

Hwang, K., Velanova, K., & Luna, B. (2010). Strengthening of Top-Down Frontal Cognitive Control Networks Underlying the Development of Inhibitory Control: A Functional Magnetic Resonance Imaging Effective Connectivity Study. *Journal of Neuroscience*, *30*(46), 15535–15545. https://doi.org/10.1523/JNEUROSCI.2825-10.2010

Insel, T., Cuthbert, B., Garvey, M., Heinssen, R., Pine, D. S., Quinn, K., Sanislow, C., & Wang, P. (2010). Research Domain Criteria (RDoC): Toward a New Classification Framework for Research on Mental Disorders. *American Journal of Psychiatry*, *167*(7), 748–751. https://doi.org/10.1176/appi.ajp.2010.09091379

Jazbec, S., Hardin, M. G., Schroth, E., McClure, E., Pine, D. S., & Ernst, M. (2006). Age-related influence of contingencies on a saccade task. *Experimental Brain Research*, *174*(4), 754–762. https://doi.org/10.1007/s00221-006-0520-9

Ji, J. L., Spronk, M., Kulkarni, K., Repovš, G., Anticevic, A., & Cole, M. W. (2019). Mapping the human brain's cortical-subcortical functional network organization. *NeuroImage*, *185*, 35–57. https://doi.org/10.1016/j.neuroimage.2018.10.006

Jiang, R., Zuo, N., Ford, J. M., Qi, S., Zhi, D., Zhuo, C., Xu, Y., Fu, Z., Bustillo, J., Turner, J. A., Calhoun, V. D., & Sui, J. (2020). Task-induced brain connectivity promotes the detection of individual differences in brain-behavior relationships. *NeuroImage*, *207*, 116370. https://doi.org/10.1016/j.neuroimage.2019.116370

Jollans, L., Zhipeng, C., Icke, I., Greene, C., Kelly, C., Banaschewski, T., Bokde, A. L. W., Bromberg, U., Büchel, C., Cattrell, A., Conrod, P. J., Desrivières, S., Flor, H., Frouin, V., Gallinat, J., Garavan, H., Gowland, P., Heinz, A., Ittermann, B., … Whelan, R. (2016). Ventral Striatum Connectivity During Reward Anticipation in Adolescent Smokers. *Developmental Neuropsychology*, *41*(1–2), 6–21. https://doi.org/10.1080/87565641.2016.1164172

Josse, J., & Husson, F. (2016). **missMDA**: A Package for Handling Missing Values in Multivariate Data Analysis. *Journal of Statistical Software*, *70*(1). https://doi.org/10.18637/jss.v070.i01

Kamkar, N. H., & Morton, J. B. (2017). CanDiD: A Framework for Linking Executive Function and Education. *Frontiers in Psychology*, *8*. https://doi.org/10.3389/fpsyg.2017.01187

Kanwisher, N. (2001). Neural events and perceptual awareness. *Cognition*, *79*(1), 89–113. https://doi.org/10.1016/S0010-0277(00)00125-6

Keren, H., O'Callaghan, G., Vidal-Ribas, P., Buzzell, G. A., Brotman, M. A., Leibenluft, E., Pan, P. M., Meffert, L., Kaiser, A., Wolke, S., Pine, D. S., & Stringaris, A. (2018). Reward Processing in Depression: A Conceptual and Meta-Analytic Review Across fMRI and EEG Studies. *American Journal of Psychiatry*, *175*(11), 1111–1120. https://doi.org/10.1176/appi.ajp.2018.17101124

Kitzbichler, M. G., Henson, R. N. A., Smith, M. L., Nathan, P. J., & Bullmore, E. T. (2011). Cognitive effort drives workspace configuration of human brain functional networks. *The Journal of Neuroscience: The Official Journal of the Society for Neuroscience*, *31*(22), 8259–8270. https://doi.org/10.1523/JNEUROSCI.0440-11.2011

Knutson, B., Westdorp, A., Kaiser, E., & Hommer, D. (2000). FMRI Visualization of Brain Activity during a Monetary Incentive Delay Task. *NeuroImage*, *12*(1), 20–27. https://doi.org/10.1006/nimg.2000.0593

Kofler, M. J., Rapport, M. D., Bolden, J., & Altro, T. A. (2008). Working Memory as a Core Deficit in ADHD: Preliminary Findings and Implications. *The ADHD Report*, *16*(6), 8–14. https://doi.org/10.1521/adhd.2008.16.6.8

Krienen, F. M., Yeo, B. T. T., & Buckner, R. L. (2014). Reconfigurable task-dependent functional coupling modes cluster around a core functional architecture. *Philosophical Transactions of the Royal Society of London. Series B, Biological Sciences*, *369*(1653). https://doi.org/10.1098/rstb.2013.0526

Latora, V., & Marchiori, M. (2001). Efficient Behavior of Small-World Networks. *Physical Review Letters*, *87*(19), 198701. https://doi.org/10.1103/PhysRevLett.87.198701

Lê, S., Josse, J., & Husson, F. (2008). **FactoMineR**: An *R* Package for Multivariate Analysis. *Journal of Statistical Software*, *25*(1). https://doi.org/10.18637/jss.v025.i01

Le, T. M., Huang, A. S., O'Rawe, J., & Leung, H.-C. (2020). Functional neural network configuration in late childhood varies by age and cognitive state. *Developmental Cognitive Neuroscience*, *45*, 100862. https://doi.org/10.1016/j.dcn.2020.100862

Lee, J., & Park, S. (2005). Working Memory Impairments in Schizophrenia: A Meta-Analysis. *Journal of Abnormal Psychology*, *114*(4), 599–611. https://doi.org/10.1037/0021-843X.114.4.599

Littman, R., & Takács, Á. (2017). Do all inhibitions act alike? A study of go/no-go and stop-signal paradigms. *PLOS ONE*, *12*(10), e0186774. https://doi.org/10.1371/journal.pone.0186774

Logan, G. D. (1994). On the ability to inhibit thought and action: A users' guide to the stop signal paradigm. In *Inhibitory processes in attention, memory, and language* (pp. 189–239). Academic Press.

Lopez, K. C., Kandala, S., Marek, S., & Barch, D. M. (2020). Development of Network Topology and Functional Connectivity of the Prefrontal Cortex. *Cerebral Cortex*, *30*(4), 2489–2505. https://doi.org/10.1093/cercor/bhz255

Luijten, M., Schellekens, A. F., Kühn, S., Machielse, M. W. J., & Sescousse, G. (2017). Disruption of Reward Processing in Addiction: An Image-Based Meta-analysis of Functional Magnetic Resonance Imaging Studies. *JAMA Psychiatry*, *74*(4), 387–398. https://doi.org/10.1001/jamapsychiatry.2016.3084

Luna, B., Garver, K. E., Urban, T. A., Lazar, N. A., & Sweeney, J. A. (2004). Maturation of Cognitive Processes From Late Childhood to Adulthood. *Child Development*, *75*(5), 1357–1372. https://doi.org/10.1111/j.1467-8624.2004.00745.x

Luna, B., Marek, S., Larsen, B., Tervo-Clemmens, B., & Chahal, R. (2015). An Integrative Model of the Maturation of Cognitive Control. *Annual Review of Neuroscience*, *38*(1), 151–170. https://doi.org/10.1146/annurev-neuro-071714-034054

Luna, B., Padmanabhan, A., & O'Hearn, K. (2010). What has fMRI told us about the Development of Cognitive Control through Adolescence? *Brain and Cognition*, *72*(1), 101–113. https://doi.org/10.1016/j.bandc.2009.08.005

Luna, B., Paulsen, D. J., Padmanabhan, A., & Geier, C. F. (2013). The Teenage Brain: Cognitive Control and Motivation. *Current Directions in Psychological Science*, *22*(2), 94–100. https://doi.org/10.1177/0963721413478416

Ma, I., van Duijvenvoorde, A., & Scheres, A. (2016). The interaction between reinforcement and inhibitory control in ADHD: A review and research guidelines. *Clinical Psychology Review*, *44*, 94–111. https://doi.org/10.1016/j.cpr.2016.01.001

Ma, I., van Holstein, M., Mies, G. W., Mennes, M., Buitelaar, J., Cools, R., Cillessen, A. H. N., Krebs, R. M., & Scheres, A. (2016). Ventral striatal hyperconnectivity during rewarded interference control in adolescents with ADHD. *Cortex*, *82*, 225–236. https://doi.org/10.1016/j.cortex.2016.05.021

Marek, S., Hwang, K., Foran, W., Hallquist, M. N., & Luna, B. (2015). The Contribution of Network Organization and Integration to the Development of Cognitive Control. *PLOS Biology*, *13*(12), e1002328. https://doi.org/10.1371/journal.pbio.1002328

Marek, S., Tervo-Clemmens, B., Nielsen, A. N., Wheelock, M. D., Miller, R. L., Laumann, T. O., Earl, E., Foran, W. W., Cordova, M., Doyle, O., Perrone, A., Miranda-Dominguez,

O., Feczko, E., Sturgeon, D., Graham, A., Hermosillo, R., Snider, K., Galassi, A., Nagel, B. J., … Dosenbach, N. U. F. (2019). Identifying reproducible individual differences in childhood functional brain networks: An ABCD study. *Developmental Cognitive Neuroscience*, *40*, 100706. https://doi.org/10.1016/j.dcn.2019.100706

Markett, S., Reuter, M., Heeren, B., Lachmann, B., Weber, B., & Montag, C. (2018). Working memory capacity and the functional connectome—Insights from resting-state fMRI and voxelwise centrality mapping. *Brain Imaging and Behavior*, *12*(1), 238–246. https://doi.org/10.1007/s11682-017-9688-9

McKenna, R., Rushe, T., & Woodcock, K. A. (2017). Informing the Structure of Executive Function in Children: A Meta-Analysis of Functional Neuroimaging Data. *Frontiers in Human Neuroscience*, *11*. https://doi.org/10.3389/fnhum.2017.00154

Mehnert, J., Akhrif, A., Telkemeyer, S., Rossi, S., Schmitz, C. H., Steinbrink, J., Wartenburger, I., Obrig, H., & Neufang, S. (2013). Developmental changes in brain activation and functional connectivity during response inhibition in the early childhood brain. *Brain and Development*, *35*(10), 894–904. https://doi.org/10.1016/j.braindev.2012.11.006

Mennes, M., Vega Potler, N., Kelly, C., Di Martino, A., Castellanos, F. X., & Milham, M. P. (2012). Resting State Functional Connectivity Correlates of Inhibitory Control in Children with Attention-Deficit/Hyperactivity Disorder. *Frontiers in Psychiatry*, *2*. https://doi.org/10.3389/fpsyt.2011.00083

Mills, K. L., Bathula, D., Costa Dias, T. G., Iyer, S. P., Fenesy, M. C., Musser, E. D., Stevens, C. A., Thurlow, B. L., Carpenter, S. D., Nagel, B. J., Nigg, J. T., & Fair, D. A. (2012). Altered Cortico-Striatal–Thalamic Connectivity in Relation to Spatial Working Memory Capacity in Children with ADHD. *Frontiers in Psychiatry*, *3*. https://doi.org/10.3389/fpsyt.2012.00002

Mitchell, M. E., Henry, T. R., Fogleman, N. D., Michael, C., Nugiel, T., & Cohen, J. R. (In Prep). *Response inhibition and rewards drive flexible reconfiguration of brain networks in children*.

Miyake, A., & Friedman, N. P. (2012). The Nature and Organization of Individual Differences in Executive Functions: Four General Conclusions. *Current Directions in Psychological Science*, *21*(1), 8–14. https://doi.org/10.1177/0963721411429458

Miyake, A., Friedman, N. P., Emerson, M. J., Witzki, A. H., Howerter, A., & Wager, T. D. (2000). The Unity and Diversity of Executive Functions and Their Contributions to Complex "Frontal Lobe" Tasks: A Latent Variable Analysis. *Cognitive Psychology*, *41*(1), 49–100. https://doi.org/10.1006/cogp.1999.0734

Norman-Haignere, S. V., McCarthy, G., Chun, M. M., & Turk-Browne, N. B. (2012). Category-Selective Background Connectivity in Ventral Visual Cortex. *Cerebral Cortex*, *22*(2), 391–402. https://doi.org/10.1093/cercor/bhr118

Nuño, L., Gómez-Benito, J., Carmona, V. R., & Pino, O. (2021). A Systematic Review of Executive Function and Information Processing Speed in Major Depression Disorder. *Brain Sciences*, *11*(2), 147. https://doi.org/10.3390/brainsci11020147

Nusslock, R., & Alloy, L. B. (2017). Reward processing and mood-related symptoms: An RDoC and translational neuroscience perspective. *Journal of Affective Disorders*, *216*, 3–16. https://doi.org/10.1016/j.jad.2017.02.001

O'Craven, K. M., & Kanwisher, N. (2000). Mental imagery of faces and places activates corresponding stiimulus-specific brain regions. *Journal of Cognitive Neuroscience*, *12*(6), 1013–1023. https://doi.org/10.1162/08989290051137549

Oldham, S., Murawski, C., Fornito, A., Youssef, G., Yücel, M., & Lorenzetti, V. (2018). The anticipation and outcome phases of reward and loss processing: A neuroimaging meta-analysis of the monetary incentive delay task. *Human Brain Mapping*, *39*(8), 3398–3418. https://doi.org/10.1002/hbm.24184

Padmanabhan, A., Geier, C. F., Ordaz, S. J., Teslovich, T., & Luna, B. (2011). Developmental changes in brain function underlying the influence of reward processing on inhibitory control. *Developmental Cognitive Neuroscience*, *1*(4), 517–529. https://doi.org/10.1016/j.dcn.2011.06.004

Padmanabhan, A., Lynn, A., Foran, W., Luna, B., & O'Hearn, K. (2013). Age related changes in striatal resting state functional connectivity in autism. *Frontiers in Human Neuroscience*, *7*. https://doi.org/10.3389/fnhum.2013.00814

Pan, P. M., Sato, J. R., Salum, G. A., Rohde, L. A., Gadelha, A., Zugman, A., Mari, J., Jackowski, A., Picon, F., Miguel, E. C., Pine, D. S., Leibenluft, E., Bressan, R. A., & Stringaris, A. (2017). Ventral Striatum Functional Connectivity as a Predictor of Adolescent Depressive Disorder in a Longitudinal Community-Based Sample. *American Journal of Psychiatry*, *174*(11), 1112–1119. https://doi.org/10.1176/appi.ajp.2017.17040430

Park, S., & Chun, M. M. (2009). Different roles of the parahippocampal place area (PPA) and retrosplenial cortex (RSC) in panoramic scene perception. *NeuroImage*, *47*(4), 1747–1756. https://doi.org/10.1016/j.neuroimage.2009.04.058

Piekarski, D. J., Johnson, C. M., Boivin, J. R., Thomas, A. W., Lin, W. C., Delevich, K., M. Galarce, E., & Wilbrecht, L. (2017). Does puberty mark a transition in sensitive periods for plasticity in the associative neocortex? *Brain Research*, *1654*, 123–144. https://doi.org/10.1016/j.brainres.2016.08.042

Porter, J. N., Roy, A. K., Benson, B., Carlisi, C., Collins, P. F., Leibenluft, E., Pine, D. S., Luciana, M., & Ernst, M. (2015). Age-related changes in the intrinsic functional connectivity of the human ventral vs. Dorsal striatum from childhood to middle age. *Developmental Cognitive Neuroscience*, *11*, 83–95. https://doi.org/10.1016/j.dcn.2014.08.011

Power, J. D., Barnes, K. A., Snyder, A. Z., Schlaggar, B. L., & Petersen, S. E. (2012). Spurious but systematic correlations in functional connectivity MRI networks arise from subject motion. *NeuroImage*, *59*(3), 2142–2154. https://doi.org/10.1016/j.neuroimage.2011.10.018

Power, J. D., Cohen, A. L., Nelson, S. M., Wig, G. S., Barnes, K. A., Church, J. A., Vogel, A. C., Laumann, T. O., Miezin, F. M., Schlaggar, B. L., & Petersen, S. E. (2011). Functional Network Organization of the Human Brain. *Neuron*, *72*(4), 665–678. https://doi.org/10.1016/j.neuron.2011.09.006

Power, J. D., & Petersen, S. E. (2013). Control-related systems in the human brain. *Current Opinion in Neurobiology*, *23*(2), 223–228. https://doi.org/10.1016/j.conb.2012.12.009

Quevedo, K., Ng, R., Scott, H., Kodavaganti, S., Smyda, G., Diwadkar, V., & Phillips, M. (2017). Ventral Striatum Functional Connectivity during Rewards and Losses and Symptomatology in Depressed Patients. *Biological Psychology*, *123*, 62–73. https://doi.org/10.1016/j.biopsycho.2016.11.004

Raud, L., Westerhausen, R., Dooley, N., & Huster, R. J. (2020). Differences in unity: The go/no-go and stop signal tasks rely on different mechanisms. *NeuroImage*, *210*, 116582. https://doi.org/10.1016/j.neuroimage.2020.116582

Ribner, A. D., Willoughby, M. T., Blair, C. B., & Investigators, T. F. L. P. K. (2017). Executive Function Buffers the Association between Early Math and Later Academic Skills. *Frontiers in Psychology*, *8*. https://doi.org/10.3389/fpsyg.2017.00869

Rosenberg, M. D., Finn, E. S., Scheinost, D., Papademetris, X., Shen, X., Constable, R. T., & Chun, M. M. (2016). A neuromarker of sustained attention from whole-brain functional connectivity. *Nature Neuroscience*, *19*(1), 165–171. https://doi.org/10.1038/nn.4179

Rosenberg, M. D., Martinez, S. A., Rapuano, K. M., Conley, M. I., Cohen, A. O., Cornejo, M. D., Hagler, D. J., Meredith, W. J., Anderson, K. M., Wager, T. D., Feczko, E., Earl, E., Fair, D. A., Barch, D. M., Watts, R., & Casey, B. J. (2020). Behavioral and Neural Signatures of Working Memory in Childhood. *The Journal of Neuroscience*, *40*(26), 5090–5104. https://doi.org/10.1523/JNEUROSCI.2841-19.2020

Rubia, K. (2013). Functional brain imaging across development. *European Child & Adolescent Psychiatry*, *22*(12), 719–731. https://doi.org/10.1007/s00787-012-0291-8

Rubia, K., Smith, A. B., Taylor, E., & Brammer, M. (2007). Linear age-correlated functional development of right inferior fronto-striato-cerebellar networks during response inhibition and anterior cingulate during error-related processes. *Human Brain Mapping*, *28*(11), 1163–1177. https://doi.org/10.1002/hbm.20347

Sadaghiani, S., Poline, J.-B., Kleinschmidt, A., & D'Esposito, M. (2015). Ongoing dynamics in large-scale functional connectivity predict perception. *Proceedings of the National Academy of Sciences*, *112*(27), 8463–8468. https://doi.org/10.1073/pnas.1420687112

Sala-Llonch, R., Peña-Gómez, C., Arenaza-Urquijo, E. M., Vidal-Piñeiro, D., Bargalló, N., Junqué, C., & Bartrés-Faz, D. (2012). Brain connectivity during resting state and subsequent working memory task predicts behavioural performance. *Cortex*, *48*(9), 1187–1196. https://doi.org/10.1016/j.cortex.2011.07.006

Salthouse, T. A., & Pink, J. E. (2008). Why is working memory related to fluid intelligence? *Psychonomic Bulletin & Review*, *15*(2), 364–371. https://doi.org/10.3758/PBR.15.2.364

Schachar, R., Logan, G. D., Robaey, P., Chen, S., Ickowicz, A., & Barr, C. (2007). Restraint and Cancellation: Multiple Inhibition Deficits in Attention Deficit Hyperactivity Disorder. *Journal of Abnormal Child Psychology*, *35*(2), 229–238. https://doi.org/10.1007/s10802-006-9075-2

Schultz, D. H., & Cole, M. W. (2016). Higher Intelligence Is Associated with Less Task-Related Brain Network Reconfiguration. *The Journal of Neuroscience*, *36*(33), 8551–8561. https://doi.org/10.1523/JNEUROSCI.0358-16.2016

Seeley, W. W., Menon, V., Schatzberg, A. F., Keller, J., Glover, G. H., Kenna, H., Reiss, A. L., & Greicius, M. D. (2007). Dissociable Intrinsic Connectivity Networks for Salience Processing and Executive Control. *Journal of Neuroscience*, *27*(9), 2349–2356. https://doi.org/10.1523/JNEUROSCI.5587-06.2007

Seitzman, B. A., Gratton, C., Marek, S., Raut, R. V., Dosenbach, N. U. F., Schlaggar, B. L., Petersen, S. E., & Greene, D. J. (2020). A set of functionally-defined brain regions with improved representation of the subcortex and cerebellum. *NeuroImage*, *206*, 116290. https://doi.org/10.1016/j.neuroimage.2019.116290

Shine, J. M., Bissett, P. G., Bell, P. T., Koyejo, O., Balsters, J. H., Gorgolewski, K. J., Moodie, C. A., & Poldrack, R. A. (2016). The Dynamics of Functional Brain Networks: Integrated Network States during Cognitive Task Performance. *Neuron*, *92*(2), 544–554. https://doi.org/10.1016/j.neuron.2016.09.018

Shine, J. M., & Poldrack, R. A. (2018). Principles of dynamic network reconfiguration across diverse brain states. *NeuroImage*, *180*, 396–405. https://doi.org/10.1016/j.neuroimage.2017.08.010

Silverstein, M. J., Faraone, S. V., Leon, T. L., Biederman, J., Spencer, T. J., & Adler, L. A. (2020). The Relationship Between Executive Function Deficits and DSM-5-Defined ADHD Symptoms. *Journal of Attention Disorders*, *24*(1), 41–51. https://doi.org/10.1177/1087054718804347

Smith, S. M., Fox, P. T., Miller, K. L., Glahn, D. C., Fox, P. M., Mackay, C. E., Filippini, N., Watkins, K. E., Toro, R., Laird, A. R., & Beckmann, C. F. (2009). Correspondence of the brain's functional architecture during activation and rest. *Proceedings of the National Academy of Sciences of the United States of America*, *106*(31), 13040–13045. https://doi.org/10.1073/pnas.0905267106

Somerville, L. H., & Casey, B. (2010). Developmental neurobiology of cognitive control and motivational systems. *Current Opinion in Neurobiology*, *20*(2), 236–241. https://doi.org/10.1016/j.conb.2010.01.006

Steinbeis, N., Haushofer, J., Fehr, E., & Singer, T. (2016). Development of Behavioral Control and Associated vmPFC–DLPFC Connectivity Explains Children's Increased Resistance to Temptation in Intertemporal Choice. *Cerebral Cortex*, *26*(1), 32–42. https://doi.org/10.1093/cercor/bhu167

Stevens, M. C. (2016). The contributions of resting state and task-based functional connectivity studies to our understanding of adolescent brain network maturation. *Neuroscience & Biobehavioral Reviews*, *70*, 13–32. https://doi.org/10.1016/j.neubiorev.2016.07.027

Stevens, M. C., Kiehl, K. A., Pearlson, G. D., & Calhoun, V. D. (2007). Functional neural networks underlying response inhibition in adolescents and adults. *Behavioural Brain Research*, *181*(1), 12–22. https://doi.org/10.1016/j.bbr.2007.03.023

Stoppel, C. M., Boehler, C. N., Strumpf, H., Heinze, H.-J., Hopf, J.-M., & Schoenfeld, M. A. (2011). Neural processing of reward magnitude under varying attentional demands. *Brain Research*, *1383*, 218–229. https://doi.org/10.1016/j.brainres.2011.01.095

Sutcubasi, B., Metin, B., Kurban, M. K., Metin, Z. E., Beser, B., & Sonuga-Barke, E. (2020). Resting-state network dysconnectivity in ADHD: A system-neuroscience-based meta-analysis. *The World Journal of Biological Psychiatry*, *21*(9), 662–672. https://doi.org/10.1080/15622975.2020.1775889

Tavor, I., Jones, O. P., Mars, R. B., Smith, S. M., Behrens, T. E., & Jbabdi, S. (2016). Task-free MRI predicts individual differences in brain activity during task performance. *Science*, *352*(6282), 216–220. https://doi.org/10.1126/science.aad8127

Teslovich, T., Mulder, M., Franklin, N. T., Ruberry, E. J., Millner, A., Somerville, L. H., Simen, P., Durston, S., & Casey, B. J. (2014). Adolescents let sufficient evidence accumulate before making a decision when large incentives are at stake. *Developmental Science*, *17*(1), 59–70. https://doi.org/10.1111/desc.12092

Tooley, U. A., Bassett, D. S., & Mackey, A. P. (2022). Functional brain network community structure in childhood: Unfinished territories and fuzzy boundaries. *NeuroImage*, *247*, 118843. https://doi.org/10.1016/j.neuroimage.2021.118843

Tottenham, N., Tanaka, J. W., Leon, A. C., McCarry, T., Nurse, M., Hare, T. A., Marcus, D. J., Westerlund, A., Casey, B., & Nelson, C. (2009). The NimStim set of facial expressions: Judgments from untrained research participants. *Psychiatry Research*, *168*(3), 242–249. https://doi.org/10.1016/j.psychres.2008.05.006

Turk-Browne, N. B. (2013). Functional Interactions as Big Data in the Human Brain. *Science*, *342*(6158), 580–584. https://doi.org/10.1126/science.1238409

Vaidya, C. J., & Gordon, E. M. (2013). Phenotypic Variability in Resting-State Functional Connectivity: Current Status. *Brain Connectivity*, *3*(2), 99–120. https://doi.org/10.1089/brain.2012.0110

van den Bos, W., Cohen, M. X., Kahnt, T., & Crone, E. A. (2012). Striatum–Medial Prefrontal Cortex Connectivity Predicts Developmental Changes in Reinforcement Learning. *Cerebral Cortex*, *22*(6), 1247–1255. https://doi.org/10.1093/cercor/bhr198

van Duijvenvoorde, A. C. K., Peters, S., Braams, B. R., & Crone, E. A. (2016). What motivates adolescents? Neural responses to rewards and their influence on adolescents' risk taking, learning, and cognitive control. *Neuroscience & Biobehavioral Reviews*, *70*, 135–147. https://doi.org/10.1016/j.neubiorev.2016.06.037

Vink, M., Zandbelt, B. B., Gladwin, T., Hillegers, M., Hoogendam, J. M., van den Wildenberg, W. P. M., Du Plessis, S., & Kahn, R. S. (2014). Frontostriatal activity and connectivity increase during proactive inhibition across adolescence and early adulthood: Activity and Functional Connectivity of Frontostriatal Network. *Human Brain Mapping*, *35*(9), 4415–4427. https://doi.org/10.1002/hbm.22483

Wang, L., Su, L., Shen, H., & Hu, D. (2012). Decoding Lifespan Changes of the Human Brain Using Resting-State Functional Connectivity MRI. *PLOS ONE*, *7*(8), e44530. https://doi.org/10.1371/journal.pone.0044530

Watson, C. G. (2020). *brainGraph: Graph Theory Analysis of Brain MRI Data* (R package version 3.0.0) [Computer software]. https://CRAN.R-project.org/package=brainGraph

Weissman, D. G., Schriber, R. A., Fassbender, C., Atherton, O., Krafft, C., Robins, R. W., Hastings, P. D., & Guyer, A. E. (2015). Earlier adolescent substance use onset predicts stronger connectivity between reward and cognitive control brain networks. *Developmental Cognitive Neuroscience*, *16*, 121–129. https://doi.org/10.1016/j.dcn.2015.07.002

White, T., Schmidt, M., Kim, D. I., & Calhoun, V. D. (2011). Disrupted Functional Brain Connectivity during Verbal Working Memory in Children and Adolescents with Schizophrenia. *Cerebral Cortex*, *21*(3), 510–518. https://doi.org/10.1093/cercor/bhq114

Wilson, R. P., Colizzi, M., Bossong, M. G., Allen, P., Kempton, M., Abe, N., Barros-Loscertales, A. R., Bayer, J., Beck, A., Bjork, J., Boecker, R., Bustamante, J. C., Choi, J. S., Delmonte, S., Dillon, D., Figee, M., Garavan, H., Hagele, C., Hermans, E. J., … MTAC. (2018). The Neural Substrate of Reward Anticipation in Health: A Meta-Analysis of fMRI Findings in the Monetary Incentive Delay Task. *Neuropsychology Review*, *28*(4), 496–506. https://doi.org/10.1007/s11065-018-9385-5

Yanes, J. A., Riedel, M. C., Ray, K. L., Kirkland, A. E., Bird, R. T., Boeving, E. R., Reid, M. A., Gonzalez, R., Robinson, J. L., Laird, A. R., & Sutherland, M. T. (2018). Neuroimaging meta-analysis of cannabis use studies reveals convergent functional alterations in brain regions supporting cognitive control and reward processing. *Journal of Psychopharmacology*, *32*(3), 283–295. https://doi.org/10.1177/0269881117744995

Yau, W.-Y. W., Zubieta, J.-K., Weiland, B. J., Samudra, P. G., Zucker, R. A., & Heitzeg, M. M. (2012). Nucleus Accumbens Response to Incentive Stimuli Anticipation in Children of Alcoholics: Relationships with Precursive Behavioral Risk and Lifetime Alcohol Use. *Journal of Neuroscience*, *32*(7), 2544–2551. https://doi.org/10.1523/JNEUROSCI.1390-11.2012

Yeo, B. T. T., Krienen, F. M., Sepulcre, J., Sabuncu, M. R., Lashkari, D., Hollinshead, M., Roffman, J. L., Smoller, J. W., Zöllei, L., Polimeni, J. R., Fischl, B., Liu, H., & Buckner, R. L. (2011). The organization of the human cerebral cortex estimated by intrinsic functional connectivity. *Journal of Neurophysiology*, *106*(3), 1125–1165. https://doi.org/10.1152/jn.00338.2011

Zald, D. H., & Treadway, M. T. (2017). Reward Processing, Neuroeconomics, and Psychopathology. *Annual Review of Clinical Psychology*, *13*(1), 471–495. https://doi.org/10.1146/annurev-clinpsy-032816-044957

Zhu, X., Cortes, C. R., Mathur, K., Tomasi, D., & Momenan, R. (2017). Model-free functional connectivity and impulsivity correlates of alcohol dependence: A resting-state study. *Addiction Biology*, *22*(1), 206–217. https://doi.org/10.1111/adb.12272